

UNIVERSITY OF BELGRADE
SCHOOL OF ELECTRICAL ENGINEERING

MOHAMED MAROUF

**HIGH FREQUENCY NOISE APPROXIMATION AND
ADAPTIVE REDUCTION IN THE ECG SIGNALS**

Doctoral Dissertation

Belgrade, 2017

UNIVERZITET U BEOGRADU
ELEKTROTEHNIČKI FAKULTET

MOHAMED MAROUF

**APROKSIMACIJA I ADAPTIVNO SMANJENJE
VISOKOFREKVENTNOG ŠUMA U EKG SIGNALIMA**

Doktorska Disertacija

Beograd, 2017

Mentor disertacije

Dr. Lazar Saranovac, vanredni profesor,
Univerzitet u Beogradu - Elektrotehnički Fakultet

Članovi komisije

Dr. Milan Prokin, redovni profesor,
Univerzitet u Beogradu - Elektrotehnički Fakultet

Dr. Miodrag Popović, redovni profesor u penziji ,
Univerzitet u Beogradu - Elektrotehnički Fakultet

Dr. Mirjana Popović, naučni savetnik,
Univerzitet u Beogradu - Institut za Medicinska Istraživanja

Dr. Jelena Popović-Božović, docent
Univerzitet u Beogradu - Elektrotehnički Fakultet

Datum odbrane

Dissertation title:

High frequency noise approximation and adaptive reduction in the ECG signals

Abstract

The ECG signal has been used since the beginning of the last century. Mainly, ECG signals are recorded to help in the diagnosis of certain group of heart, artery, and pulmonary diseases. Therefore, ECG signal processing is not a new theme for research. Plenty of methods that address the main challenges in ECG signal preprocessing and analysis pipeline were presented in the literature. One of the challenges that are still a subject of research is the high frequency noise presence in ECG signal recording.

Due to the overspread of the internet of things (IOT) solutions and developed telecommunication infrastructure, new application of the ECG signal recording were presented and integrated in telemedicine platforms. Additionally, ECG signal recording applications are not limited anymore to the standard clinical and holter recording. Post event and loop recording has become more popular, cheaper, and available to patients. Moreover, several recording methodologies, using dry and wearable fashion, have appeared to replace the classic adhesive electrodes recording. The question that often arises when dealing with signals recorded with these devices is the reliability of recorded signals regardless of the used recording method.

The most important factor that determines the reliability of ECG signals is the amount of high frequency noise present in the signal. However, the noise presence (offset and onset), ratio to the signal, nature, and color are variable over the whole recording. This is because noise is not stationary in ECG signal, especially in the long-term recording which is the case of loop event recorders and holters. Hence, there is no measure that could be applied on the whole signal to estimate the overall signal quality. Thus, noise level estimation or approximation should be considered in translation invariant manner in the time domain. Developing a method to approximate the noise level over time can be utilized to estimate the reliability of ECG signal in sliding local windows of any length rather than estimating the signal quality in overall.

In this context, a noise level estimation over time in translation-invariant manner is introduced. Due to the non-stationarity of noise presence, strength, and color, the word

approximation is more accurate than estimation. So, the proposed method is called noise level approximation or just noise approximation.

The stationary wavelet transform (SWT) is used to find the translation-invariant approximation of the high frequency noise. This is accomplished in the form of reference signal extracted as an estimation of the signal quality in two modes. In the first mode, the reference signal (noise approximation signal) is extracted after the exclusion of possible QRS complexes candidates which could be found using multi-resolutional analysis on the details of SWT transform. The second mode is the same as the first but without the exclusion of QRS complexes when the reference signal is calculated.

In order to increase the robustness and the reliability of the extracted reference signal, different heart rates and rhythms were used in the normalization of the reference signal. The corresponding waves, caused by heart electrical activity in these rhythms and heart rates, show fast changes with irregular morphology. Taking such arrhythmias into consideration is important for avoiding misclassification between them and noise intervals, because of high ratio of amplitude changes in the ECG signal waves in these arrhythmias. Thus, noise level approximation is reliable and applicable regardless of the rhythm included in the input signal. Smoothing of the reference signal provides suitable guiding signal that could be thresholded and quantized to several noise levels corresponding to the amplitude of the reference signal. This was the motivation behinds the proposal of the extracted signal in noise suppression framework such as adaptive filtering, filters banks, or adaptive Wiener wavelet denoising. Considering arrhythmias when the building the reference signal increases its reliability to give good filtering results regardless of input signal rhythm. This enhances the whole signal fidelity. Where, signal fidelity after processing measures how close the result of digital processing represents the "true" input signal. The lack of reliability and fidelity of filtering algorithms are the main reasons why physicians prefer to disable all ECG signal filtering methods before interpretation.

Additionally, the exclusion of possible QRS complexes candidates will be translated in a reference signal that reflects the noise in the S-Q interval between each consecutive two beats and therefore, reference signal will drop during the QRS complex. This reduces the QRS complexes attenuation and minimizes the distortion of filtering methodology guided by the built reference signal. This is important due to the fact that these complexes are associated with higher frequencies than other segments or waves in the ECG signal and they are usually distorted when ECG signals are filtering.

Finally, application of noise level approximation and adaptive reduction are discussed in real case where an ECG recorder was presented to record ECG signals in different recording modes. Algorithms integration is discussed as well as the proposed device design and implementation. Noise level approximation and adaptive reduction are integrated in the processing pipeline of the recorded signals using both dry and wet electrodes.

Key words: Adaptive noise reduction, ECG, Noise approximation, Telemedicine

Scientific area: Electrical engineering

Scientific subarea: Electronics

UDC number: 621.3

Naslov teze:

Aproksimacija i adaptivno smanjenje visokofrekventnog šuma u EKG signalima

Rezime

EKG signali su korišćeni još početkom prošlog veka. Uglavnom su se koristili za dijagnozu određenih grupa srčanih, arterijskih i plućnih bolesti. Stoga, obrada EKG signala nije nova tema za istraživanje. Mnogo metoda koje se odnose na glavne izazove koji su prisutni u postupcima za obradu i analizu EKG signala, su predstavljeni u literaturi. Jedan od izazova koji je i dalje predmet istraživanja je prisustvo visokofrekventnog šuma u snimanju EKG signala.

Zbog širenja upotrebe “*internet of things*” (IOT) rešenja i razvijene telekomunikacijske infrastrukture, nove primene za snimanje EKG singala su predstavljene i integrisane u telemedicinskim platformama. Tako da primena EKG snimanja više nije ograničena na standardna klinička i holter snimanja. *Post-event* i *loop* snimanja su postala popularnija, jeftinija i pristupnija pacijentima.

U cilju zamene klasičnog snimanja sa adhezivnim elektrodama, pojavilo se i nekoliko različitih metodologija koje koriste suve elektrode i prenosive uređaje.

Pitanje koje se često javlja u radu sa snimljenim signalima ovih uređaja, je pouzdanosti snimljenih signala bez obzira na metodu snimanja.

Najvažniji faktor koji određuje pouzdanost EKG signala je količina visokofrekventnog šuma prisutnog u signalu.

Međutim, prisustvo šuma (početak i kraj), njegov odnos u signalu, priroda i boja su varijabilni kroz vreme u celom signalu, zato što taj šum je nestacionaran u EKG signalima. Ovo se posebno odnosi na dugoročno snimanje, pogotovo u *loop event recorder* i *holter*.

Imajući to u vidu, ne postoji mera koja može da se primeni na celi signal za estimaciju celokupnog kvaliteta signala. Tako da treba da se razmatra estimacija ili aproksimacija nivoa šuma na *translation-invariant* način. Razvijanje metode za aproksimaciju nivoa šuma kroz vreme može da se koristi za estimaciju celokupnog kvaliteta singala.

U ovom kontekstu, predstavljena je estimacija nivoa šuma kroz vreme na *translation-invariant* način. Zbog nestacionarnog prisustva šuma, njegove jačine i boje, upotreba termina aproksimacija je tačnija od termina estimacija. Tako da je navedena metoda nazvana aproksimacija nivoa šuma ili samo aproksimacija šuma.

Stationary wavlet transformacija (SWT) je korišćena metoda za nalaženje *translation-invariant* aproksimacije visokofrekventnog šuma. Ovo je ostvareno u formi referentnog signala izdvojenog kao estimacija kvaliteta signala u dva režima rada. Prvi režim je posle izbacivanja potencijalnih QRS kompleksa, koji mogu da se detektuju sa *multi-resolutonal* analizom na detalje SWT transformacije. Drugi režim je isti kao prvi samo što nisu izbačeni QRS kompleksi iz kalkulacije referentnog signala.

Različite srčane frekvencije i srčani ritmovi su korišćeni za normalizaciju referentnog signala u cilju povećanja robustnosti i pouzdanosti ekstrahovanog referentnog signala. Odgovarajući talasi, izazvani električnom aktivnošću srca u ovim srčanim ritmovima i srčanim frekvencijama, pokazuju brze promene sa neregularnom morfologijom. Uzimajući to u obzir važno je izbegavanja pogrešne klasifikacije između tih ritmova i zašumljenih intervala. To povećava pouzdanosti i primenljivosti aproksimacije šuma bez obzira na ritam koji postoji u ulaznom EKG signalu.

“*Smoothing*“ referentnog singala daje prikladan vodeći singal koji može da se koristi za određivanje praga i kvantizaciju amplitude referentnog singala na nekoliko nivoa šuma.

Ovo je i bio motiv za predlog nove metode za korišćenje ekstrahovanog signala u platformi za uklanjanje šuma kao što su adaptivno filtriranje, banka filtara, i adaptivno *Wavelet Wiener* filtriranje. Uzimajući aritmije u obzir, metoda za izdvajanje referentnog vodećeg signala, povećava pouzdanost rezultata filtriranja bez obzira na ritam koji postoji u signalu.

Ovo poboljšava celokupnu tačnost signala posle filtriranja. Tačnost signala nakon obrade meri koliko je rezultat posle filtriranja sličan tačnom ulaznom signalu.

Nedostatak tačnosti algoritma za filtriranja je glavni razlog zašto lekari daju prednost isključivanju svih filtara pre interpretacije EKG signala.

Dodatno, izbacivanje potencijalnih QRS kompleksa će proizvesti referentni signal koji reflektuje šum u S-Q intervalu između dva otkucaja za redom. Zbog toga će amplituda referentnog signala opasti za vreme QRS kompleksa. Ovo smanjuje slabljenje QRS kompleksa i minimizira distorziju izazvanu filtriranjem koje je vođeno sa izdvojenim referentnim signalom. Ovo je važno zbog toga što su ti kompleksi asocirani sa najvišim frekvencijama za razliku od ostalih talasa koji postoje u EKG signalima a uglavnom postaju neprepoznatljiv posle filtriranja EKG signala.

Na kraju su analizirani metode za apoksimaciju i adaptivno filteriranje šuma u EKG signalima u realnim primenama. Nova arhitektura EKG uređaja je predstavljena za snimanje EKG signala u različitim režimima rada. Takođe su predstavljene integracije navedenih

algoritma i njihova implementacija u procesu analize snimljenih signala sa suvimi i vlažnim adhezvnim elektrodamama.

Ključne reči: Adaptivno smanjenje šuma, EKG, Aproksimacija šuma, Telemedicina

Naučna oblast: Elektrotehnika

Uža naučna oblast: Elektronika

UDK broj: 621.3

List of Contents

List of Figures	I
List of Tables	VI
Abbreviations	VII
1. Introduction.....	1
2. The Cardiac Physiology.....	7
2.1 The heart Anatomy and physiology	7
2.2 The heart conduction system and function.....	8
2.3 The Electrocardiography (ECG)	9
2.4 ECG measurement.....	12
2.5 Recording modes.....	14
2.5.1 Standard ECG	14
2.5.2 Stress test	15
2.5.3 Signal-averaged ECG	15
2.5.4 HOLTER monitoring.....	16
2.5.5 Event Recorders.....	17
2.6 ECG signal Applications.....	19
2.7 ECG signals Analysis pipeline.....	19
2.8 Current challenges in the analysis pipeline	21
2.8.1 Variability among individuals	21
2.8.2 ECG signal are non-stationarity	22
2.8.3 Noise susceptibility.....	23
3. Noise Sources and Measurement in the ECG signals.....	25
3.1 Noise And Artifacts Sources	26
3.1.1 Motion Artifacts	26
3.1.2 Baseline Wandering.....	27
3.1.3 Power Line Interference	27
3.1.4 EMG Noise	29
3.1.5 Electrode Popup Or Contact Noise.....	30
3.1.6 Other Noise Sources	30
3.2 The Main Properties Of Noise In The ECG Signals	31

3.2.1	Non-stationarity	31
3.2.2	Spectral Overlapping With Arrhythmias	31
3.2.3	Noise Coloration.....	32
3.3	Measuring Noise In The ECG Signal.....	34
3.4	Review Of Noise Level Estimation/Approximation Methods	35
3.4.1	Route Mean Square (RMS) Power In The Isoelectric Region	35
3.4.2	WWD.....	36
3.4.3	RMSSD-R and SD-R:.....	38
3.4.4	Activity	39
3.4.5	PCA	41
3.4.6	KLT	43
3.4.7	Frequency Content In Six Bandwidths and Out Of Range Event	45
3.4.8	Moving Average	46
3.4.9	T-P Interval Average Power Divided By QRS.....	47
3.4.10	Cumulative Mismatch Histogram.....	47
3.4.11	Moving Variance	49
3.4.12	Kurtosis.....	49
3.4.13	LMS Adaptive Filtering.....	50
3.5	Conclusion (Noise Level Estimation vs. Approximation).....	50
4.	Short-time Noise level Approximation	53
4.1	Proposed Approach Flow Diagram	54
4.2	Wavelet Transform Of ECG Signal	54
4.3	Extraction Of Zero-Crossings, Peaks, And Valleys	59
4.4	Smoothing	61
4.5	Smoothed Reference Signal Normalization	62
4.6	Discussion And Results.....	66
4.6.1	Evaluation ECG Database	66
4.6.2	Noise Generation and Addition	66
4.6.3	Evaluation Results	68
4.7	Reference Signal Sensitivity And Dynamic Range.....	73
4.8	Reference Signal Implementation	73
4.9	Applications	73
4.9.1	Guided Leads Selection.....	73

4.10 Conclusion.....	75
5. Adaptive Noise Reduction	76
5.1 Related work	77
5.2 Noise Level Approximation As A Guiding Signal For Filters Bank	79
5.3 Adaptive noise reduction.....	80
5.4 Discussion And Results.....	82
5.4.1 Noise Generation And Tested Signals.....	82
5.4.2 Benchmark Methods And Validation	82
5.5 Noise Level Approximation as a Guiding Signal For Wiener Filter.....	90
5.6 Conclusion.....	94
6. Algorithms integration in a multi-purpose ECG telemetry system	95
6.1 Background	96
6.2 System Architecture and Design.....	97
6.4 Dry And Wet Electrodes	99
6.5 ECG Acquisition Module.....	100
6.6 Mobile Application	102
6.7 Algorithms and Offline Analysis	104
6.8 Evaluation and Results	108
6.8.1 Device Placement Versus Signal Quality.....	108
6.8.2 Correlation With ECG Golden Standard Leads	110
6.8.3 Peer review of clinical acceptability.....	111
6.8.4 Accuracy Evaluation For Heart Rate Detection	113
6.8.5 Noise Influence On Heart Rate Accuracy	114
6.8.6 Comparison With The Available Commercial Solutions	114
6.9 Conclusions	116
7. Conclusions and Perspectives	117
References.....	119
Biography.....	129
Author's publications	129

List of Figures

2.1	The cardiac muscle wall structure	8
2.2	The structure diagram of the human heart	8
2.3	Blood flow diagram of the human heart. Blue components indicate oxygen-rich blood pathways and red components indicate oxygen-poor blood pathways	9
2.4	Heart electrical conduction system	10
2.5	Normal features and intervals of the ECG signal. P, Q, R, S, T waves are shown as they are supposed to be in ideal sinus rhythm	11
2.6	The Einthoven's triangle. Leads are calculated as the difference in potential between two different body points	11
2.7	The P, Q, R, S, T, U waves resulting from one depolarization / repolarization cycle .	12
2.8	The six standard precordial leads	13
2.9	The limb leads on the top and augmented limb leads on the bottom	14
2.10	Typical treadmill stress test procedure	15
2.11	Holter monitoring test	16
2.12	Recent 12 lead ECG harness developed by NASA used as ECG loop recorder. Orbital dry electrodes shown in A are embedded in special belt C. Signals are sent wirelessly via Bluetooth to the receiving smart phone D. Finally, a print out of 12 lead ECG is obtained	17
2.13	Photograph of the patient-operated ECG system	18
2.14	ECG signal analysis general pipeline	20
2.15	Heartbeats averaged by subject	22
2.16	ECG interval with arrhythmias from the first channel of MIT-BIH record 207. Changes in the morphology and heart rate have a non-stationary nature	23
3.1	ECG signal from MIT-BIH record 103 shows motion artifacts contaminating the signal	26
3.2	Baseline wandering from MIT-BIH record 103	27
3.3	Power line interference added to ECG signal. Nominal frequency is 50 Hz in this case	28
3.4	Two different intervals corrupted by EMG noise from the origin. Intervals are from the MIT-BIH record 108	29
3.5	Relative power spectra of QRS complex, P and T waves, muscle noise and motion artifacts	32
3.6	Several ECG rhythms on left side and the corresponding PSD for them on the right side. From top to bottom, Sinus rhythm, Ventricular Tachycardia, Ventricular flutter, and Ventricular fibrillation. It is clear how arrhythmia impact the spectrum of the ECG signal over time and how it is possible to occupy the whole spectrum of the recorded signal	33

3.7	Comparing a zero-mean unit-variance clean ECG (upper plot) with the same signal with additive noise of decreasing coloration (lower autocorrelation). In each case, the noise is set to be zero-mean with unit variance, and therefore has the same power as the ECG (SNR = 1). It is obvious that the whiter the noise, the more significant the distortion for a given SNR	34
3.8	Some of the amplitude and duration features used in WWD algorithm	38
3.9	Short-time RMS values; turns count using Willison's procedure. Both signals were computed using a causal moving window of 70 ms duration	40
3.10	SVD of 25 QRS complexes: (a) Stacked QRS complexes from MIT-BIH record 108, (b) Stack of first 10 principal components after applying PCA on the QRS complexes array, (c) Stem representation of singular spectrum shows how eigenvalues magnitude associated with principal components decreases, (d) reconstruction of the new bases using only the first 5 principal components	42
3.11	Left figure is for the first four principal components. Right, is for the bases 5-8; we can notice how correlation with the non-signal component in the original signal increases as eigenvalues decreases	43
3.12	KL bases functions extracted from MIT-BIH following the procedure proposed in [56]	44
3.13	Computation of coefficients using the KL bases functions. Summation of KL bases functions is used to represent each QRS complex in the signal. On the top of the figure, the original signal is shown. The first and second coefficient a, b and their contributions to the representation of QRS are shown in the center. In the lower part of the figure, three numbered QRS complexes are mapped onto the a-b plane illustrating how the KLT preserves morphologic similarities. Image adapted from[56]	45
3.14	Filtered residue (FR) method. (A) Action potentials recorded from cultured neonatal rat cardiac myocytes ($m = 48$). (B) Signal-averaged trace. Note that all action potentials are identical. (C) Residue (light trace) and FR (dark trace), superimposed on top. See text for details of the algorithm. (D) Final output (dark trace) superimposed on the signal-averaged trace (gray). Horizontal scale bars represent 50 ms.	46
3.15	Signals and signal quality histogram plots for MIT-BIH record 203	48
3.16	Signals and signal quality histogram plots for MIT-BIH record 207	48
3.17	Flow diagram of the EMG detection algorithm using moving variance	49
3.18	Kurtosis and tailness of Gaussian distribution	50
4.1	Flow diagram for the reference signal extraction or the short-time noise level approximation method	54
4.2	The adopted prototype wavelet $\Psi(t)$ and smoothing function $\Theta(t)$	56
4.3	Equivalent frequency responses of the DWT at scales 2^k , $k = 1; \dots; 5$ for 250-Hz sampling rate.	56
4.4	Two filter-bank implementations of DWT. (a) Mallat's algorithm.(b) Implementation without decimation (algorithme à trous)	58
4.5	SWT at the first five scales of ECG-like simulated waves	59
4.6	The A_{zpv} array extraction from ECG signal details. ECG signal interval from Lead 1 of	

MIT-BIH record 106 on the top with extracted reference signal (solid red line), and at the bottom are the details of ECG signal of scale 2^2 . Peaks and valleys are in red squares, zero-crossings are in green dots, and QRS complexes are marked as black circles	60
4.7 Several intervals from the MIT-BIH database for arrhythmia that show fast heart rate and irregular waves' morphology. (a) is for atrial fibrillation, (b) is for ventricular flutter, (c) is for idioventricular rhythm, (d) is for ventricular tachycardia, (e) is for supraventricular tachycardia, and (f) is for Torsade De Pointes	64
4.8 Histogram of samples number vs. smoothed reference signal values	65
4.9 The process of noise addition to the ECG evaluation signals	67
4.10 Signals with original noise. In the top is 108 record while in the bottom is the 109 record. Reference signal with (red line) and without (dashed-dotted black line) QRS exclusion. ECG signals here are noisy from the origin	69
4.11 Heart block rhythms MIT-BIH record (109), Reference signal with (red line) and without (dashed-dotted black line) QRS exclusion. Clean ECG signal from MIT-BIH record (Top), and the same signal after noise addition (bottom)	70
4.12 Atrial Fibrillation MIT-BIH record (201) , Reference signal with (red line) and without (dashed-dotted black line) QRS exclusion. Clean ECG signal from MIT-BIH record (Top), and the same signal after noise addition (bottom)	70
4.13 Ventricular beats (106) record, Reference signal with (red line) and without (dashed-dotted black line) QRS exclusion. Clean ECG signal from MIT-BIH record (Top), and the same signal after noise addition (bottom)	71
4.14 Idio Ventricular (207) record, Reference signal with (red line) and without (dashed-dotted black line) QRS exclusion. Clean ECG signal from MIT-BIH record (Top), and the same signal after noise addition (bottom)	71
4.15 Atrial Fibrillation (201) record, Reference signal with (red line) and without (dashed-dotted black line) QRS exclusion. Clean ECG signal from MIT-BIH record (Top), and the same signal after noise addition (bottom)	72
5.1 Flow diagram for the reference signal extraction and adaptive denoising	80
5.2 Equivalent frequency responses of filters at degree 1,...,10 for 250-Hz frequency sampling	81
5.3 Reference signal with and without QRS exclusion.(up) Noisy ECG signal from MIT-BIH record 106, (middle) filtered signal in solid blue and reference signal extracted with exclusion of QRS components in solid red, (bottom) filtered signal in continuous blue and reference signal extracted without exclusion of QRS components in solid red	82
5.4 Comparison with other methods results.(a) original signal 106 record from MIT-BIH data base, (b) signal after real EMG noise addition with SNR = 5, (c) filtered signal with BPF,(d) filtered signal with WD, (e) filtered signal with SVD, (f) the results without the exclusion of QRS candidates, (g) the results with the exclusion of QRS candidates	84
5.5 Normal sinus rhythm MIT-BIH record(103). Adaptive denoising results. Clean ECG signal is at top of figures (a,b,c, and d), signal after noise addition is in the middle in solid blue line, while the extracted reference signal (red), and filtered signal are at the	

bottom	85
5.6 Idio Ventricular Rhythm MIT-BIH record(207) Adaptive denoising results. Clean ECG signal is at top of figures (a,b,c, and d), signal after noise addition is in the middle in solid blue line, while the extracted reference signal (red), and filtered signal are at the bottom	85
5.7 Heart block rhythms MIT-BIH record(109) Adaptive denoising results. Clean ECG signal is at top of figures (a,b,c, and d), signal after noise addition is in the middle in solid blue line, while the extracted reference signal (red), and filtered signal are at the bottom	86
5.8 Atrial Fibrillation MIT-BIH record(201) Adaptive denoising results. Clean ECG signal is at top of figures (a,b,c, and d), signal after noise addition is in the middle in solid blue line, while the extracted reference signal (red), and filtered signal are at the bottom	86
5.9 Adaptive denoising results. Filtering results of different ECG rhythms from MIT-BIH records. Noisy ECG signal from origin is at the top of figures in solid blue line, while extracted reference signal (red), and filtered signal are shown at the bottom	87
5.10 Adaptive denoising results. Filtering results of different ECG rhythms from MIT-BIH records. Noisy ECG signal from origin is at the top of figures in solid blue line, while extracted reference signal (red), and filtered signal are shown at the bottom	87
5.11 SNR improvement after adaptive denoising of Lead I of MIT-BIH records (from top to bottom 103,117,119) computed for four types of noises	89
5.12 A log representation of the power spectral components of a signal for Wiener filter .	91
5.13 The block diagram of the Wavelet Wiener Filtering approach. The upper path is used to estimate the noise-free signal and the lower for wiener filtering using the noise-free estimation	92
5.14 The block diagram of the proposed Adaptive Wavelet filtering using the extracted noise level approximation (NLA) which is used to adapt the filtering of wavelet coefficients to get adaptively filtered noise free estimation. The estimated noise free coefficients are then used to compute the filtering factor of Wiener filter (WWF)	94
6.1 The basic diagram of the presented platform and its principal components, where the proposed device is wirelessly transmitting the recordings to a handheld mobile phone which transmits the signals to a cloud server. Signals could be directly transmitted to the cloud server using GSM connection	97
6.2 The principal components and mechanical design of proposed ECG device, where short-term post-event recorder is enabled b inserting the ECG acquisition body in the short-term post-event recorder housing. Holter or long-term recording mode is enabled by connecting the cable of wet adhesive electrodes to the ECG acquisition body	98
6.3 ECG acquisition module architecture	101
6.4 The flowchart of ECG signal processing pipeline implemented on smart phone applications	102
6.5 The flowchart of ECG signals analysis for both short-term and long-term modes	104
6.6 Clustering of ECG beats of first channel of MIT-BIH recording 106 using KLT coefficients vector and RR features. Noise level approximation is used in this step in the validation of clustered beats. Average cluster was calculated and beats which have	

Euclidean distance large larger than 2 standard deviations and whose corresponding noise level approximation value larger than 0.5 were classified as noises and isolated	106
6.7 Screen-shot of the web analysis platform. Automatic analysis results are seen in the bottom part, while the signal is shown with colors annotating the beats classification. Physicians have an access to their patients' recordings so they can confirm the automatic analysis results and follow their status	107
6.8 Tested device placement; two vertical (V1–V2), three horizontal (H1–H3), and finally the corresponding positions of electrodes of H2, V1 placement on human chest ribs	109
6.9 Short-term post-event signals L1–L3 (left column) versus golden standard channels V1–V3 (right column). The morphological variability could be noticed among leads recorded using short-term post-event recorder as well as golden standard leads	111
6.10 Histogram of isolated beats or detected on each lead that are not detected on all leads	113

List of Tables

3.1	Shows features used to build the features vector which is then used to assess signal quality using statistical study	37
4.1	Signals used for histograms generation	63
4.2	Correlation coefficient of reference signal with estimated SNR	69
5.1	Single lead delineation results with and without the usage of adaptive denoising	90
6.1	The average correlation values of short-term post-event recorder Leads (L1–L3) and corresponding ECG Golden standard leads (V1–V3).....	110
6.2	Signal quality and clinical acceptability for selected placements H1, V1	111
6.3	Results of peer review of event and best match leads from golden standard ECG ...	112
6.4	QRS complex delineation results on both short term event leads and best matched three standard ECG leads event	114
6.5	Features comparison with similar available commercial solutions	115

Abbreviations

ECG	<i>Electrocardiography</i>
SWT	<i>Stationary Wavelet Transform</i>
EMG	<i>Electromyogram</i>
QRS	<i>QRS Complex</i>
SNR	<i>Signal To Noise Ratio</i>
IOT	<i>Internet of things</i>
RMS	<i>Root Mean Square</i>
WDD	<i>Weighted Diagnostic Distortion</i>
RMSSD	<i>Root Mean Square Of Successive Differences</i>
SD-R	<i>Standard Deviation Of The Residuum</i>
PCA	<i>Principal Components Analysis</i>
KLT	<i>“Karhunen –Loeve” Transform</i>
ORE	<i>Out Of Range Event</i>
A-V	<i>Atrioventricular</i>
SA	<i>Sinoatrial Node</i>
NN	<i>Neural Network</i>
FIR	<i>Finit Impulse Response</i>
IIR	<i>Infinit Impulse Response</i>
PSD	<i>Power Spectral Density</i>
RMS	<i>Route Mean Square</i>
PRD	<i>Percentage Root Mean Square Difference</i>
ZCR	<i>Zero-Crossing Rate</i>
ZC	<i>Zero-Crossing</i>
TC	<i>Turns Counts</i>
SVD	<i>Singular Value Decomposition</i>

GPU	<i>Graphics Processing Unit</i>
FR	<i>Filtered Residue</i>
NS	<i>Noise Score</i>
MRA	<i>Mutiresolutional Analysis</i>
LPF	<i>Low Pass Filtering</i>
HPF	<i>High Pass Filtering</i>
DWT	<i>Discrete Wavelet Transform</i>
BPM.	<i>Beats Per Minute</i>
NST	<i>Noise Stress Test Database</i>
PPV	Positive Predictive Value
PC	<i>Personal Computer</i>
WD	<i>Wavelet Details</i>
SURE	<i>Stein's Unbiased Risk Estimate</i>
ISWT	<i>Inverse Stationary Wavelet Transform</i>
MCU	<i>Microcontroller</i>
eMMC	<i>Embedded Multi-Media Controller</i>
LED	<i>Light-Emitting Diode</i>
NFC	<i>Near Field Communication</i>
UART	<i>Universal Asynchronous Receiver/Transmitter</i>
RFID	<i>Radio-Frequency Identification</i>

Chapter 1

1. Introduction

The ECG signal has been used since the beginning of the last century. Mainly, it has been used to diagnose a certain group of heart, artery, and pulmonary diseases. Therefore, ECG signal processing is not a new theme for research. Plenty of methods that address the major challenges in the ECG signal preprocessing and analysis pipeline were presented in the literature. One of these challenges that are still a subject of research is the noise presence during the recording of ECG signals.

Due to the overspread of internet of things IOT solutions and developed telecommunication infrastructure, new applications for ECG signal recording were proposed as portable or wearable devices integrated in telemedicine platforms. So, ECG signal recording applications are not limited anymore to the standard clinical and holter recording. Moreover, the post event and loop recording applications have become more popular, cheaper, and available to patients especially after the widespread usage of the dry electrodes and wearable fashion instead of the classic recording methods using of adhesive electrodes.

Anyway, the question that often arises when dealing with signals recorded with these devices is the reliability of recorded signals regardless of the adopted method.

The ECG contains very distinctive features which are essential for detection and interpretation of heart arrhythmias. However, automatic identification of these features is not a tractable problem, because of the presence of diverse non-cardiac contaminants that influence the ECG signal during the acquisition process. These artifacts and noises are the main causes of imprecise delineation, and the false classification of heartbeats which lead to false alarms and misleading analysis.

Therefore, signal quality estimation and enhancement is essential in order to reduce the number of false alarms induced by analysis algorithms enabling more efficient heartbeats detection and classification, especially in the long term and fetal ECG signals.

The main sources of contaminates are patient's electrodes motion artifacts, power line interference, baseline wander, and EMG noise caused by muscle tremors on the chest wall. Unlike power line interference and baseline drift, the EMG noise and patient-electrode motion artifacts are difficult to detect and eliminate using linear filtering, because of the non-stationary nature of these noises and the big overlaps on the whole frequency bands of ECG and EMG signals [1, 2, 3, 4]. Therefore, because of the different sources and consequently nature of contaminants that affect the ECG signal, special approaches should be used to handle each kind of contamination.

In this thesis, the EMG noise contamination is addressed. Due to the wide frequency band and large coloration of this particular noise source, it encompasses other high frequency noises such as Gaussian noise. Hence, from now on, EMG noise will be referred to as high frequency noise or just noise if not otherwise specified. Two aspects of dealing with high frequency noises are addressed in this thesis; noise level estimation as well as adaptive reduction.

Noise level estimation is fundamental phase in the ECG signal processing pipeline, because it could be used in all other places in the analysis pipeline. The following major usages highlight the importance of noise estimation:

1. It provides reliable confidence measures. Appropriate noise level estimation could be used to identify when the noise level is high. This information along with other parameters contributes to defining the “level of trust” of the ECG interval which is consequently used to belittle the importance of possible alarms.
2. It could be used for noise suppression. Appropriate noise level estimation could be utilized to guide the adaptive filtering approaches by controlling the filtering strength according to the corresponding noise level estimated in the ECG signal.
3. Find the best channels to be used for the combination of leads' delineation results. This could be done by studying the amount of noise present in each channel over time and selecting leads interchangeably according to the estimated noise variance. Thus, delineation combination algorithm prefers results from cleaner intervals when there is a mismatch in the delineation of other leads.

4. Make a decision about an interval's quality, and, afterwards, isolate intervals of EMG noises where noise is present.
5. Find precise dominant heartbeat morphology from the ECG signal. This also requires suitable noise level estimation over time in the ECG signal. Thus, only Heartbeats with high SNR values contribute in the averaging procedure.

Several methodologies that address noise level estimation or equivalently signal quality estimation are presented in the literature. Sometimes this issue is presented as noise approximation, noise estimation, signal quality estimation, or short-time noise assessment. A review of the most important methods is presented in this thesis.

Actually, noise is random and uncertain. So, it could not be computed precisely. Anyway, its variance or level to the signal could be somehow estimated. Moreover, from the statistical point of view, there is no way to compute noise precisely even if the same measurement is repeated for large number of times due to the fact that noise is not systematic but random and uncertain occurrence.

It is important to distinguish noise from the systematic error, which is an error in the measurement arising from a defeat or physical effect during the measurement. Systematic errors could be computed using standards and then used to re-calibrate the measurement devices. Noise, on the other hand, is more random and uncertain as mentioned above.

Therefore, the most appropriate terminologies for the aforementioned problem could be “noise free signal estimation” or “noise level approximation” which is the term adopted and used in this context henceforth.

Most of the published methods that address noise estimation suffer from two drawbacks. Firstly, the focus of most of presented methods is to estimate noise level over discrete intervals of different lengths. There is a need to estimate noise level over time in time-translation manner, rather. Secondly, ignoring arrhythmia with fast changing rhythms in these methods reduce their reliability. This is mainly due to the great overlapping in the frequency spectrum of both arrhythmia and noise which leads to imprecise estimation of noise when these rhythms are present in the signal.

In this thesis, a new approach to deal with the EMG and high frequency noises is proposed. The main goal of the presented algorithm is to find a smooth time-translation approximation of the noise level. In order to ensure that the extracted noise level approximation will work

properly in the presence of arrhythmia, several arrhythmias with different heart rates and morphologies are considered when the noise approximation is built.

Afterwards, several applications of the noise approximation methodology in the ECG signal analysis pipeline are presented. Special attention is paid to the usage of noise level approximation signal in adaptive noise suppression. This is realized as guiding the filtering approach to reduce noise adaptively in the signal. Results of this application proved the suitability and reliability of this noise level approximation in the analysis pipeline.

The proposed noise approximation and its application in adaptive noise reduction are evaluated using signals recorded by both dry and wet adhesive electrodes. Both real EMG and artificial noises are used in the validation procedures.

The outline and contributions of this thesis are summarized below.

Chapter 2

This chapter is an introduction to the Cardiac physiology and Electrocardiogram recording. Firstly, a brief introduction of the heart Anatomy and structure is presented. Then, an overview of the heart conduction system, whose activity is monitored when the ECG signals are recorded, is introduced and discussed. It is important to understand the ECG measurement system in order to understand its drawbacks and defeats. Therefore, a section dedicated to how ECG signals are recorded is included. Additionally, an overview of ECG application is added to give an insight into the applicability of the presented approaches in both already developed and currently developing technologies.

Afterwards, the ECG analysis pipeline and its main challenges are introduced and explained. The goal of this thesis is to study the challenge of noise presence, so this problem is introduced in this section and discussed in details in the next one.

Chapter 3

In this chapter, the problem of noise level or relevantly signal quality estimation will be studied in details. First of all, a subsection is dedicated to present the noise and contaminants in the ECG signal. A review of noise types and sources is included. Secondly, the main properties of noise are studied in both spectral and time domains. Dealing with the Non-stationarity, coloration, and spectral overlapping with arrhythmia is of paramount importance when noise approximation of reduction is addressed.

In order to explain the different methodologies presented in the literature, a review of the most important methods used to address noise level estimation and approximation in the ECG signals is added. It is worthy to mention that noise in this context will be limited to EMG and high frequency noises only. The presented review encompasses methods used for signal quality, noise level, and noise free estimation. The following methods are included in the review:

- Root mean square (RMS) power in the isoelectric region
- Weighted Diagnostic Distortion (WDD)
- root mean square of successive differences (RMSSD) and The standard deviation of the residuum SD-R
- Activity
- Principal Components Analysis (PCA)
- “*Karhunen –Loeve*” transform KLT
- Frequency content in six bandwidths and Out of range event (ORE)
- Moving average
- T-P interval average power divided by QRS
- Cumulative mismatch histogram
- Moving variance
- Kurtosis
- LMS adaptive filtering

Chapter 4

This chapter is dedicated to the new method presented for time-invariant high frequency noise approximation. Thus, the representation of ECG features in the time-scale domain, after applying the Stationary Wavelet Transform (SWT), is discussed. Afterwards, the usage of multi-resolutinal analysis approach is presented to find wavelet correspondents to noise in the wavelet details of the ECG signal. The resulted signal after smoothing is considered as non-global approximation of the EMG noise.

Afterwards, detailed analysis of the arrhythmia and noise spectrums is provided in this chapter. This is important to understand the next step in the presented approach where two thresholds σ_1 and σ_2 are used in the normalization of the previously resulted smooth approximation.

The evaluation of the noise approximation method is also presented in this chapter. Firstly, the adopted procedure for evaluation is introduced. Several metrics were introduced and calculated for this purpose.

The extracted noise approximation has several applications in the ECG analysis pipeline. Some of these applications are discussed in this chapter including: Guided Leads selection, Noisy intervals isolation, Classification and Clustering confidence, and Dominant beat finding.

Chapter 5

As mentioned above, the noise level approximation signal is suitable to be used as guiding signal in an adaptive noise reduction framework. This chapter is dedicated for this application.

Firstly, the most important methodologies regarding adaptive noise reduction from the ECG signals are discussed. A review of three main methodologies is presented; adaptive filtering, wavelet based filtering, filters bank.

In the next section, two approaches are suggested for adaptive Electromyogram (EMG) noise reduction in the Electrocardiogram (ECG) signals. In the first one, noise level approximation, presented in chapter 3, is utilized to guide a filters bank. This method is implemented and evaluated. The second method adopts the usage of translation-invariant noise level approximation in adaptive Wiener Wavelet filtering approach to achieve the adequate adaptiveness. This method is not implemented, though. The algorithm workflow only is presented for future work.

Chapter 6

In this chapter, the design and implementation of multi-purpose ECG recorder is presented. The algorithms proposed in this thesis are integrated in the analysis workflow of signals recorded using this device. Two recording modes are enabled using two different electrodes types. Therefore, two customized pipelines for the ECG signal analysis are introduced and the noise approximation and adaptive reduction methods are integrated in each of them.

Chapter 2

2. The Cardiac Physiology

Before digging into the details of advanced ECG processing algorithms, it is important to understand the cardiac physiology and how the electrical activity of the heart conduction system is measured. This is important because the next chapters address issues related to noise approximation and adaptive reduction in the ECG signals as well as a new design proposed to record the ECG signal. Therefore, a brief introduction about the heart physiology and anatomy is included in this chapter.

Afterwards, the different modes in which experts analyze electrical activity of the heart conduction system are introduced. Signal analysis pipeline is introduced to understand the conventional processing pathway applied to recorded signal before it reaches to the hands of an expert. Finally, the most difficult challenges facing algorithms in the ECG signal analysis pipeline are presented and discussed in details.

2.1 The heart Anatomy and physiology

The human heart is a specific muscle that is different from the other two muscles types of muscles; skeletal and smooth muscles. The muscle tissue of the heart is called the myocardium. It forms a thick middle layer between the outer epicardium and the inner endocardium layers. Both layers form the double-walled sac containing the heart and the roots of the great vessels [5].

The cardiac muscle has cross striations formed by rotating segments of thick and thin protein filaments. However, in contrast to skeletal muscle, cardiac muscle cells are typically grouped in branch-like structures instead of linear (see Figure 2.1). The primary structural proteins of cardiac muscle are myosin and actin.

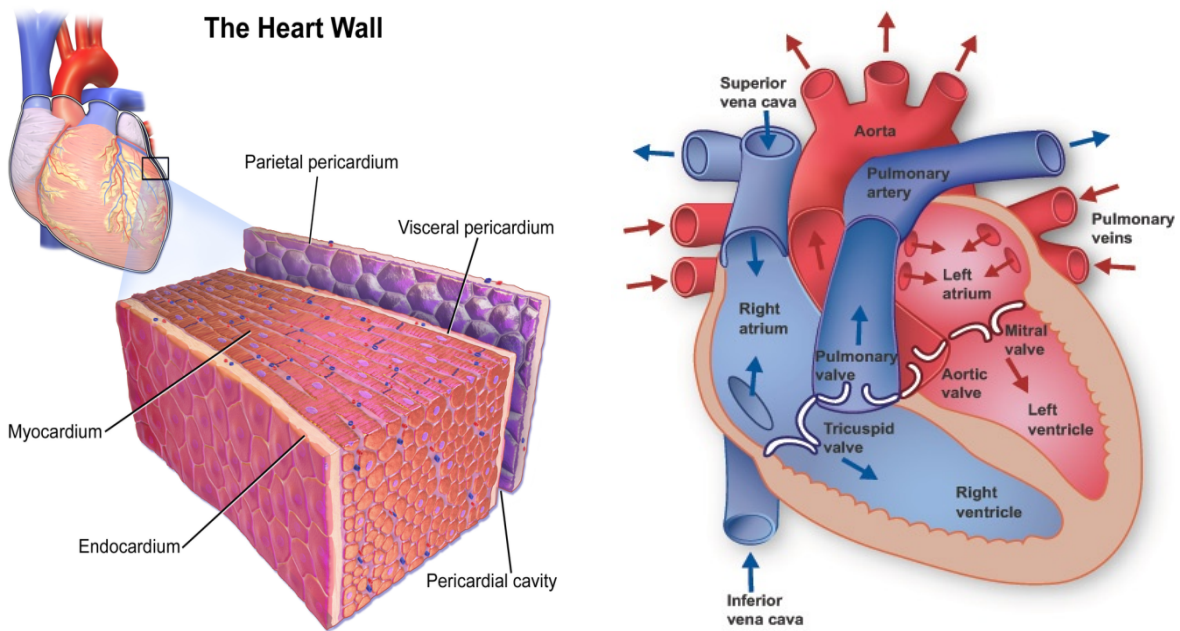


Figure 2.1 The cardiac muscle wall structure. Image adapted from [6]

Figure 2.2 The structure diagram of the human heart. Image adapted from [7]

Unlike the action potential in skeletal muscle cells, the cardiac action potential is not initiated by nervous activity. Instead, it arises from a group of specialized cells that have automatic action potential generation. Therefore, it is not under the control of the somatic nervous system. Another difference that distinguishes cardiac muscle cells is there need to extracellular calcium ions for contraction to occur [8].

The heart has four chambers, two upper atria, the receiving chambers, and two lower ventricles, the discharging chambers (see Figure 2.2). Atrioventricular septum separates the atria from the ventricles. The atrioventricular (A-V) valves which are located in the atrioventricular septum allow blood transfer between atria and ventricle from the same heart side (see Figure 2.2 and Figure 2.3).

2.2 The heart conduction system and function

As mentioned above, the heart functionality is triggered by the heart conduction system - a group of cells in the heart that have the ability to generate electrical activity. It maintains the cardiac muscle rhythmical contraction by generating the Action potential which keeps the chambers works synchronized to pump blood. On the other hand, the autonomic nervous system plays a different role by regulating the heart rate and the contractility of cardiac cells [10].

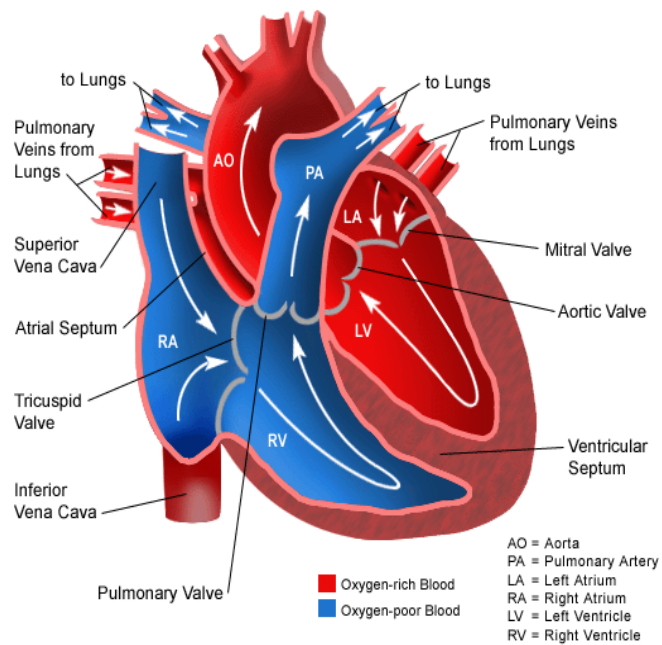


Figure 2.3 Blood flow diagram of the human heart. Blue components indicate oxygen-rich blood pathways and red components indicate oxygen-poor blood pathways. Image adapted from [9]

The heart conduction system consists of specialized heart muscle cells. The whole system is embedded in myocardium (see Figure 2.4). Its main components are the SA node, AV node, bundle of His, bundle branches, and Purkinje fibers. The work of these components cause electrical impulses to spread over the heart and make it contract and any dysfunction of the conduction system is reflected in the speed and regularity of heart rhythms which makes it irregular, fast, or slow. The produced electrical activity can be measured at electrodes placed at special positions on the skin. The recording is then produced in the form of a graph or ECG.

2.3 The Electrocardiography (ECG)

It has been more than 100 years since the first electrocardiograph machine was invented by the Nobel prizewinning Dutch doctor and physiologist, Willem Einthoven. He used the string galvanometer (the first practical electrocardiograph) to record ECG signals [10]. He named later the waves of ECG signal using the P, Q, R, S, and T letters which are still in use today (see Figure 2.5 which illustrates these waves). Einthoven also described the electrocardiographic features of a number of cardiovascular disorders [10].

Over the last century, several devices for recording ECG signals were invented and massively produced. Nevertheless, the basics of ECG recording have not changed a lot. The heart called Einthoven's triangle is still the essential method to find ECG leads (see Figure 2.6). However, special interest in the ECG processing arose to help physicians in handling

increasing amount of ECG recordings taking advantage of the advances in digital processing platforms and computers. So, what happens in a single ECG beat and how these events are depicted in the ECG?

In the normal heart, the action potential of each beat begins in the right atrium from the SA node (see Figure 2.7). This node is sometimes referred to as the natural pacemaker of the heart. The potential spreads across both atria causing the muscle cells to depolarize and contract inducing the phase known as atrial systole (this is presented on the ECG as P wave). The period of conduction that follows atrial systole P wave and precedes the contraction of ventricles is depicted as PR interval – a flat line following P. Then the signal leaves the atria and enters the AV node located in the septum, and then it enters the bundle of HIS to propagate through the bundle branches and purkinje fibers along ventricles. As the signal spreads in the ventricles, the cells depolarize and the ventricles contract very rapidly inducing the ventricles sys. Finally as the signal passes out, the ventricular wall starts to relax and recover. This act of repolarization is depicted in the T wave in the ECG signal. Therefore, ST segment is the period when ventricles are depolarized, while QT interval represents the time needed from the depolarization to the repolarization of ventricles [14]. The sequence of events just described and the associated ECG trace repeats with every heartbeat.

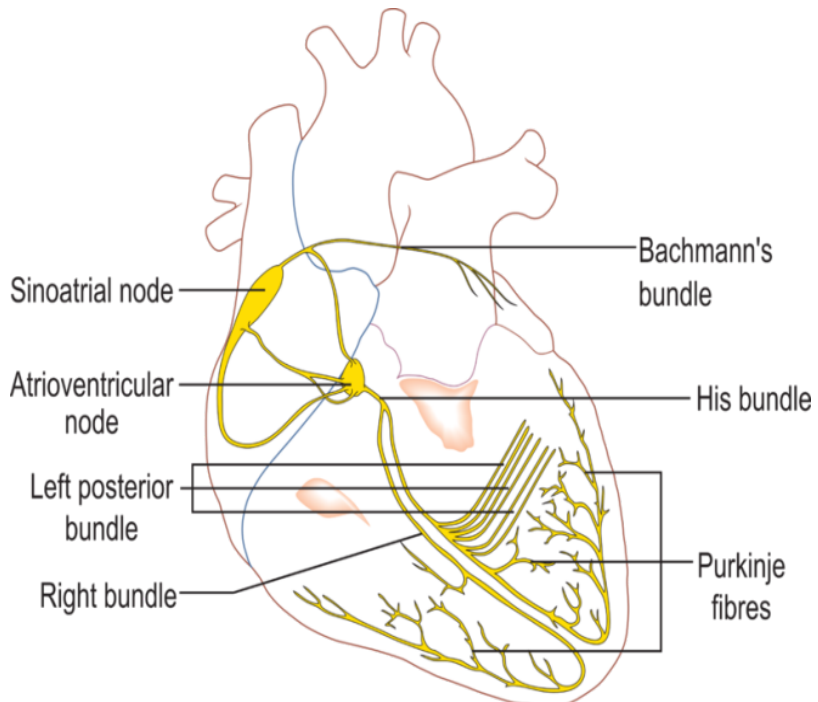


Figure 2.4 Heart electrical conduction system. Image adapted from [11]

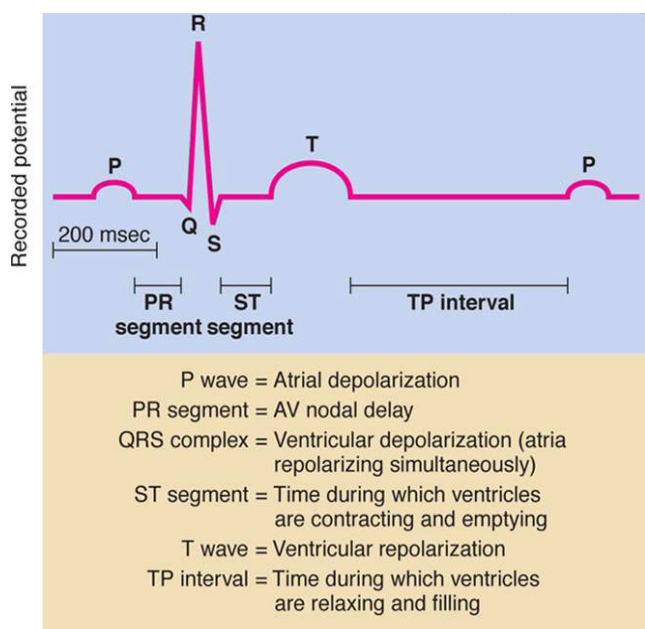


Figure 2.5 Normal features and intervals of the ECG signal. P, Q, R, S, T waves are shown as they are supposed to be in ideal sinus rhythm. Image adapted from [12]

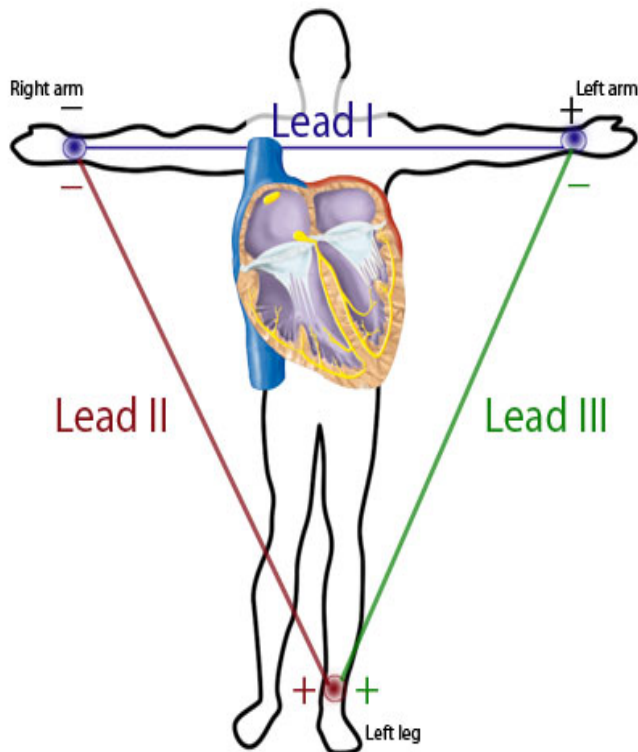


Figure 2.6 The Einthoven's triangle. Leads are calculated as the difference in potential between two different body points. Image adapted from [13]

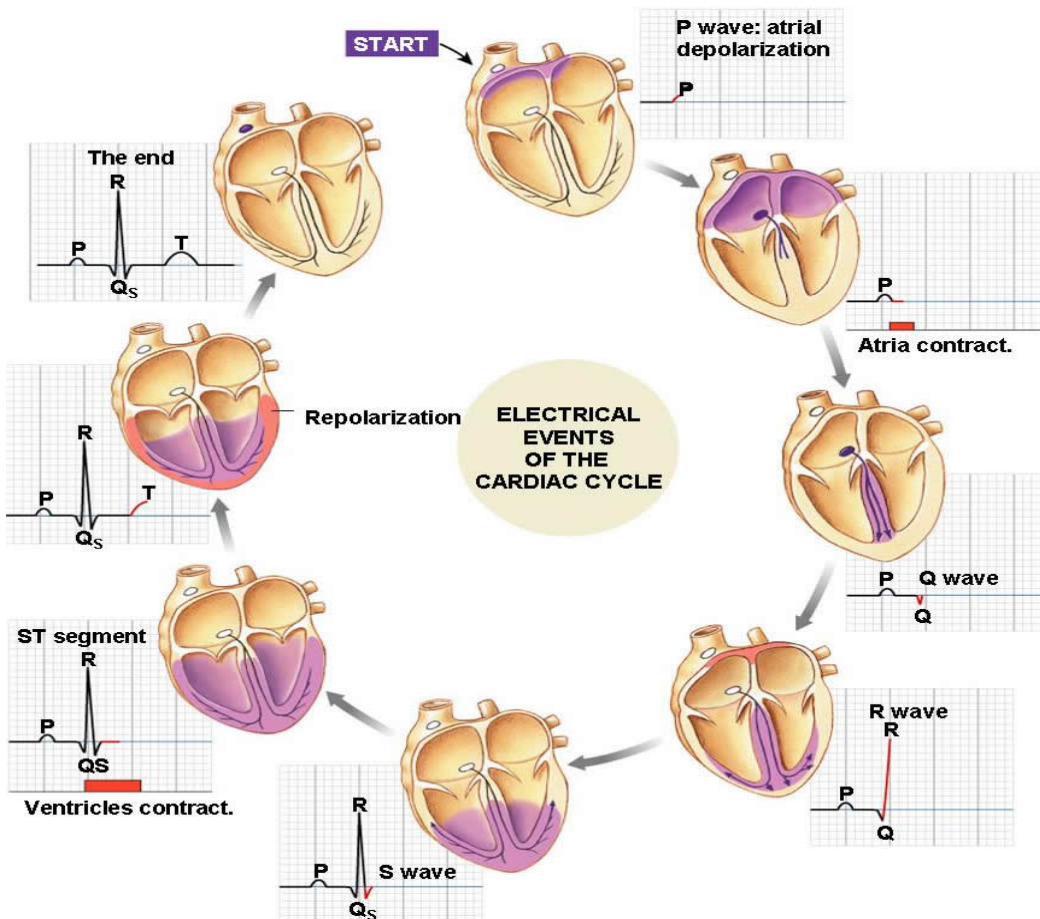


Figure 2.7 The P, Q, R, S, T, U waves resulting from one depolarization / repolarization cycle. Image adapted from [15]

Under the influence of this electrical provocation, the heart muscle cells shrink, which as a result, causes a mechanical effect in the form of cyclic shrinking of heart atria and ventricles. As an effect of heart muscle shrinking, the blood circulates in the human organs.

Schematic representation of normal ECG waves is shown in Figure 2.5. Each normal ECG beat consists of P wave that represent the atrial depolarization phase, QRS complex that represents the ventricular depolarization, T wave that depicts the ventricular repolarization and finally U wave that represents the papillary muscle repolarization.

2.4 ECG measurement

The depolarization and repolarization phenomena of the heart muscle cells are caused by the movement of ions. This is the essence of the heart electric activity as it induces the electric current, which generates the electromagnetic field around the heart. There is possibility to measure the electric potential at each point of the electromagnetic field. The potential difference recorded at the two points of the electromagnetic field reflects the ECG signal. The shape of the ECG signal and a cyclic repetition of its characteristic parts including

P-QRS-T complex, constitute essential information about operation of the electrical conduction system of the heart.

The Electrocardiograph is measured by sensing the electrical activity using electrodes in contact with the body on the limbs and on the rib cage. The difference in potential between two electrodes is considered as one ECG lead/channel. So, the "lead" is not the same as the "electrode". Since leads can share the same electrode, a standard 12-lead ECG happens to need only 10 electrodes.

There are limbs, precordial and augmented limbs leads. The presence of these leads and the way they are measured depends on the ECG recording device and ECG application. In essence, the precordial leads are "unipolar" and represent the difference between each of precordial electrodes (V₁-V₆) and the central terminal compared to a common lead (commonly the Wilson's central terminal). Figure 2.8 illustrates the electrodes position on the subject chest and how precordial leads are computed from them. On the other hand, the limb leads are "bipolar" and are the comparison between two electrodes

There is also a group of leads called the augmented limb. They are derived from the same three electrodes as limbs leads, but they use Goldberger's central terminal as their negative pole. Figure 2.9 shows a graphical representation of Einthoven triangle. It explains how limbs and augmented limbs leads are calculated.

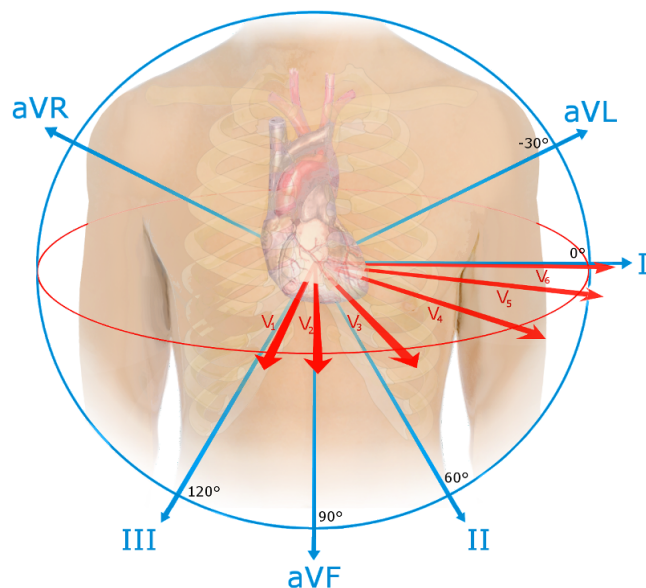


Figure 2.8 The six standard precordial leads. Image adapted from [16]

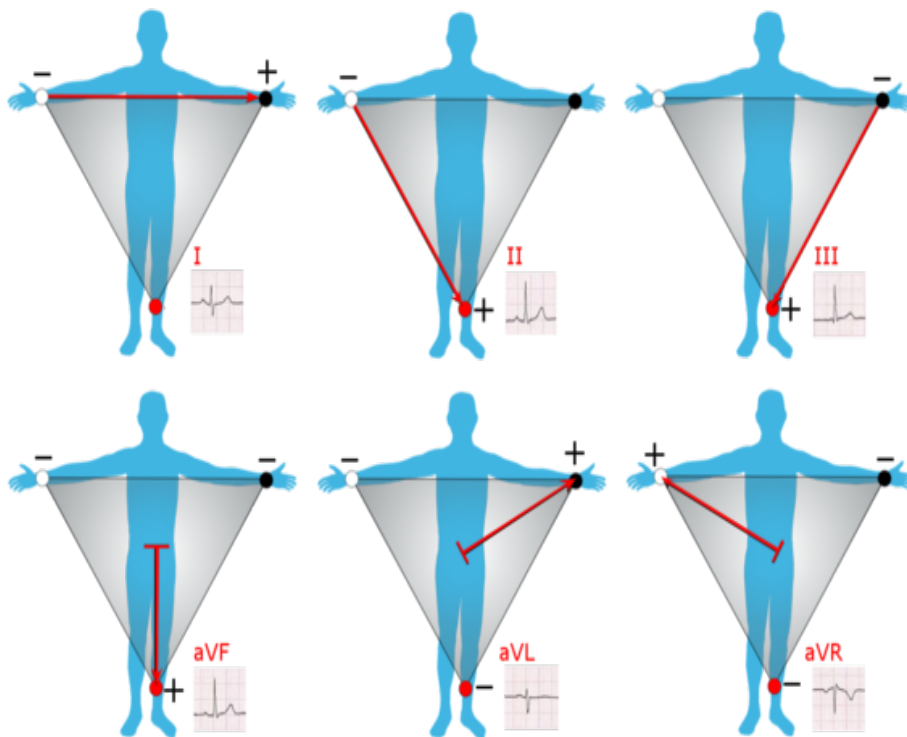


Figure 2. 9 The limb leads on the top and augmented limb leads on the bottom. Image adapted from [16]

An important point to highlight is the polarity of ECG waves. Each wave has an origin and direction of spreading. Polarity of the ECG waves is determined by the direction of depolarization or repolarization in the heart muscle cells. Thus, if the depolarization of the heart spreads toward the positive electrode, it produces a positive deflection and vice versa. In a similar manner, if the repolarization of the heart spreads toward the positive electrode, it produces a negative deflection and vice versa [14].

2.5 Recording modes

2.5.1 Standard ECG

This kind of recording is done generally in controlled conditions such as hospitals and clinics. Standard ECG monitoring could be performed to monitor the cardiac muscle activity of patients or to check the heart's status after a myocardial infarction, or after a heart-related procedure such as a cardiac catheterization, heart surgery, electrophysiological studies, etc. On the other hand, clinical ECG recording could be used in the diagnosis of a certain group of cardiac, artery, and pulmonary diseases.

2.5.2 Stress test

One of the most important procedures performed by specialists is the so-called stress test (also called treadmill test or exercise EKG). A stress test is given while a patient is walking on a treadmill or pedaling a stationary exercise bicycle ergometer. The stress response could be also induced by drug stimulation. This kind of tests is aimed to assess the changes in the ECG during a physical activity, such as exercises, and to evaluate patients for coronary artery disease or arrhythmias [18].

The electrocardiogram (ECG) in this mode is recorded by the means of 10 electrodes that are attached to the skin of the chest, arms, and legs (see Figure 2.10). The whole procedure is done in a controlled clinical environment and patient must be supervised by a specialist all the time.

2.5.3 Signal-averaged ECG

Another important clinical ECG recording is the signal averaged ECG. This procedure is done in the same manner as the standard ECG recorded. However, special algorithms are used to align the ECG of multiple heartbeats and then average them in order to remove interference. Usually, 15-20 minutes ECG is recorded for this purpose [3].

After averaging, important variations, so-called "late potentials", in the QRS complexes are revealed. Information extracted by analyzing late potentials is crucial to diagnose certain group of potentially dangerous disease.

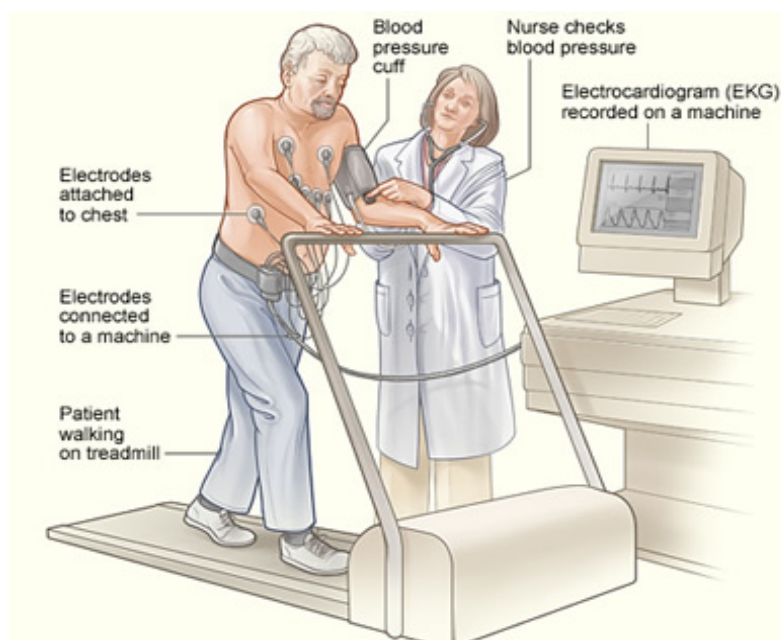


Figure 2. 10 Typical treadmill stress test procedure. Image adapted from [19].

2.5.4 HOLTER monitoring

Holters are small electronics devices with electrodes attached to them, generally by lead wires [20]. Usually, they are used to record 24 hour of ECG signal; however, some holters are able to record up to 7 days.

While wearing a holter, patients keep a diary of their symptoms and function normally with their daily activities (see Figure 2.11). Activities that cause the electrodes to become loose or detached during recording are an exception. For instance, patients are asked to avoid taking a shower, swimming, or any activity causing an excessive amount of sweating. Once the monitor is returned, the data are analyzed in digital format using special analysis software. Diaries are used to understand the correlation between analysis results on the one hand and activities and symptoms on the other hand.

Physicians decide to go for this kind of recording for observing occasional cardiac arrhythmias which is difficult to be identified in a shorter periods because their symptoms are infrequent. In this case, the short duration of monitoring can be inadequate.

Analyzing software is crucial when dealing with holter signals due to the long duration of recorded signal. On average, there is more than 100.000 beats that should be delineated and analyzed. Moreover, the presence of noises and artifacts in the HOLTER ECG signal is inevitable. Therefore, it would be extremely time-demanding to analyze or even manually browse through such a long signal.

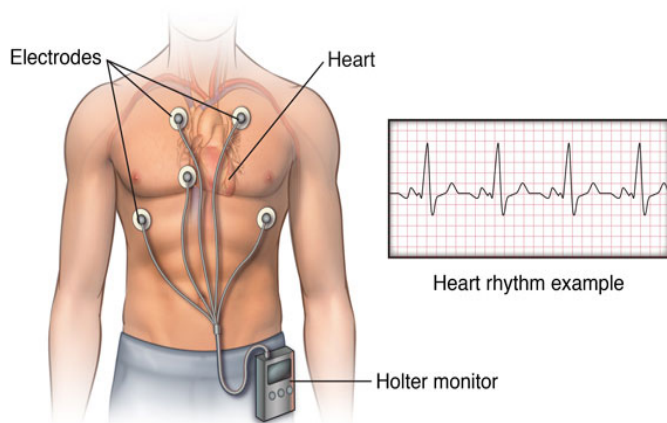


Figure 2. 11 Holter monitoring test. Image adapted from [21]

The automatic analysis commonly provides the physician with information about heart beat morphology, beat interval measurement, heart rate variability. However, the success of the automatic analysis is very closely associated with the signal quality and noise presence patterns in the signal. Noise approximation and signal quality estimation are of paramount importance for a successful analysis.

The main limitation of Holter monitoring is the detection of intermittent arrhythmias, because symptoms happen infrequently. Additionally, there is no real-time analysis of the recorded signals. In these cases, event monitor could be used [22, 23, 24, 25].

2.5.5 Event Recorders

For patients having more transient symptoms, a cardiac event monitor is considered. Such devices could be used for a month or more in order to catch the arrhythmic ECG signal. Event recording devices can be divided into loop and post-event recorders [22].

Loop

In loop recording approach, electrodes are in long-term continuous contact with patient's skin and the event signal storing and processing is triggered by patients or by embedded algorithm [24, 20, 22]. Some of these devices rely on patients to activate the recording of ECG signal when the symptoms happen. Other devices have automatic triggers that recognize slow, fast, or irregular heart rates.

Once activated, data are stored for a programmable fixed amount of time before the activation (looping memory) and a period of time after the activation.

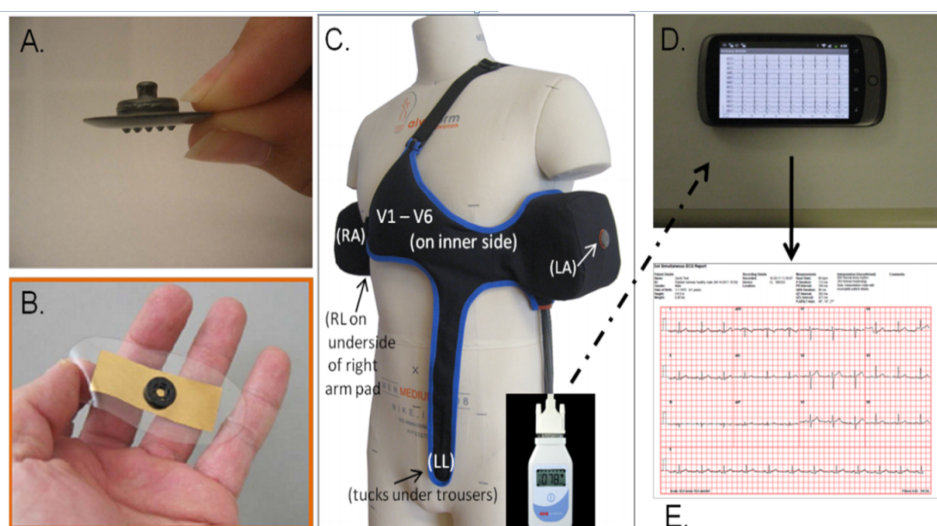


Figure2. 12 Recent 12 lead ECG harness developed by NASA used as ECG loop recorder. Orbital dry electrodes shown in A are embedded in special belt C. Signals are sent wirelessly via Bluetooth to the receiving smart phone D. Finally, a print out of 12 lead ECG is obtained. Image adapted from [28]

Over the last few years, there has been more interest in developing loop recorder. Different devices emerged to make the loop ECG event recording easier and wireless [26, 27] using wearable fashion such as belts (see Figure 2.12) and T-shirts. However, the quality of the recorded signals is still the major impediment facing the efforts to replace signals recorded with standard wet adhesive electrodes which are still the favored choice for long-term recording [29]. Self activated devices suffer from the false alarms because noise and artifacts which are very common in such devices. False alarms are usually misclassified as arrhythmia. On the other hand, wearable technology is prone to artifacts and noises more than the classic approaches of ECG signal recording. This also applies on the new recording approaches using capacitive electrodes.

Poor signal quality and, consequently, poor clinical acceptability are the main reason for imprecise delineation and misclassification of heart beats with artifacts. Moreover, the lack of signal quality makes the algorithm event-activated devices generate false alarms and store misleading intervals which increase the physician cost [22]

Post-event monitoring

The second type of event monitoring is the patient-activated post-event ECG recording where the device is not worn continuously, but applied and triggered by patients once symptoms develop [23, 30, 31]. Event ECG intervals are then recorded and transmitted directly to a data center where signals can be processed and analyzed by both algorithms and physicians.

The major advantage of these devices is that they are small and allow ECG recording for longer time periods because such devices are off most of the time and used only when symptoms develop (see Figure 2.13). They can also provide real-time data analysis when the patient transmits a recording in proximity to the symptomatic event [22].



Figure2. 13 Photograph of the patient-operated ECG system. Image adapted from [31]

2.6 ECG signal Applications

Medical uses for ECG information are varied and are generally related to having a need for knowledge of the structural or the functional changes of heart muscle. Some applications of ECG are:

- Diagnose certain group of heart disease (Ischemia , myocardial infarction, Conduction disorders, Pericarditis, Valvular heart disease, Enlarged heart, Electrolyte disturbances , Chest trauma, etc);
- diagnose certain group of artery and pulmonary diseases;
- obtain a baseline tracing of the heart's function;
- check the function of an implanted pacemaker;
- check the effectiveness of certain heart medications;
- Study the side effects of new medications on heart muscle.
- preoperative monitoring when any form of anesthesia is used;
- Check the heart's status after a myocardial infarction, or after a heart-related procedure such as a cardiac catheterization, heart surgery, electrophysiological studies, etc.
- Hypertrophic cardiomyopathy screening in adolescents as part of a sports physical out of concern for sudden cardiac death;

2.7 ECG signals Analysis pipeline

Figure 2.14 illustrates the three necessary steps in any ECG signal analysis software, regardless of the recording mode. First, the recorded signal should be preprocessed. Afterwards, a set of algorithms is applied on the preprocessed signal to delineate it and to extract features needed for the different analysis purposes.

Preprocessing of the ECG signal is essential for good analysis results due to the fact it affects all other subsequent steps in the signal. It includes several crucial steps in the general pipeline.

First, a calibration of the ECG signal amplitude should be done. Calibration is important to ensure that ECG waves are accurately measured and presented over the whole signal. The standard calibration of the ECG is 10mm/mV. Therefore, if the recording speed is adjusted at 50 mm/second, 1 miliVolt calibration signal is expected to produce a perfect square with a 10 mm height and 10mm width. Calibration pulses are generated and measured by the acquisition circuit and then used to calibrate the amplification gain periodically.

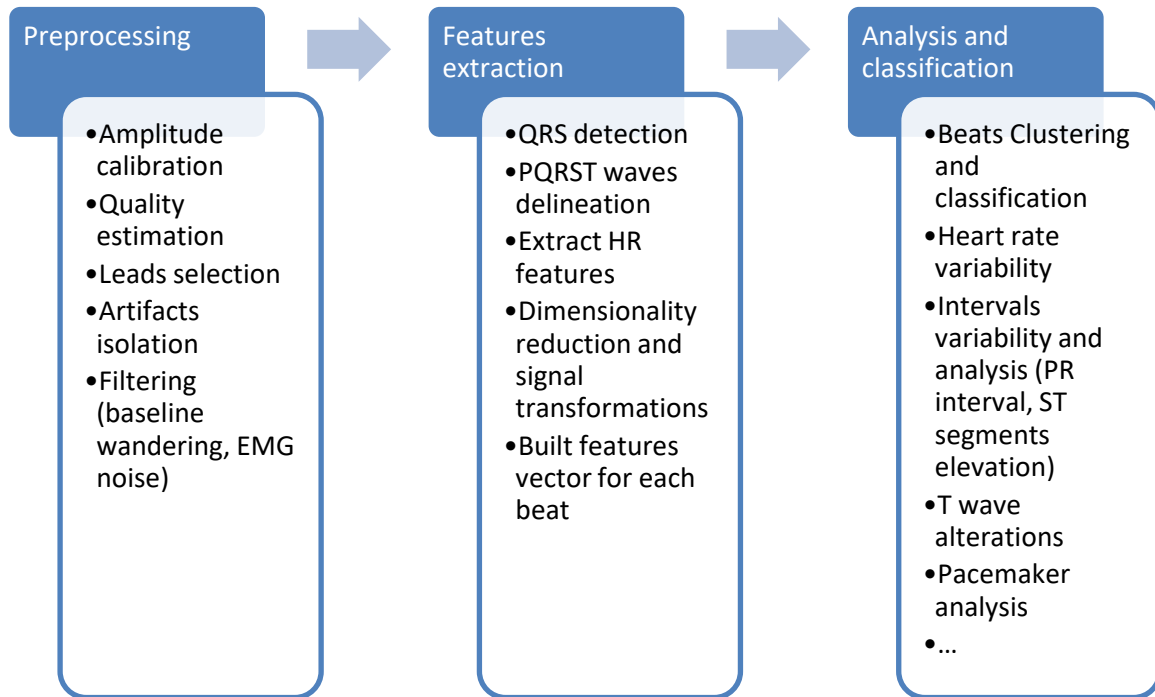


Figure 2.14 ECG signal analysis general pipeline.

Quality estimation and noise approximation is the next step in the preprocessing phase. Signal quality could be enhanced when it is possible or estimated to be used to determine the confidence of analysis results. Signal quality is measured as the presence of any non-cardiac contaminants in the ECG signal. This step is the subject of this thesis and it will be discussed in details in next sections.

A set of filtering algorithms should be applied on the ECG channels. Several kinds of noises and artifacts are present in the ECG signal; each of them should be processed in a different manner. For instance, baseline wandering removal is usually achieved using algorithms that find the low frequency component and then subtract it from the signal. On the other hand, high frequency and EMG noise are removed using special filtering approaches under some strict conditions defined in special standards [32]. Finally, motion artifacts should be detected and isolated if possible. This is essential to prevent such contamination from affecting negatively on the analysis results.

The next step after preprocessing is feature extraction. A lot of information could be extracted from the ECG signal and used for diagnosis. Generally, most information relies on ECG waves' intrabeat timings and amplitudes. When analyzing an ECG record, physicians focus on both the morphological and the timing changes of ECG waves over time. The process of extracting this information from the ECG signal is called delineation. It is worthy to mention that all analysis algorithms depend largely on the features provided to them. In

essence, the accuracy of features extraction has great impact on the number of false positives (false alarms). On the other hand, accuracy of features extraction depends on the signal quality.

Features extraction is not limited to the delineation of PQRST waves. Consequently, features' vectors are not limited to the timing intervals of these waves. Depending on the analysis algorithm used, other features could be required. For instance, analysis of atrial fibrillation requires heart Rate features to be extracted upon intervals of different lengths.

Besides delineation, dimensionality reduction and signal transformation algorithms could be used to find features vectors. For example, a lot of analysis algorithms depend on features extracted using transformation like the wavelet transformation. Another example is the Hermite functions usage to present QRS complexes [33]. In this case, each QRS complex is decomposed into Hermite bases functions taking advantage of the orthonormality of Hermite function bases. Therefore, resulting coefficients as well as heart rate based features are used to represent each complex. The formed feature vector is then fed to unsupervised self-organizing NN's to cluster QRS complexes in leads into a specific number of clusters.

Third and final phase after features extraction is the analysis phase. In this phase, a set of specialized algorithms step in. Several approaches could be found in the literature to analyze ECG signal. Algorithms vary depending on the purpose of the analysis results. Classification of the ECG beat, heart rate analysis, ST segment analysis, T wave alternans, signal-averaged ECG, late potential analysis, are usually performed depending on the diagnosis procedure followed by cardiologist.

2.8 Current challenges in the analysis pipeline

2.8.1 Variability among individuals

The signal morphology as well as its repeatability to the characteristic regions change over time and are dependent on each individual. Variability across individuals (patients) is the biggest obstacle of using globally extracted data sets to train supervised machine learning approaches to work on all individuals. This implies that in the analysis of ECG signals it is hard to rely on some global templates as such do not exist [3, 34].

The limitation associated with this is quite substantial, as we cannot consider typical methods of signal processing and classification where we often rely on the use of such templates. Therefore, there is always a need to add some locally extracted features to improve the accuracy of any supervised approach.

For instance, in exercise tests the muscle noise suppression is eliminated after averaging parts of the ECG signals including QRS complexes. Usually, physicians select a dominant beat pattern for the given patient. It is essential to exclude QRS complexes which are totally different from the dominant beat pattern from the averaging process. However, automatic averaging algorithms have to exhibit some abilities of unsupervised learning given the fact that such a dominant shape cannot be determined in advance in automatic analysis.

If we consider a shape of the ECG signal present in a certain lead within the population of healthy individuals, there will be differences among these signals (see Figure 2.15). A similar situation will be encountered in case of patients with some heart problems. This was the motivation to develop methods to use the ECG signal to identify individuals taking advantage from the unique expression of cardiac features among individuals [35].

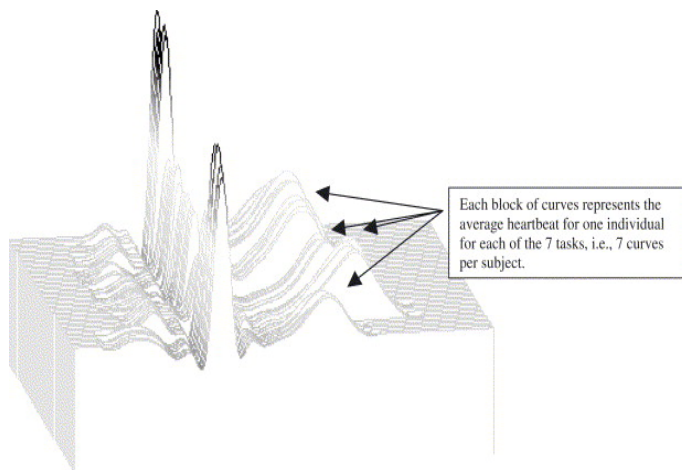


Figure 2.15 Heartbeats averaged by subject. Image adapted from [35]

2.8.2 ECG signal are non-stationarity

Variability across time is the second challenge when dealing with ECG automatic analysis. The transitions between rhythms are a non-stationary process. Non-stationarity includes, the morphological properties of heart beats, Intrabeat basis: RR intervals. Thus, there is also probability for abnormal changes in beat morphology or rhythm. The etiology of these changes is often intricately connected [3, 34].

The dynamics of ECG signal's waves morphological changes could not be predicted. Some papers consider some periodicity [36] in the signal to apply some algorithms, this assumption is not correct, though. Figure 2.16 shows one intervals of ECG signals with arrhythmias which explain this property.

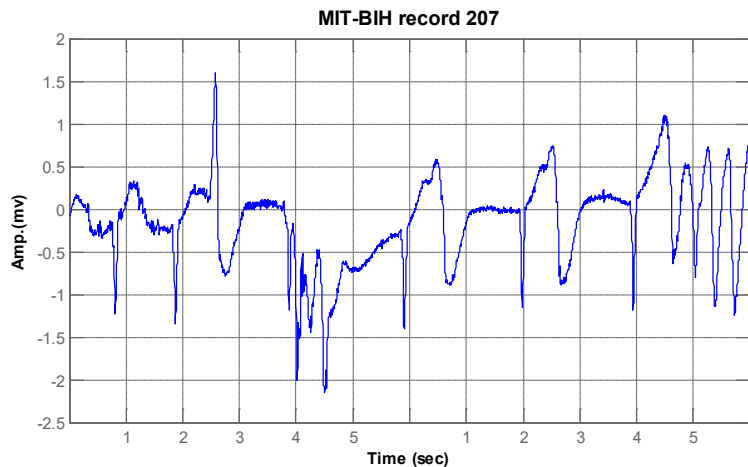


Figure2. 16 shows ECG interval with arrhythmias from the first channel of MIT-BIH record 207. Changes in the morphology and heart rate have a non-stationary nature.

2.8.3 Noise susceptibility

Unfortunately, noise is omnipresent and its presence in the ECG signal is inevitable. Noise is definitely the biggest obstacle facing efforts to automate the whole process from the ECG signal recording to the providing of a feedback from analysis results [39]. Unlike in other stationary signals, noise presence in the ECG signals is hard to be separated from the input signal. Thus, it has a huge and adverse effect on the interpretation potentials of ECG signal. Therefore, noise reduction and isolation is extremely important to elevate the diagnostic value of ECG signals. For example, it is essential to have a clean signal when physicians study the alternans - a subtle beat-to-beat change in the repeating pattern of an electrocardiogram (ECG) waveform that can be indicative of electrical instability of the heart and increased susceptibility to sudden cardiac death. In order to analyze such subtle changes in the waveforms, a clean signal is required [34].

Unfortunately, noises that affect the ECG signal could be within the frequency band of the signal most important waves. Furthermore, noise can manifest with similar morphologies as these waves [1].

Several noises contaminate the ECG signal. They can be categorized according to the noise source during the recording process [1]. Each noise category has its own characteristics and properties. Consequently, each category should be addressed using customized algorithms built especially to deal with it. It is relatively easier to deal with noises that originate from the stationary sources such as power line interference or those with low correlation with the ECG signal characteristics such as baseline wandering. These kinds are less problematic than those with high correlation or overlapping with the ECG signal characteristics such as motion

artifacts or EMG noise. In the next chapter, the most damaging and frequent noise classes are presented in further details.

Chapter 3

3. Noise Sources and Measurement in the ECG signals

In this chapter, noise which is the main topic of this thesis is discussed in details. First of all, the most damaging and frequent noise sources that contaminate the electrocardiography are explained and categorized according to their characteristics. Afterwards, concise discussion about noise properties in the ECG is presented. Both the signal's and noise's spectrums are analyzed. Moreover, the spectrums of some arrhythmias are also presented in order to pave the way for the detailed review of noise level estimation methods.

Hence, the problem of noise level or equivalently signal quality estimation is studied in details in this chapter. Firstly, noise level estimation issue in the ECG signal is defined. Noise level estimation and noise level approximation are correlated approaches; both are intended to address the problem of signal quality estimation vs. noise and artifacts by computing a noise level measure in.

It is important to understand the current approaches addressed in literature related to the above mentioned problem. Therefore, a review of the most important methods used for noise level estimation and approximation in the ECG signals is included. The presented review encompasses methods used for signal quality, noise level, and noise free signal estimation which are only different methodologies/ terminologies used when this issue is addressed.

The presented review is aimed to pave the way for introducing the concept of noise level approximation over time which is one of the claimed contributions in this thesis and the main them of chapter 3.

3.1 Noise And Artifacts Sources

3.1.1 Motion Artifacts

These artifacts are caused by the electrodes movement away from the contact area with the skin. These artifacts are sometimes considered the most difficult contaminants to deal with. This is due to the fact that there is no way to anticipate neither the morphology nor the frequency of these artifacts (see Figure 3.1). Indeed, motion artifacts' nature tends to be different from the classic defined noise's nature. Thus, special approaches should be employed to solve the problem of motion artifacts presence in the ECG signal. Generally, the detection and isolation of corrupted intervals with motion artifacts is more adequate strategy than filtering because their presence damages the ECG signal properties. Nonlinear methods, generally machine learning based methods, are applied for this purpose.

In an attempt to reduce the negative impact on interpretation results caused by motion artifacts, new ECG devices include hardware solution to this kind of artifacts. Lead off detection circuits are added to detect the situation when some lead detaches due to loose contact [37]. Moreover, some devices provide secondary signals correlated with the patients' motions and movements or electrode-skin properties. These secondary signals are then used in the detection and isolation of motion artifacts by determining the relationship between the noise content of the primary ECG signal and noise content of the secondary input signal; and combining the primary input signal and the secondary input signal in consideration of the determined relationship to produce a noise-reduced result [38].

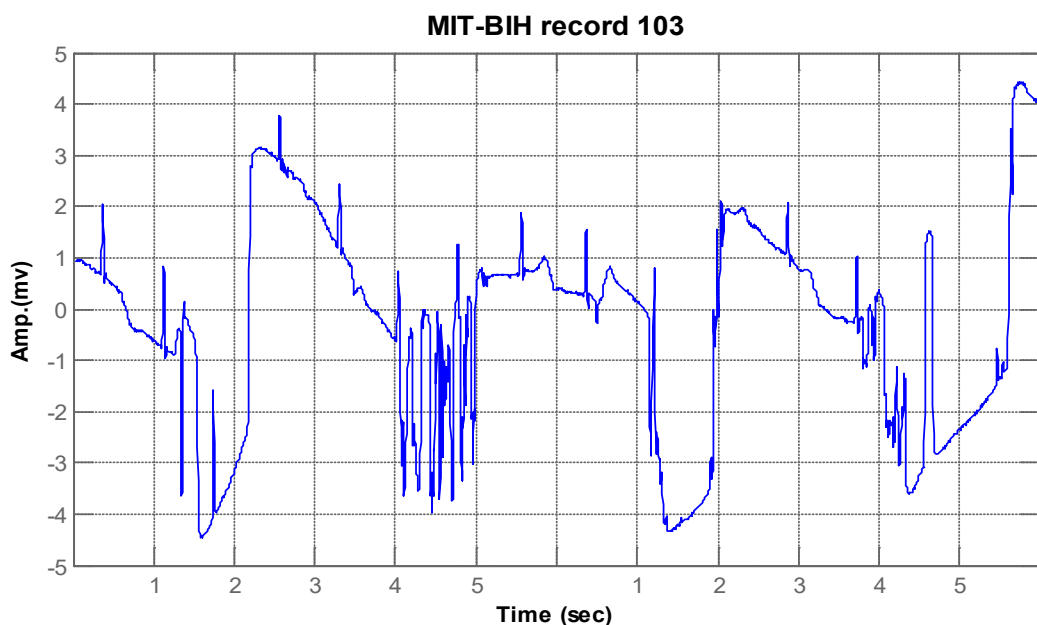


Figure 3.1 ECG signal from MIT-BIH record 103 shows motion artifacts contaminating the signal.

3.1.2 Baseline Wandering

Baseline wandering is slow-varying distortions. It is mainly caused by changing of the body-electrode impedance which is reflected in the form of low frequency component added to the signal. Impedance changes are caused by patients' respiratory movements or any other smooth movements that affect the electrode-skin contact (see Figure 3.2).

Several methodologies are presented in the literature to solve this issue. The most important point that should be taken into consideration when filtering low frequency noise is the distortion of low frequency segments in the ECG signal especially the ST segment or even the T wave offset. Linear methods (FIR and IIR filtering) are usually used but also a nonlinear (the empirical mode decomposition [39], Polynomial Fitting [40]). Wavelet transform-based methods (linear and non-linear [40]) were also proposed to solve this issue.

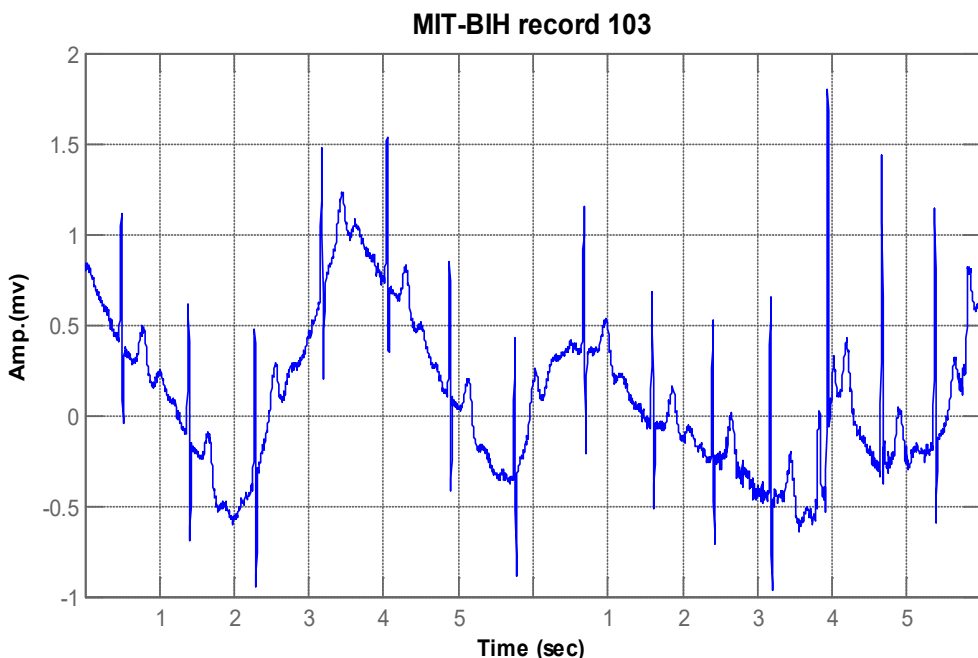


Figure 3.2 Baseline wandering from MIT-BIH record 103.

3.1.3 Power Line Interference

The power line interference is a usual disturbance that could ruin the visual diagnostic potential of the whole signal. As the name shows, this kind of noise is originated from the power line electromagnetic field. Depending on the utility electrical network frequency used, the nominal frequency of the alternating current overlap with recorded ECG signal through capacitive and inductive coupling [34].

Capacitive coupling refers to the transfer of energy between two circuits by means of a coupling capacitance present between the two circuits. The coupling capacitance value decreases with increasing separation of the circuits and vice versa. Inductive coupling on the other hand is caused by mutual inductance between two conductors. Magnetic flux is produced when the current flows through wires. This induces a current in the adjacent circuits causing the addition of frequency component to the current in the affected circuit.

In the frequency domain of the ECG signal, power line interference manifests in a peak in (50 or 60) ± 0.2 Hz. Unlike other noise sources, the nature of this noise is stationary in terms of its frequency (see Figure 3.3) in the affected intervals. However, the appearance of these contaminants is unpredictable in terms of its onset, offset, length, and power in the affected interval.

Although it looks easy to remove from the ECG signal, it is still an important challenge to provide a method that minimize the distortion and suppress the interference noise in the affected intervals only. Several approaches were introduced to treat this noise type. The renowned notch filtering, such as filter proposed in [41], are the most used ones.

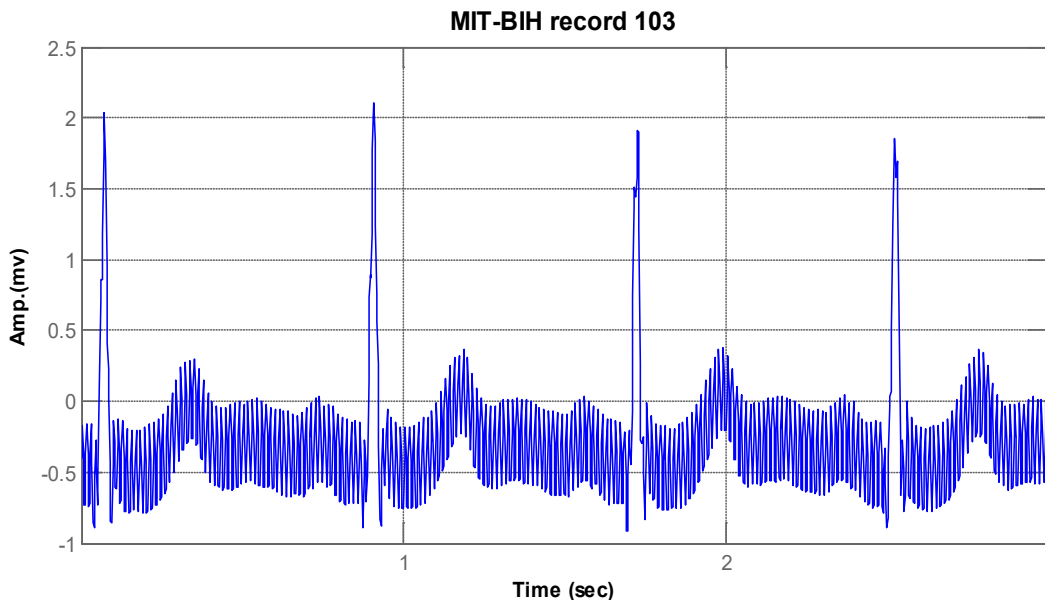


Figure 3.3 Power line interference added to ECG signal. Nominal frequency is 50 Hz in this case.

3.1.4 EMG Noise

The electromyography signal is produced by the skeletal muscles contractions (see Figure 3.4). The recorded electrical activity is generated by the muscle cells when these cells are electrically activated. Because of these muscles are in the vicinity of cardiac muscle it is expected to catch the EMG signal while recording ECG signal [37].

Because, ECG and EMG signals share the frequency spectrum with significant energy of both, it is inevitable to have the EMG noise overlapped with the ECG signal while recording of the heart electrical activity.

The amplitude of EMG signal is stochastic (random). However, the amplitude distribution of this kind of noise could be reasonably approximated by a Gaussian function. It can range from 0-100 mV. On the other hand, the amplitude of ECG signal ranges from 0.1-5 mV [42]. This means that ECG signal could be completely obscured by the EMG noise.

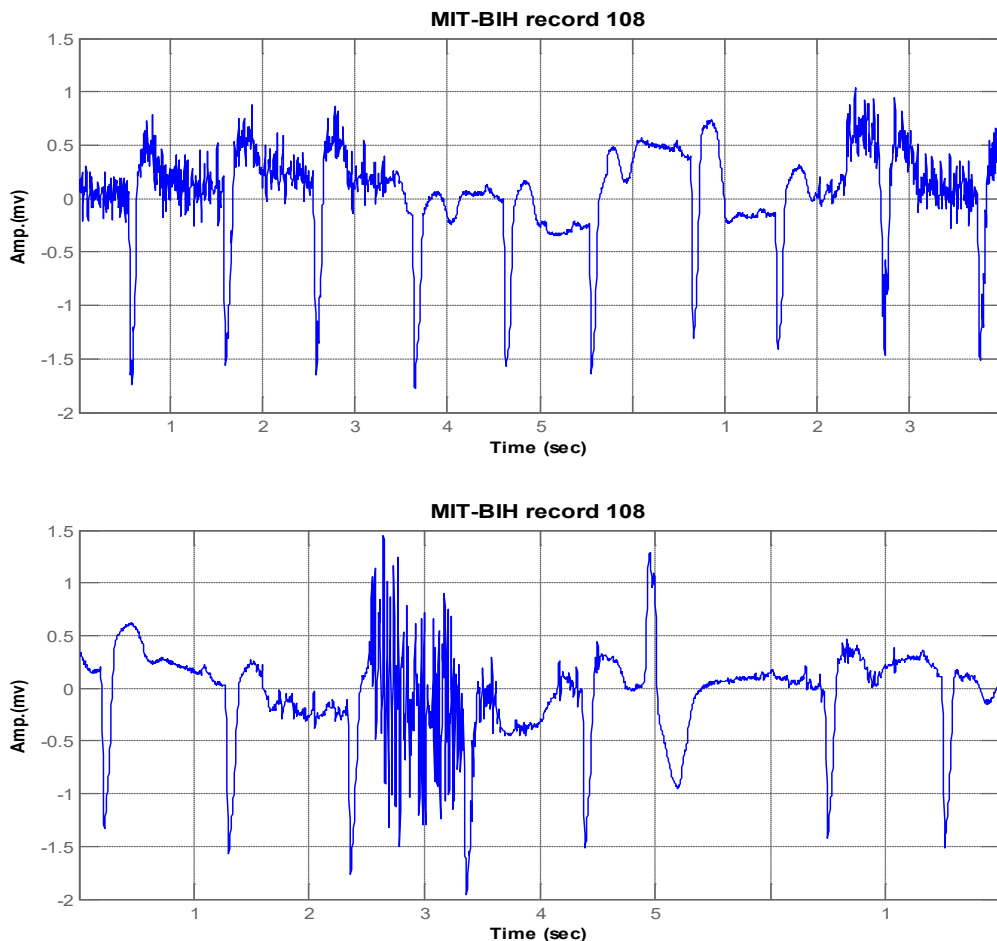


Figure 3. 4 Two different intervals corrupted by EMG noise from the origin. Intervals are form the MIT-BIH record 108.

Nevertheless, because of the different time-scale characteristics of both signals, it is possible to separate them using an appropriate time-scale transformation. These characteristics manifest relatively clearly using a multi-resolutonal approach such as the stationary wavelet transform as it will be discussed later in Chapter 4.

Generally, the QRS complex could be found and delineated after a separation of EMG noise from the ECG signal. This means that an interpreter can deduce the heart rate. Unfortunately, such separation is usually done at the expense of late potential and other ECG signal waves including the QRS complex itself. Nevertheless, sometimes it is still worthy to conclude the heart rate as such information could be used to analyze heart rate variability. So, a filtering algorithm is essential in order to get better performance of delineation algorithms and to extract representative features that can be passed to the analysis algorithms.

The fact that EMG noise is non-stationary in terms of its presence and properties (see Figure 3.4) limits the usage of linear filtering methods such as standard FIR or IIR filters [43].

Finally, this noise type is main noise type addressed in this thesis. Thus, its properties as well as filtering techniques used will be discussed in details in the subsequent chapters.

3.1.5 Electrode Popup Or Contact Noise

Similar to motion artifacts, this kind of noise is caused by the changes in the propagation medium between the heart and the electrodes. Sudden changes in the skin-electrode impedance induce sharp transients in signal baseline which decay exponentially to the baseline value [3]. Sometimes these changes occur rapidly several times in succession. They cause sudden changes in the amplitude of the ECG signal as well as low frequency baseline shifts.

3.1.6 Other Noise Sources

Other noise sources affect the ECG signal such as the instrumentation noise which is noise originated in the data collecting device. This noise refers to any kind of noise caused by the electrical equipments that are used in the recording. This may include Electrode probes, cables, signal processor/amplifier, and the Analog-to-Digital converters. Nowadays, this kind of noise could be significantly reduced in ECG devices by using higher quality chips, shielding, and the careful circuit design [37, 34].

Another noise source that affects the ECG signal is the electronic noise which is a specific kind of the instrumentation noise. This kind of noise is sometimes referred to as flicker noise or pink noise. Its power spectral density is inversely proportional to the frequency of the

signal. Flicker noise overlaps in the frequency domain with EMG noise. Therefore, filtering the EMG noise leads to the reduction of this kind of noise too. Pink noise is used in the literature to simulate this kind of noise presence in the ECG signal as well as to evaluate EMG noise filtering techniques [43].

There are also other sources of noises that could be caused by the quantization process or by the later signal processing algorithms. Dealing with these noises is usually preventive because it is possible to avoid them when special attention is paid while developing the algorithms or designing the ECG device hardware.

3.2 The Main Properties Of Noise In The ECG Signals

This section is devoted to address the properties of high frequency noise in the ECG signal. High frequency noise encompasses EMG noise as well as other noises that overlap with the EMG noise in their spectra. Other noises may share some of these characteristics, though.

3.2.1 Non-stationarity

As previously mentioned, non-stationarity in the ECG manifests both in an interbeat timing basis (as RR interval timing changes) and on an intrabeat shape basis (as morphological changes) [3]. Non-stationarity also applies for noises that corrupt the ECG signal such as EMG, motion artifacts, and baseline wandering (see Figure 3.4, Figure 3.2, and Figure 3.1). These noises are also of non-stationary nature, transient, and time-varying phenomena. So, the noise presence and ratio to the signal are variable and hard to be anticipated over time [3, 34]. Therefore, adaptive techniques are required to deal with these noises, because such techniques allow the detection of time varying noise characteristics and dynamic variations.

3.2.2 Spectral Overlapping With Arrhythmias

The accepted range of the diagnostic ECG is from 0.05Hz to 100 Hz [34]. However, for some applications such as the diagnosis of acute myocardial ischemia or late potentials analysis high frequency ECG is required especially for the analysis of ST segments as information exist beyond these limits [44, 45]. Unfortunately, noise spectra that contaminate the ECG signal extends over the whole spectra of the recorded signal [2] (see Figure 3.5). Generally, EMG noise and other high frequency noises overlap with the high frequency components of the normal ECG signals such as Q, S, and R peaks/valleys. Moreover, the morphological and frequency changes of some arrhythmias tend to be fast and unpredictable.

The energy of ECG signals containing rhythms such as ventricular and atrial fibrillation, flutters, and tachycardia is distributed over the spectrum (see Figure 3.6). Therefore, spectral separation of noise and ECG rhythms is difficult. Due to this overlapping linear filtering techniques are unsuitable [45].

On the other hand, special attention should be paid, when filtering is done using non-linear adaptive techniques, in order to prevent filtering from damaging the fine characteristics in the ECG signal in the intervals where arrhythmia is present.

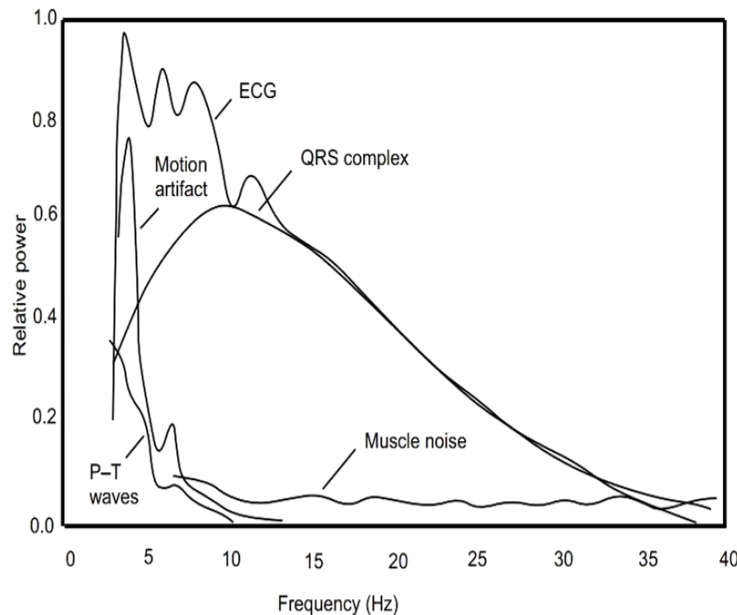


Figure 3.5 Relative power spectra of QRS complex, P and T waves, muscle noise and motion artifacts. Image adapted from [2]

3.2.3 Noise Coloration

Noise color has a great impact on the way it corrupts the signal because different noise colors have significantly different properties. There are different ways of generating colored noise [46, 47], and realistic ECG artifacts. One method is to rely on the slope of the power spectrum of the signal β . Thus, noise color is defined as

$$S(f) \propto \frac{1}{f^\beta}, \quad (3.1)$$

where β is the density slope. White noise is generated using ($\beta = 0$), pink noise or flicker noise using ($\beta = 1$), and the random walk noise or brown noise using ($\beta = 2$). Colored noise is usually generated by passing white noise through a filter with a rational transfer function.

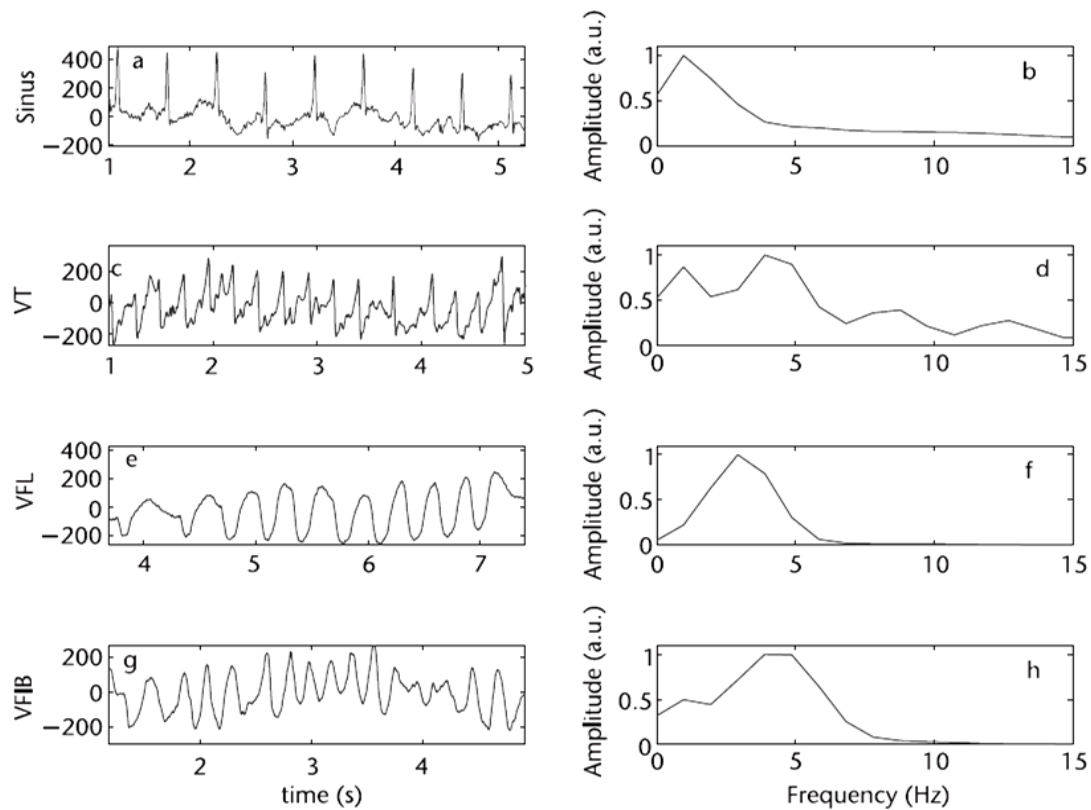


Figure 3.6 Several ECG rhythms on left side and the corresponding PSD for them on the right side. From top to bottom, Sinus rhythm, Ventricular Tachycardia, Ventricular flutter, and Ventricular fibrillation. It is clear how arrhythmias impact the spectrum of the ECG signal over time and how it is possible to occupy the whole spectrum of the recorded signal. Image adapted from [3]

Except the power line interference, there is no specific noise color for other noise sources. Noise coloration is determined by the power spectral density characteristics. Therefore, for the same noise type, coloration is variable. Due to this variability and non-stationarity in noise coloration, simple noise measurement methods suffer from the lack of adaptability to noise coloration. For instance, signal-to-noise ratio (SNR) for a brown noise contaminated ECG equates to a much cleaner ECG than the same SNR for an ECG contaminated by pink noise [3]. Figure 3.7 illustrates this.

So, the coloration of the noise can significantly affect the signal visual appearance. Sometimes, noise associated with high SNR value could be more damaging than noise with low SNR value. Consequently, ECG analysis algorithms could perform differently depending on the noise coloration, and therefore it is important to take the coloration of the noise in the signal as well as the SNR into consideration when developing algorithms to deal with noise in the ECG signals.

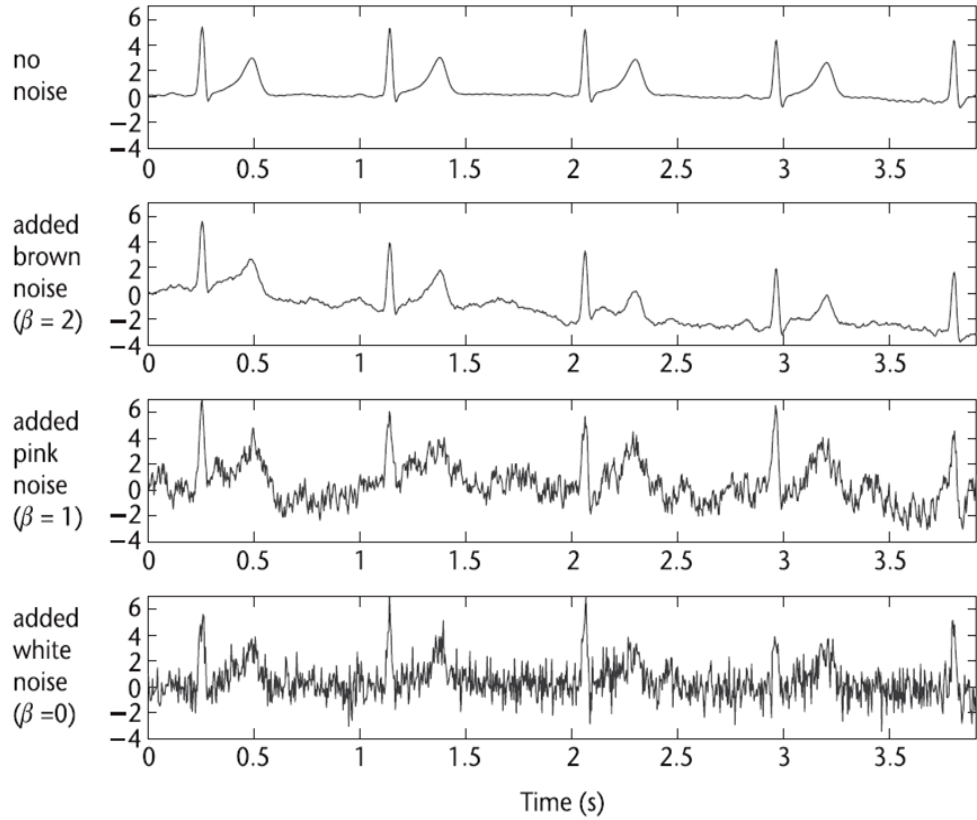


Figure 3.7 comparing a zero-mean unit-variance clean ECG (upper plot) with the same signal with additive noise of decreasing coloration (lower autocorrelation). In each case, the noise is set to be zero-mean with unit variance, and therefore has the same power as the ECG ($\text{SNR} = 1$). It is obvious that the whiter the noise, the more significant the distortion for a given SNR. Image adapted from [3]

3.3 Measuring Noise In The ECG Signal

Noise in general and EMG noise in particular are shown to be consisted of chaotic processes [48]. It is impossible to accurately predict its dynamics or characteristics over time. There are methods to estimate the noise level over time or equivalently to estimate signal quality vs. noise. However, noise estimation is not straightforward task especially in the ECG signal. This is partially due to the deceptive noise properties and partially due to the ECG signal subtle and fine characteristics that tend to overlap with noise over the whole ECG diagnostic spectra [1].

Noise diverse coloration over time and non-stationarity in terms of onset offset and strength reduce the usability of classical noise measuring methods that deal with noise on whole without taking these changing characteristics and dynamics.

On the other hand, the ECG signal is non-stationary. Thus, it is hard to anticipate its dynamics and characteristics over time. As a result, noise measuring using the residue after signal estimation is also limited, especially when arrhythmias are present.

Several methods for ECG signal quality estimation are presented in literature. Some of them are designed to work for all types of noises, while others are designed specifically for EMG noise detection and estimation. Some methods were not originally built to work with the ECG signal; however they were adapted and customized to be deployed for noise level estimation in the Electrocardiograph.

In this chapter, a review of the most important methods used to estimate noise is presented. Some methods that were originally introduced to deal with signal quality on whole are also included because signal quality is mainly related to noise presence in the signal.

Because of the diversity of noise sources, and consequent diversity of their characteristics, more accurate approximation could be obtained when addressing each of these noise sources separately. This however is not the case in all presented methods. Anyway, the included methods could be all used to deal with the EMG noise. As mentioned above, noise in this context will be limited to EMG and high frequency noises that overlap with it.

3.4 Review Of Noise Level Estimation/Approximation Methods

3.4.1 Route Mean Square (RMS) Power In The Isoelectric Region

This method rely on the assumption that signal in the isoelectric region should be flat with low amplitude variation. Consequently, Route mean square (RMS) based method provides a measure of the signal distortion by measuring the power of noise or non-signal variations. Ideally, isoelectric regions in the ECG signal should be associated with zero amplitude after the removal of baseline wandering. This means that the ideal quadratic mean or RMS value should be also zero when calculated in this region. Thus, low RMS values denote to high signal to noise ratio.

However, isoelectric region should be found firstly. Isoelectric line estimation includes filtering the baseline wandering from the ECG signal. Moreover, it depends largely on the precise fiducial point detection in each heartbeat which is a prerequisite for the automatic identification of the isoelectric levels [49]. This is troublesome especially when noise is present.

The formula used to compute RMS value is

$$x_{rms} = \sqrt{\frac{1}{n}(x_1^2 + x_2^2 + \dots + x_{n-1}^2 + x_n^2)}, \quad (3.2)$$

where x_1, x_2, \dots, x_n are the amplitude values of the signal samples in the isoelectric region.

Finally, this method is general and cannot be used to estimate one specific type of noise or to define the noise color. Rather, it is prone to shifts especially in the presence of notches or motion artifacts that could impact small interval but with high amplitude values. Hence, it is not suitable to study noise in non-stationary random signals and noises such as the case of the Electrocardiograph signals [37]. Generally speaking noise-power is the computed parameter but without considering the stationarity in the dynamics and coloration of the noise or of the signal.

3.4.2 WWD

The distortion of the electrocardiogram (ECG) signal is measured after comparing the distortion between original signal and the reconstructed signal from compression coefficients [50]. Unlike the Percentage Root Mean Square Difference (PRD) which is used to evaluate ECG compression algorithms, the Weighted Diagnostic Distortion (WDD) focuses on the most important diagnostic features only.

The PRD measure is given as

$$PRD = \sqrt{\frac{\sum_{n=1}^N (x(n) - \tilde{x}(n))^2}{\sum_{n=1}^N (x(n))^2}} \times 100 \quad (3.3)$$

where x is the original signal, \tilde{x} is the reconstructed signal after compression, and \bar{x} is the signal's mean.

On the other hand, the WDD method takes the relevant diagnostic information present in the ECG signal into consideration when the measure is computed (see Figure 3.8.). This information exists in the PQRST waves and denotes to the morphology, amplitude, onset, offset and duration. So, the first step must be the utilization of specialized algorithms for delineation in order to delineate these waves. Afterwards, features vectors are formed for both the original and the reconstructed signals as the following

$$\begin{aligned} \beta^T &= [\beta_1, \beta_2, \dots, \beta_p] \\ \hat{\beta}^T &= [\hat{\beta}_1, \hat{\beta}_2, \dots, \hat{\beta}_p], \end{aligned} \quad (3.4)$$

where P is the number of features in the formed vectors, β is the features vector for the original signal, and $\hat{\beta}$ is the features vector for the reconstructed signal.

Table 3.1 Shows features used to build the features vector which is then used to assess signal quality using statistical study.

Feature symbol	Description	Unites
RR _{int}	The time between two successive R peaks	Ms
QRS _{dur}	From Q onset to S offset	Ms
QT _{int}	Interval from QRS onset to T offset	Ms
QTP _{int}	From QRS onset to T peak	Ms
P _{dur}	P wave duration	Ms
PR _{int}	From P onset to R offset	Ms
QRS _{peaks}	Peaks/valleys total number in QRS complex	>=1
QRS _{sign}	The sign of first peak in QRS complex	1 or -1
Δ _{wave}	The existence of Δ wave	0 or 1
T _{shape}	The shape of T wave encoded in integer	
ST _{shape}	The shape of ST segment encoded in integer	
QRS _{amp} ⁺	Minimum positive amplitude of QRS complex	
QRS _{amp} ⁻	Minimum negative amplitude of QRS complex	
P _{amp}	P wave amplitude	Mm
T _{amp}	T wave amplitude	Mm
ST _{elev}	The ST elevation	Mm
ST _{slope}	ST slope	mm/sec

Table 3.1 describes the diagnostic features used in this method. The WDD is found after the computation of normalized difference between these vectors after the multiplication with a diagonal matrix of weights Λ defined in [50]. This could be written like so,

$$WDD(\beta, \hat{\beta}) = \Delta\beta^T \frac{\Lambda}{tr[\Lambda]} \cdot \Delta\beta \times 100 , \quad (3.5)$$

where $\Delta\beta^T$ is the normalized difference vector and it is given as

$$\Delta\beta^T = [\Delta\beta_1, \Delta\beta_2, \dots, \Delta\beta_p]. \quad (3.6)$$

The evaluation of this method was conducted using expert-based approach where three independent expert cardiologists, who studied the reconstructed ECG signals in a blind and a semi-blind tests. Results are reported in [50] and show good correlation with experts' opinions about the diagnostic features of the evaluated signals.

The main disadvantage of this method is the fact that it is expensive to calculate. Furthermore, it requires the detection of the main diagnostic features which is in turn a great drawback taking into account the difficulty of these detection especially onsets and offsets of ECG waves in the presence of noise. Finally, time resolution is not considered, so it cannot be used to estimate quality over time. It is intended for assessment of ECG excerpts with several ECG beats.

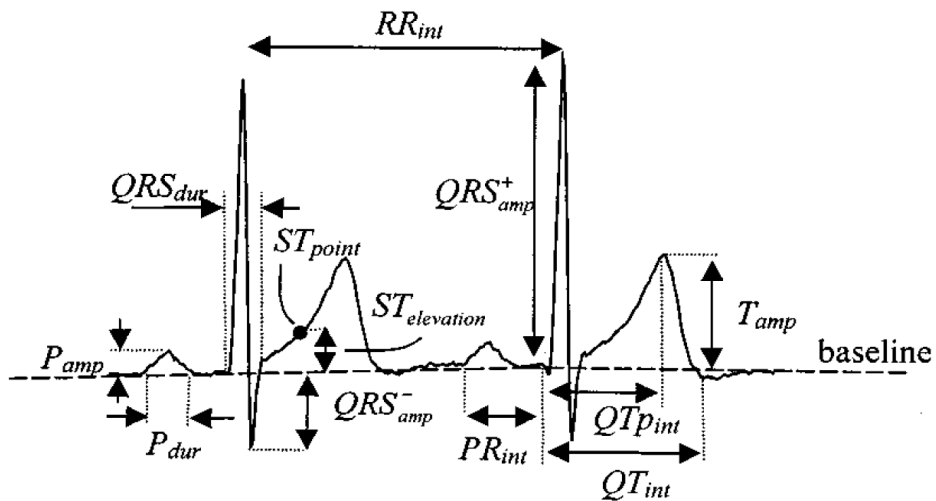


Figure 3.8 Some of the amplitude and duration features used in WWD algorithm. Image adapted from[50]

3.4.3 RMSSD-R and SD-R:

These two measures were presented in [51]. Authors propose these measures to assess the quality of digital electrocardiogram recordings. Firstly they calculated the average QRS-T complexes from all beats with normal morphology in recordings of 10 seconds. Then, they calculated the residuum after subtracting each beat's QRS-T from the average QRS-T. This residuum is introduced as the noise level expression and further computation is done on it. The standard deviation of the residuum (SD) and the root mean square of successive differences (RMSSD) are calculated are calculated over the whole 10-second recording. Formulas for these calculation are given like so

$$SD - R = STD(x) \quad (3.7)$$

$$RMSSD - R = \sqrt{Exp(Dx^2)} , \quad (3.8)$$

where x is the residuum signal and Dx is the successive differences computed from the residuum.

The SD-R is mostly influenced by the overall magnitude of the residuum, thus it predominantly measures the respiration related noise and the slow baseline wander. On the other hand, the root mean square of successive differences RMSSD-R reflects the EMG noise and other high frequency noises present in the signal. The limitation of this algorithm is its dependence on normal QRS-T waves' morphologies without extrasystoles, so it cannot be applied on abnormal ECG recordings. This limits the usability of this signal quality assessment method.

3.4.4 Activity

Several measures could be grouped under the study of signal activity. Activity refers to the measure of waveform complexity of variability over time. Activity study is originally proposed to analyze the extent of variability in signals such as PCG and EMG [37].

Variance of the signal is one of the measures that could be used as simple and fast expression of the activity in ECG signals, especially when high frequency and EMG noised are the target noise group [52]. Variance is simply given as

$$\sigma_x^2 = E[(x - \mu_x)^2] \quad (3.9)$$

Variance measures the variability in ECG signal and when the signal has zero mean its square root is equivalent to the RMS value. In ECG signals, this is the case in the ideal isoelectric line.

Another important indication of the activity or variability in ECG signals is the number of zero-crossings within a specified interval. The zero-crossing rate (ZCR) increases as the high-frequency content of the signal increases [53, 54, 37]. In the case of ECG signal, ZCR is suitable to measure EMG and high frequency noises due to the fact that ECG signal show low ZC rates comparing to these noises.

ZCR is used as suitable approximation of noise levels in an ECG recording after counting of the number of times the signal change its amplitude from positive to negative value and then the counted value should be normalized by dividing by the number of samples in the signal segment under study.

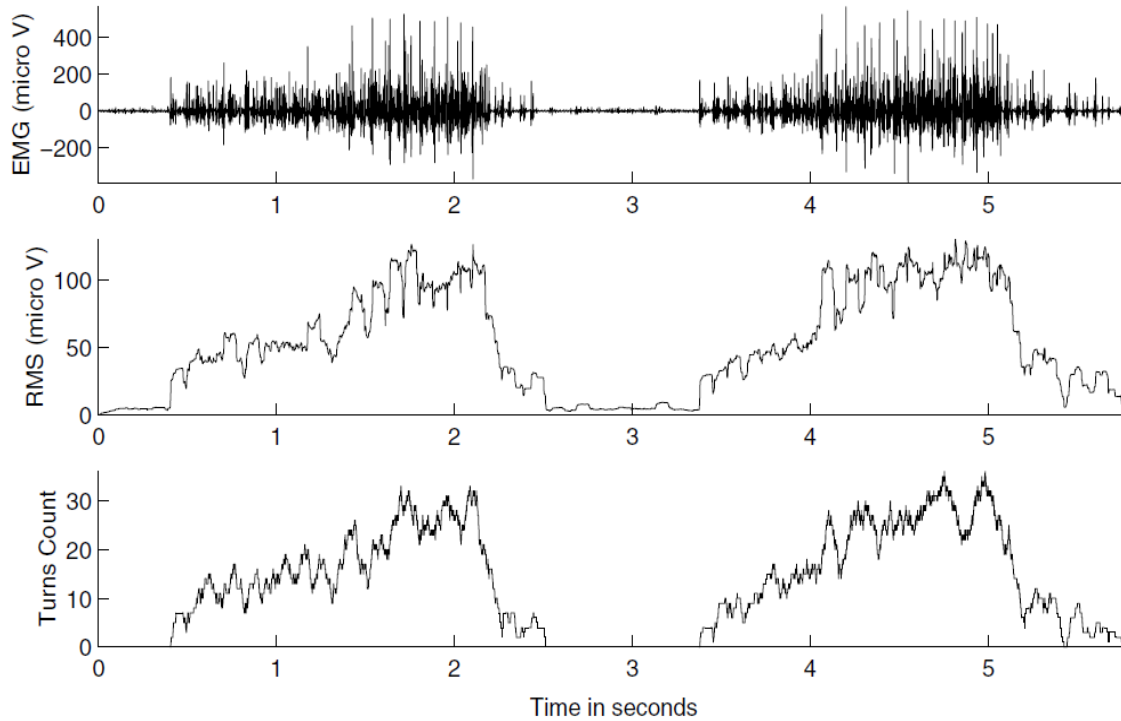


Figure 3.9 Short-time RMS values; turns count using Willison's procedure. Both signals were computed using a causal moving window of 70 ms duration. Image adapted from [37]

As mentioned above, this method is not intended to work for low frequency noise. Thus, in order to reduce the negative impact of baseline wandering on the results of this approach, it is preferred to count zero-crossing in the derivative of the signal instead of using the signal itself.

Finally, Wilson in [55] proposed a method called Turns counts (TC) which is applied directly on EMG signals. It is also a measure of the activity originally proposed to study EMG signals. In this method, the number of local minimums with amplitude higher than a threshold is counted. The threshold was defined as 0.1mV. The threshold was selected carefully in order to avoid counting insignificant fluctuations due to neglected high frequency noise. The method is expected to be robust in the presence of noise due to the threshold imposed.

Figure 3.9 shows two signals extracted from the EMG signal to study its activity. Both could be used to approximate noise in the ECG signals. However, the first one represents the energy of sharp variation while the other reflects the speed at which these sharp changes occur. Using these two methods together, is more accurate approach than using one of them only.

3.4.5 PCA

The well-known Principal component analysis method is an orthogonal linear transformation that transforms the data set of observation from its original coordinate system to a new one in which the observations are represented by a set of orthogonal bases. The transform is given as the following

$$C = \frac{X^T X}{n-1}, \quad (3.10)$$

where C is the covariance matrix which is a symmetric matrix and hence it can be diagonalized like so

$$C = V\lambda V^T, \quad (3.11)$$

where V is the matrix of eigenvectors or principal components, and λ is the matrix of eigenvalues. Eigenvalues could be arranged in descending order. The smaller the eigenvalues are, the less energy along the corresponding eigenvector there is. Therefore, the smallest eigenvalues are often considered to be associated with the noise in the signal.

Principal component analysis is largely used to separate the non-signal components from the ECG signal without using any spectral analysis of the signal. Moody et al. [56, 57] have shown that the QRS complexes can be encoded in the first five principal components (PCs). Singular value decomposition, or SVD, is the most commonly used technique by which the PCA is conducted to compress multi-dimensional signals such as the ECG signal. Consider X as $N \times M$ matrix of the signal observation; in this case each row represents one beat centered in the R peak of the QRS complex. N is the number of samples used to represent the beat which depends on the sampling frequency as well as on the time interval around R peak employed for the transform. M is the total number of beats used in the transform. The signal observations X could be written as

$$X = USV^T \quad (3.12)$$

$$XV=USV^T V=US, \quad (3.13)$$

where XV are called the principal components of the signal, S is $N \times M$ non-square matrix with zero elements everywhere, except on the leading diagonal with elements arranged in descending order of magnitude. Each element is equal to root square of the computer eigenvalues.

The data set could be reconstructed by choosing only those eigenvalues associated with much of the energy along the eigenvectors. As a result, the dimensionality is reduced from $N \times M$ to $M \times P$ where P is the number of left principal components. This could be written as

$$X_p V_p = U_p S_p \quad (3.14)$$

Using the left principal components, QRS complexes could be rebuilt as in

$$X_p = U_p S_p V_p^T \quad (3.15)$$

The residue resulted by subtracting the original data and the new bases X_p could be used as noise assessment in the ECG signal. Figure 3.10 and Figure 3.11 show how this method is applied on an ECG signal and illustrates several aspects of using it for ECG signal quality estimation.

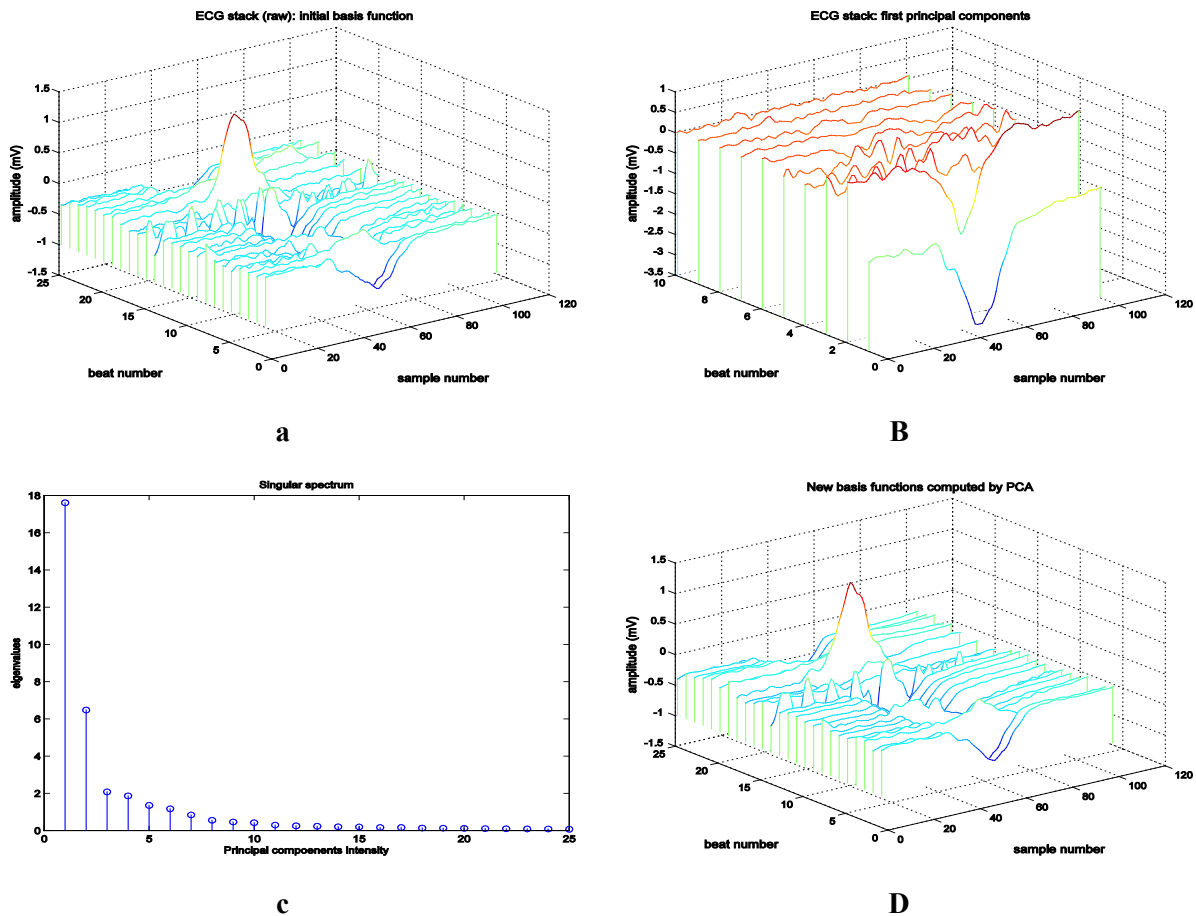


Figure 3.10 SVD of 25 QRS complexes: (a) Stacked QRS complexes from MIT-BIH record 108, (b) Stack of first 10 principal components after applying PCA on the QRS complexes array, (c) Stem representation of singular spectrum shows how eigenvalues magnitude associated with principal components decreases, (d) reconstruction of the new bases using only the first 5 principal components.

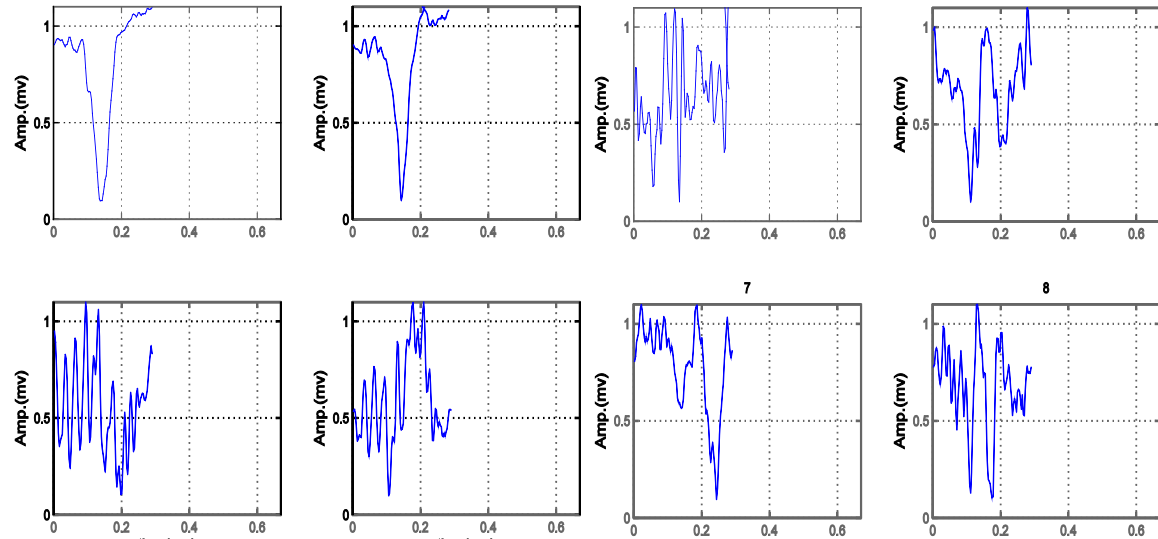


Figure 3.11 Left figure is for the first four principal components. Right, is for the bases 5-8; we can notice how correlation with the non-signal component in the original signal increases as eigenvalues decreases.

3.4.6 KLT

The “*Karhusnen –Loeve*” transform KLT presented in [56] is one of the most robust methods used for ECG signal morphological representation and noise estimation. This transform relies on the assumption that noise is not completely separable in the frequency domain, but it is separable in KLT domain. Similar to principal component analysis, this method relies on the reconstruction of the signal using a set of bases. KLT is a Rotational transformation of the n-dimensional Euclidean pattern space E^n , where n is the number of possible morphological clusters the QRS complex can have.

Authors in [56] propose a procedure to compute KL bases from the MIT-BIH data base [58]. They cluster all waves from 44-nonpaced records from this data base, approximately 100,000 QRS complexes. The resulted clusters, 300, are then used to find the principal direction or the eigenvectors which are then truncated to find 6 most correlated eigenvectors with all clusters. The procedure could be written as follows

$$C = E[(X - E(X))(X - E(X))'] \quad (3.14)$$

$$C = V\lambda V^T \quad (3.15)$$

$$\lambda_K \geq \lambda_{K+1}, k = 1, 2, \dots, n-1, \quad (3.16)$$

where X is $N \times M$ matrix containing 300 QRS clusters, $E(x)$ is the average QRS complex in the vectors ensemble, C is covariance matrix whose eigenvectors are used as the bases eigenvectors V for the transform, and finally λ is the eigenvalues matrix. The KL bases

functions extracted from MIT-BIH database, after downsampling to 250 Hz, are shown in Figure 3.12.

Afterwards, using these eigenvectors each QRS complex is then represented (see Figure 3.13) as follows

$$x_{QRS} = \alpha_0 \gamma_0 + \alpha_1 \gamma_1 + \alpha_2 \gamma_2 + \dots + \alpha_r \gamma_r \quad (3.17)$$

Finally, after reconstruction of the QRS complexes using the KLT bases, the difference between the reconstructed wave and the original one is used as an estimation of noise presence in the ECG signal.

This method is superior to classic methods which rely on isoelectric line because it can estimate noise presence in the QRS complexes and it can be used to detect motion artifacts as well as other noises. However, there are several disadvantages to using the KLT. First of all it requires QRS delineation and then representation using the KL bases.

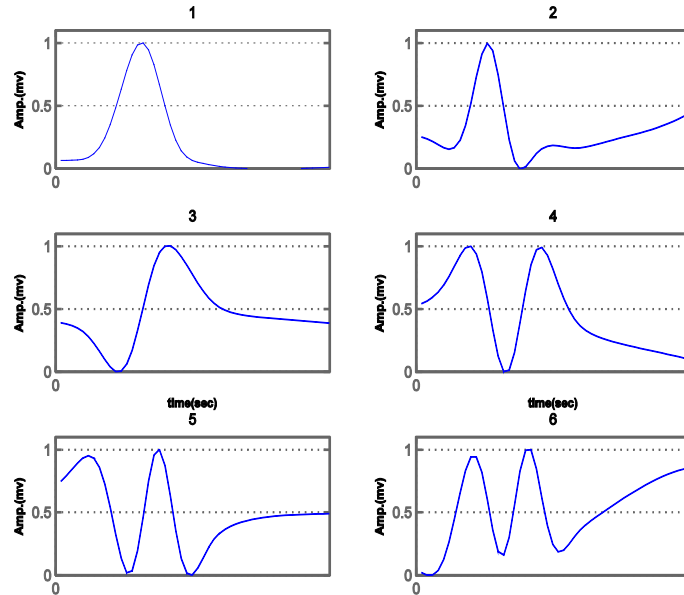


Figure 3. 12 KL bases functions extracted from MIT-BIH following the procedure proposed in [56]

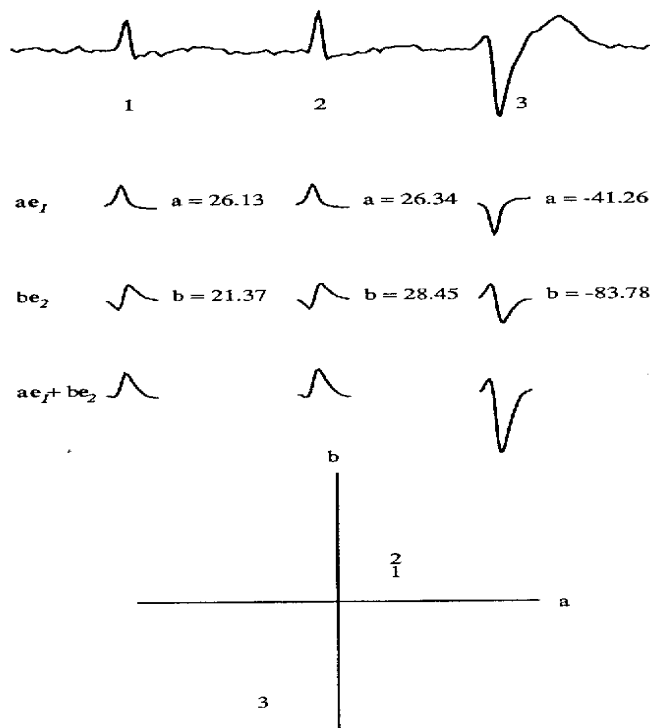


Figure 3.13 shows how coefficients are computed using the KL bases functions. Summation of KL bases functions is used to represent each QRS complex in the signal. On the top of the figure, the original signal is shown. The first and second coefficient a, b and their contributions to the representation of QRS are shown in the center. In the lower part of the figure, three numbered QRS complexes are mapped onto the a-b plane illustrating how the KLT preserves morphologic similarities. Image adapted from[56]

On the one hand, Delineation of QRS complexes is a tricky process in the presence of noise in the ECG signal. On the other hand, reconstruction and subtraction process are time consuming processes and requires efforts to be parallelized or implemented to use GPU processors. Additionally, the whole transform and its later usage depends on the good selection of training data and later clustering, therefore the accuracy of this algorithm depends significantly on the training set. Finally, ectopic beats are usually classified as noise when KLT is used to assess the noise in the electrocardiograph.

3.4.7 Frequency Content In Six Bandwidths and Out Of Range Event

Authors in [59] establish simple quantitative measures that can be used to demonstrate signal quality problems. This method is a combination of the frequency content and signal amplitude features.

The signal energy is firstly computed in six different bandwidths within the frequency of the diagnostic ECG (0.05–100 Hz); Low frequency (LF, 0.05–0.25 Hz), lower ECG bandwidth (ECG1, 0.25–10 Hz), higher ECG bandwidth (ECG2, 10–20 Hz), medium frequency (MF, 20– 48 Hz), power-line noise (50 Hz, 48–52 Hz), and high frequency (HF, 52–100 Hz).

Afterwards, the number of occurrences the signal exceeds a predefined threshold (out-of-range event, ± 4 mV) is counted. Finally, the signal quality is estimated from the extracted features using statistical analysis. This method is intended to estimate the overall signal quality and to assess its diagnostic potentials.

3.4.8 Moving Average

This method relies on the periodicity of the ECG signal. The assumption behind signal averaging is that the noise at different sample times is uncorrelated, but that the signals at these times are highly correlated. Therefore, using signal averaging in time, it is possible to find the stationary portion of the signal [36].

However, ECG signals are not periodic; therefore, it is important to solve this issue before applying averaging. Otherwise, this will have a negative impact on the final results. Stretching and shrinking operations are the bases for the conversion of quasi-periodic signals into periodic signals.

The proposed algorithm takes advantage of this feature in filtering signals with a minimum amount of distortion. After filtering the ECG signal, the residue is found by subtracting the signal average from the corresponding points of the input. Then the filtered residue (FR) is added back to the signal average to reconstruct the output with minimal distortion. The residue can be used as an estimate of noise ratio in the signal. Figure 3.14 illustrates this method.

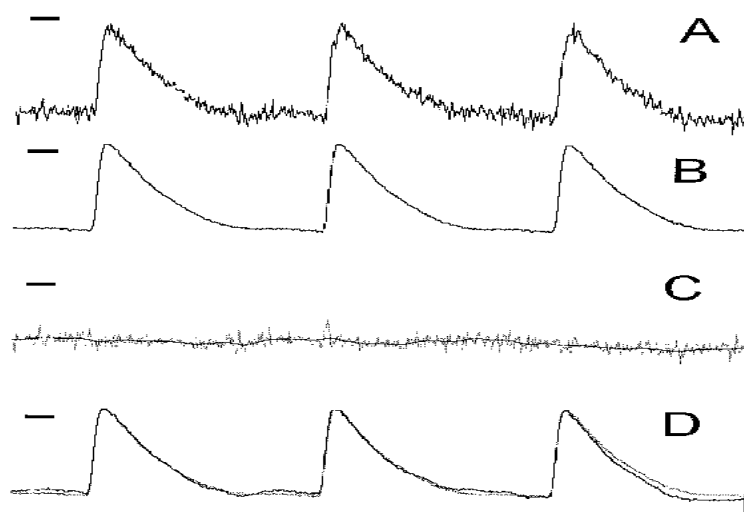


Figure 3.14 Filtered residue (FR) method. (A) Action potentials recorded from cultured neonatal rat cardiac myocytes ($m = 48$). (B) Signal-averaged trace. Note that all action potentials are identical. (C) Residue (light trace) and FR (dark trace), superimposed on top. See text for details of the algorithm. (D) Final output (dark trace) superimposed on the signal-averaged trace (gray). Horizontal scale bars represent 50 ms. Image adapted from [36].

The main drawback of this method is its dependence on timing information which is crucial to allow the beats alignment and averaging. Moreover, this algorithm is not tested on real ECG signals with arrhythmias. Furthermore, the reported results are valid only when signal is reasonably periodic. This is not the case in real ECG signals.

3.4.9 T-P Interval Average Power Divided By QRS

For each detected beat, the QRS average power is estimated as the square average of the samples in a 100 ms interval located around the detected R-peak [60]. The T-P interval power is evaluated as the square average of the samples in an interval obtained by approximate estimation of the end of T-wave and the onset of the following P-wave. For each detected QRS, a noise index (NI) is defined as the T-P interval average power divided by the QRS average power. The NI is quantized in three levels: $NI < NI_{0.2}$ (high). The weights 0, 1, 2 are respectively assigned to each of these levels and, for any interval of an ECG, the Noise Score (NS) is estimated by averaging the weights of the QRSs detected in that interval. This method also relies on the correct delineation of P and T waves and its results could be misleading when P and T waves are not detected precisely.

3.4.10 Cumulative Mismatch Histogram

The values of amplitude differences for consecutive QRS complexes are stored over a period of time in frequency histograms. Afterwards, a cumulative histogram is derived from the previously built histograms and then the signal quality is determined based on how fast the cumulative histogram curves rise. Cumulative histograms of signals with higher quality will rise faster than the signals with lower quality [61].

This method was tested and evaluated on real ECG with arrhythmias. Additionally, authors evaluate the improvement in PVC beats classification when this algorithm is used to select leads with better quality for the beats classification purposes. They found that leads identified by this algorithm with higher quality provide better classification performance. Figure 3.15 and Figure 3.16 illustrates this methodology using MIT-BIH records 207 and 203, both including arrhythmias.

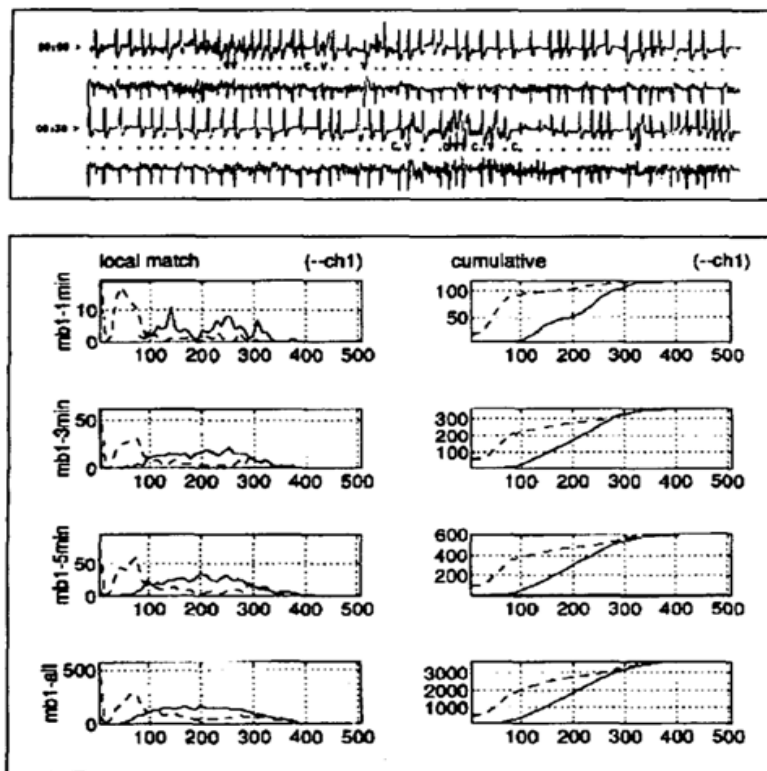


Figure 3.15 signals and signal quality histogram plots for MIT-BIH record 203. Image adapted from [61]

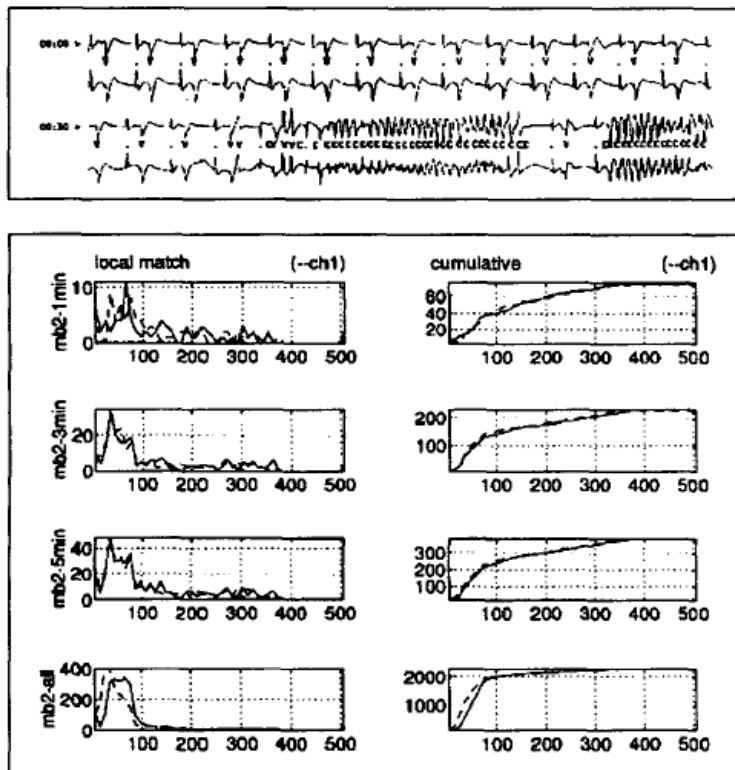


Figure 3.16 signals and signal quality histogram plots for MIT-BIH record 207. Image adapted from [61].

3.4.11 Moving Variance

In [62], an automated algorithm for detecting EMG noise in large ECG data is presented based on the moving variance in the signal after suppressing of QRS complexes. QRS are detected using well-known beats detection algorithm. Afterwards, authors propose the usage of morphological filtering to extract only the EMG noise corrupting the ECG signal. Moving variance is then calculated in time-invariant fashion with a sliding window to measure degree of signal fluctuation, excluding the fluctuations of QRS complexes. Figure 3.17 shows the main steps of this algorithm.

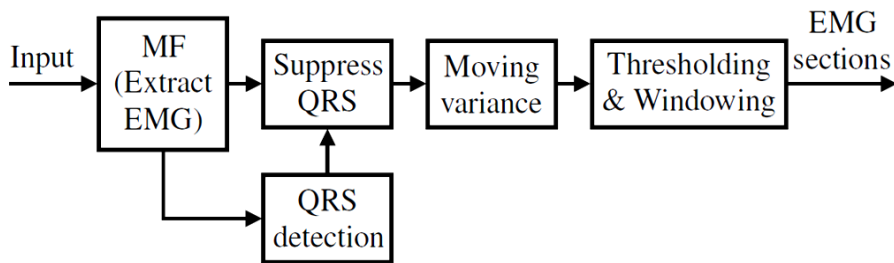


Figure 3.17 Flow diagram of the EMG detection algorithm using moving variance. Image adapted from [62].

Finally, normalization, followed by windowing and thresholding, is done based on the calculated moving variance. Thus, using the short-time variance signal one can find and isolate noise. This algorithm was evaluated on signals recorded on rats while noise was artificially added to the signals. Therefore, this algorithm is not tested on real signals or in the presence of arrhythmia.

3.4.12 Kurtosis

Kurtosis based method measures the Gaussianity of signal amplitude distribution based on the assumption that ECG signals are hyper-Gaussian [63]. Thus, higher kurtosis values are associated with lower quality in the ECG signal.

The kurtosis is the fourth standardized moment, defined as:

$$\text{Kurt}[X] = \frac{\mu_4}{\sigma^4} \quad (3.19)$$

Gaussianity of the signal amplitude distribution is computed and used, later, as quality estimation.

Kurtosis is computed to measure of the "tailedness" of the ECG signal amplitude distribution (see Figure 3.18). Whereby, higher kurtosis value is associated with the signal whose amplitude values are dispersed around its expectations. Furthermore, as a measure to

“tailedness”, it is suitable to measure the presence of outliers because outliers are reflected in the extreme tail of the amplitude distribution [64].

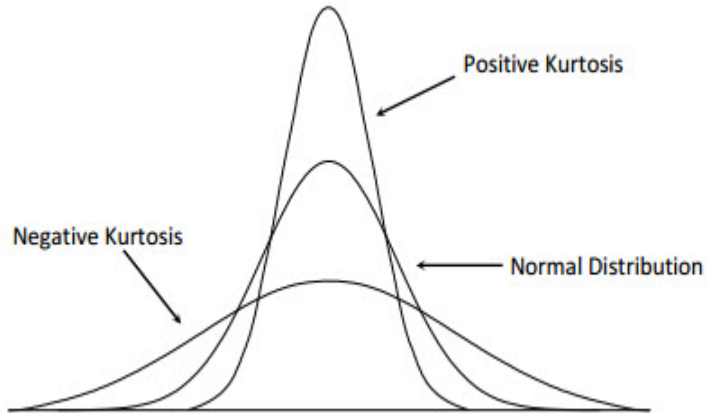


Figure 3. 18 Kurtosis and tailedness of Gaussian distribution.

3.4.13 LMS Adaptive Filtering

LMS adaptive filtering is used originally to separate the ECG signal from the noisy input. Therefore, it can be used to estimate the SNR value after subtracting the clean extracted ECG from the noisy input. The reference signal input for this algorithm is selected to be a template of the clean ECG signal. This method is proposed in [63]. Authors compare the performance with other algorithms.

This method relies significantly on the reference signal used for filtering. It is impossible to anticipate the template of a clean ECG signal that should be used as reference. Furthermore, signals with arrhythmias are not considered when this method was developed.

3.5 Conclusion (Noise Level Estimation vs. Approximation)

Signal quality estimation or equivalent noise estimation has a major impact on the final results of the ECG analysis pipeline. Its presence is crucial as it affects how the ECG channels are used later in the processing and analysis.

From the previous review it can be concluded that this is done usually depending on specific mathematical or statistical properties of the noise or the ECG signal. These properties are employed in order to separate the noise from the ECG signal or vice versa. The performance of these algorithms is measured by studying the error which resulted from the estimation procedure. Let $x(t)$ be the observed signal with noise $n(t)$. The original clean signal is $\hat{x}(t)$. In the estimation algorithms, the estimated clean signal $\hat{x}(t)$ is found with the estimation

error $e_x(t)$, while the estimated noise is found with the estimation error $e_n(t)$ as in the following

$$\begin{aligned} X(t) &= X'(t) + n(t) \\ \hat{X}(t) &= X'(t) + e_x(t) \\ \hat{n}(t) &= n(t) + e_n(t) \end{aligned} \quad (3.20)$$

These errors, however, depend significantly on the statistical model with which the noise/noise-free signal estimation is calculated. Noise or signal quality estimation models are usually built on the approximation of some statistical property of the ECG signal which is extracted based on the signals cohort statistics. Notwithstanding the foregoing, the estimation error varies from signal to signal even when the same approach is used. This is due to the non-stationary nature of signal dynamics, particularly with the existence of arrhythmia. Noise, as well as ECG waves, has different unpredictable characteristics that differ from patient to patient and from signal to signal.

Therefore, it is important to focus on one specific noise type at a time. Such approach enables building algorithms that can take all aspects of one specific noise into consideration. Otherwise, signal quality estimation will try to approximate the overall ratio of noises and artifacts. Such algorithms have limited usage in the processing pipeline and their role is restricted to leads selection for later analysis.

On the other hand, considering the usage of the comprehensive knowledge base is a decisive factor to the reliability of any noise or signal quality estimation. Besides the normal ECG signals, knowledge base should include noisy signals with real noises and all possible rhythms present while recording the signal. Because of the overlapping spectrum and fast changing dynamics or arrhythmia over time, noise estimation algorithms tend to misclassify arrhythmia intervals as noises. That is why some noise estimation algorithms could be used to detect arrhythmia as well for instance, KLT. Thus, reliability of any algorithm for noise estimation is restricted unless arrhythmia is taken into account.

There are several purposes for the development of noise estimation or overall signal quality estimation algorithms. Despite this, it is still an overall assessment of noise presence in the signal, so such estimation still has limited usages.

Algorithm with good time resolution could increase the usability of such algorithms. For instance, instead of rejecting the whole channel because of its estimated poor quality, special algorithm could isolate only those parts of the channel with poor quality while others could

be used for the delineation and classification purposes. Developing a short-time noise level approximation is the most appropriate solution in this case.

Using a time invariant short-time noise level approximation, signal quality is estimated with high time resolution following the dynamic changes of noise and ECG signal. All of this expands the applicability area of such a method, making it a suitable or automatic over-time lead selection; where channels selection is alternating over time according to the signal quality. Moreover, this enables the usage of such an algorithm for noise isolation and signal quality enhancement. Details about the application of short time noise level approximation are presented in details in the next chapter.

Finally, it is important to mention that methods that require precise QRS detection cannot be used in signals with low SNR because the average of detected beats itself is affected by noise unless a large number of ECG beats is considered. Unfortunately, including large number of ECG beats in the computation could negatively affect the averaged beat morphology, especially in the case of an ECG signal with multiform PVC's (MIT-BIH signals of 105 and 207).

Chapter 4

4. Short-time Noise level Approximation

In this chapter, a novel approach for Electromyogram (EMG) noise level approximation in Electrocardiogram (ECG) signals is introduced in details. The presented short time noise level approximation works also for all high frequency noises which overlap with the Electromyogram (EMG) spectrum.

The stationary wavelet transform (SWT) is used to find efficient translation-invariant approximation of EMG noise. This is accomplished in the form of reference signal extracted as an estimation of the signal quality vs. EMG noise. The reference signal is built and then normalized after considering different heart rates and rhythms which increases its robustness and reliability to give accurate results regardless the input signal rhythm.

Additionally, several applications of the extracted reference signal in the ECG signal analysis and processing pipeline are suggested in this chapter. The variety of applications stems from the robustness and the reliability of the proposed method due to the usage of different heart rates and rhythms when building the reference signal. This makes it suitable to be used regardless of the rhythm present in the ECG signal.

For evaluation purposes, both real EMG and artificial noises were used. The tested ECG signals are from MIT-BIH Arrhythmia Database Directory. The correlation coefficient between the added noise and the reference signal were computed for moving windows over the signal. Finally, the correlation between beats detection and reference signal was computed and presented. Reference signal gave a high correlation with false positive values. Most false positives caused by EMG noise occur in intervals of a greater amplitude reference signal and vice versa.

4.1 Proposed Approach Flow Diagram

In order to illustrate the presented approach a flow diagram is presented (see Figure 4.1). The first block in the flow diagram is the Stationary Wavelet Transform (SWT). This transform is applied on the raw ECG signal to find signal details.

Afterwards, a multi-resolutional analysis (MRA) is used to detect the most likely QRS complexes. Henceforth, the detected points are called QRS candidates. The corresponding zero-crossings, peaks, and valleys of QRS complexes candidates are excluded from any later computation.

The remaining zero-crossings, peaks and valleys in the wavelet details at scale 2^2 are used to build the array of zero-crossing, peaks, and valleys A_{zpv} . This array is supposed to contain all non-signal components in its wavelet details and using it a noise level approximation could be conducted.

So, the next step is to smooth the formed array A_{zpv} . The resulted signal after smoothing is considered as non-normalized approximation of EMG noise level. Finally, two thresholds σ_1 and σ_2 are used in the normalization of the resulted smooth signal. The thresholds were found after the analysis of several recordings with different cardiac activities which helps to globalize this method for all ECG signals.

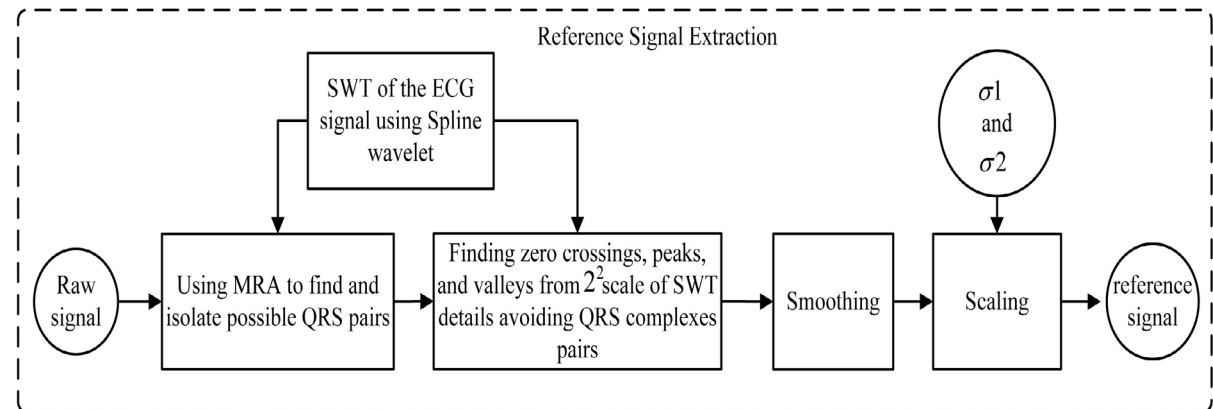


Figure 4. 1 Flow diagram for the reference signal extraction or the short-time noise level approximation method.

4.2 Wavelet Transform Of ECG Signal

The first step of the proposed approach is the Wavelet Transform which is one of the most used methods for ECG signal delineation, denoising, and arrhythmias recognition. Thus, in order to capture time-scale variations of the ECG signal, Wavelet Transform (WT) is used. The WT of signal $x(t)$ is defined as

$$W_{a,b}[x(t)] = \frac{1}{\sqrt{a}} \int_{-\infty}^{+\infty} x(t) \psi\left(\frac{t-b}{a}\right) dt, a > 0, \quad (4.1)$$

where $\psi(t)$ is the mother wavelet, a is positive and defines the scale, and b defines the shift and could be any real number. From (4.1) one can conclude that the greater the scale factor a , the wider the bases function and consequently, the corresponding coefficient gives information about lower frequency components of the signal, and vice versa. This is crucial to do a multi-resolutonal analysis.

Mallat in [66] shows that in case the mother wavelet is derivative of a smoothing function $\theta(t)$, the wavelet transform equation could be written like so

$$\psi(t) = \frac{d\theta(t)}{dt} \quad (4.2)$$

$$W_{a,b}[x(t)] = -a\left(\frac{d}{db}\right) \int_{-\infty}^{+\infty} x(t)\theta(t-b) dt, \quad (4.3)$$

For the previous equation, it is easy to conclude that the wavelet transform of the signal is the derivative of the filtered version of the signal with the smoothing function $\theta(t)$ at scale a . It can be concluded from (4.2) that zero-crossings (when $W_{a,b}x(t) = 0$) correspond to the inflection points of $x(t)\theta(t-b)$. So, they indicate the location of signal's sharp-variation points at each scale a [65].

Quadratic Spline wave proposed by Mallat in [66] (see Figure 4.2) is adopted in this method. For this wavelet, the filters $H(z)$ and $G(z)$ (see Figure 4.3 for their frequency responses) used in the implementation of DWT in this method are given as

$$H(e^{jw}) = e^{jw/2} (\cos \frac{w}{2})^3 \quad (4.4)$$

$$G(e^{jw}) = 4je^{jw/2} (\sin \frac{w}{2}), \quad (4.5)$$

Both of them the LPF and the HPF are FIR filters with impulse responses given as

$$h[n] = \frac{1}{8} \{ \delta[n+2] + 3\delta[n+1] + 3\delta[n] + \delta[n-1] \} \quad (4.6)$$

$$g[n] = 2\{\delta[n+1] - \delta[n]\} \quad (4.7)$$

As the Spline wave is an anti-symmetric wavelet, the points of maximum slopes of amplitude variations in the ECG signal will correspond to local minima and maxima in the WT details,

while the ECG signal local minima and maxima will be associated with zero-crossings at different scales [65, 66]. Therefore, finding zero-crossings points in the details of wavelet transform is equivalent to finding sharp changes in the ECG signal, which is the ultimate goal, since sharp changes are most likely originated by noise.

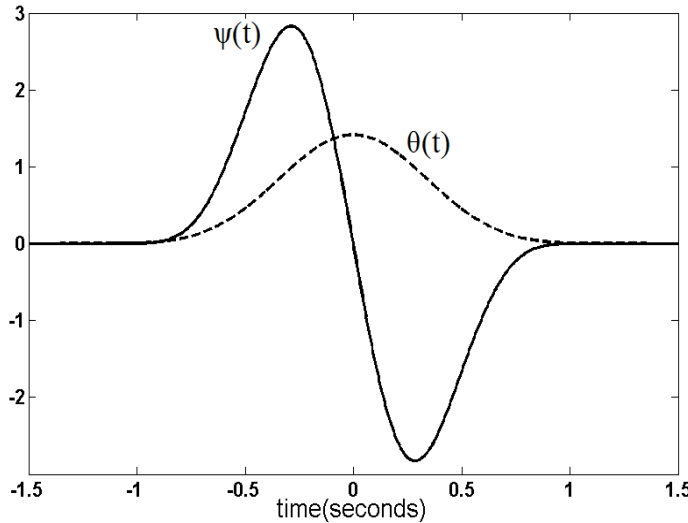


Figure 4.2 The adopted prototype wavelet $\Psi(t)$ and smoothing function $\Theta(t)$

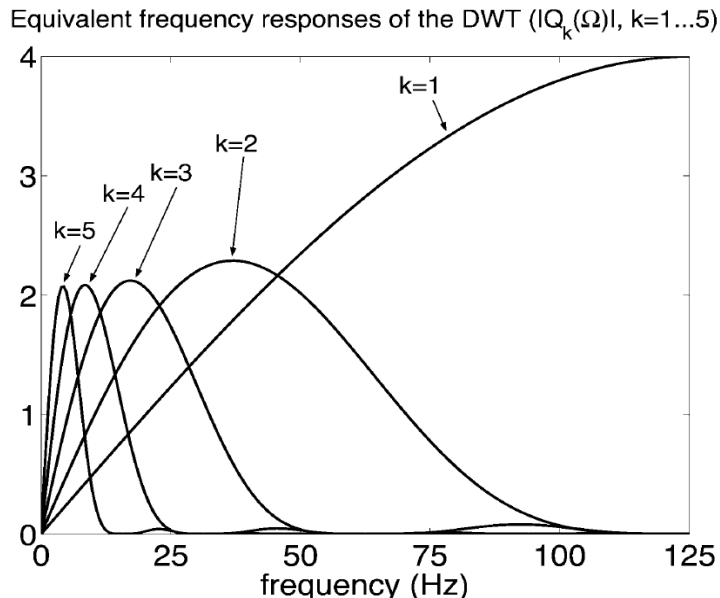


Figure 4.3 Equivalent frequency responses of the DWT at scales 2^k , $k = 1; \dots; 5$ for 250-Hz sampling rate. Image adapted from [68]

An important issue is to know whether zero-crossings obtained from multiscale sharp variations points could be a sufficient representation of the information carried in the signal, regardless of their origin (noise source of the original signal source). Authors in [79] have

shown that it is possible to obtain the multi-scale sharp-variation points from zero-crossings of the signal convolved with the Laplacian of a Gaussian. This method is extensively used in singularity detection and in other pattern recognition applications. Mallat in his paper [65] discusses the issue of completeness and stability of signals representation based on the study of their zero-crossings in other domains, especially in using a multi-scale transform such as wavelet transform. In his paper, he stated that “The positions of zero-crossings may provide a complete representation under certain assumptions but such representation is not stable” [65]. However, he concluded that such representation could be stabilized by adding a complement of information that measures the size of the structure between two consecutive zero-crossings.

So, zero-crossings in wavelet details give only position information about the multi-scale sharp variations, especially when they are detected in a limited number of scales. Therefore, it is hard to differentiate small amplitude fluctuations from important discontinuities [65, 66, 69] using zero-crossings representations. Thus, the usage of local minima/maxima in the wavelet details is adopted in this method in addition to zero-crossings. Peaks and valleys in the wavelet details assess the structure between two consecutive zero-crossings taking into account that peaks and valleys correspond to the maximum absolute slope of the signal’s sharp multiscale variations. This provides sufficient representation of the corresponding signal changes, originated by both heart electrical activity and by EMG and high-frequency contaminants.

Let the noisy signal $x(t)$. It could be written as

$$x(t) = x'(t) + n(t), \quad (4.8)$$

where $x'(t)$ stands for the clean signal, and $n(t)$ stands for the EMG and other high-frequency noises. Replacing (4.8) in (4.3) allows us to rewrite equation (4.3) as

$$\begin{aligned} W_a x(b) &= -a \left(\frac{d}{db} \right) \int_{-\infty}^{+\infty} x'(t) \theta(t-b) dt \\ &\quad - a \left(\frac{d}{db} \right) \int_{-\infty}^{+\infty} n(t) \theta(t-b) dt. \end{aligned} \quad (4.9)$$

Two unknown variables are in (4), the wavelet coefficients of the clean signal $x(t)$ and wavelet coefficients of noise $n(t)$. Thus, estimating the coefficients of signal directly means to estimate the noise coefficients. This is discussed in details in next sections.

Finally, in order to overcome the lack of translation-invariance of the discrete version of wavelet transform (DWT), the stationary wavelet transform (SWT) is used. The stationary wavelet transform (SWT) allows us to perform a time-invariant multi-resolutonal analysis using the “algorithme à trous” approach [67] (see Figure 4.3). The downsampling of the signal over levels will be replaced by interpolating the filter impulse response from previous levels (see Figure 4.4). This process is called “algorithme à trous” [60]. The approximations of SWT wavelet transform are smoothed versions of the signal taking into consideration that the maximum frequency in each level will be $2^{-n} F_s$.

Stationary Wavelet transform’s muti-resolutonal properties enables large temporal support for lower frequencies while maintaining short temporal widths for higher frequencies, by the scaling properties of the wavelet transform. This property extends conventional time-frequency analysis into time-scale analysis, and makes it suitable to analyze and isolate non-stationary signals such as an ECG signal which contains components (P, Q, R, S, T waves) as well as contaminants of different frequencies or more accurately different time-scales.

Figure 4.4 shows several simulated waves similar to those in the ECG, together with the first five scales of their DWT (2^k ; $k = 1, \dots, 5$). The local maxima and minima of the SWT indicate the local singular points of the considered signal. The same sampling rate is applied in all scales to keep the time-invariance as well as the temporal resolution. This is achieved by removing the decimation stages and interpolating the filter impulse responses of the previous scale as illustrated in Figure 4.4 (b). See Figure 4.3 for the filters impulse responses.

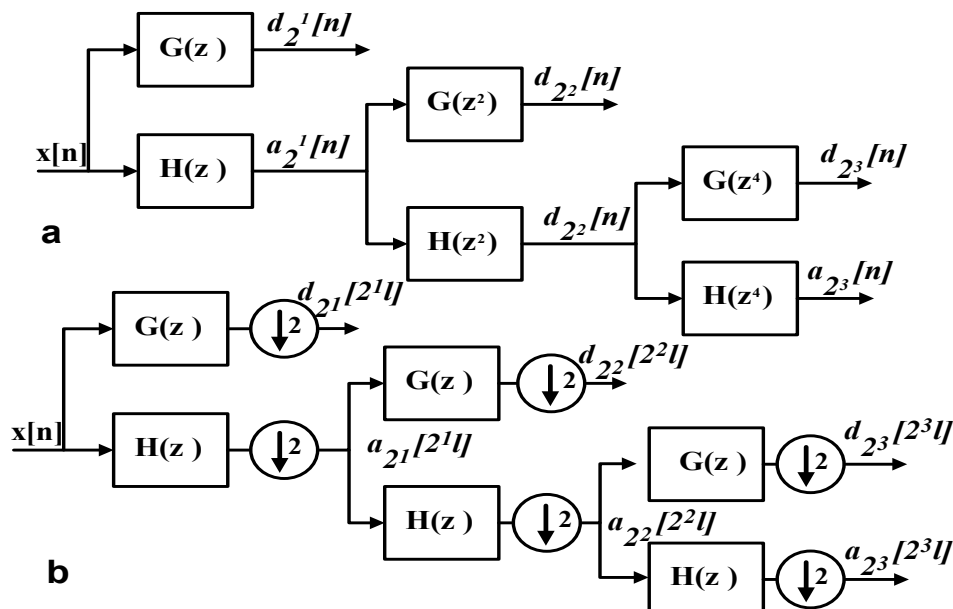


Figure 4.4 Two filter-bank implementations of DWT. (a) Mallat’s algorithm.(b) Implementation without decimation (algorithme à trous).

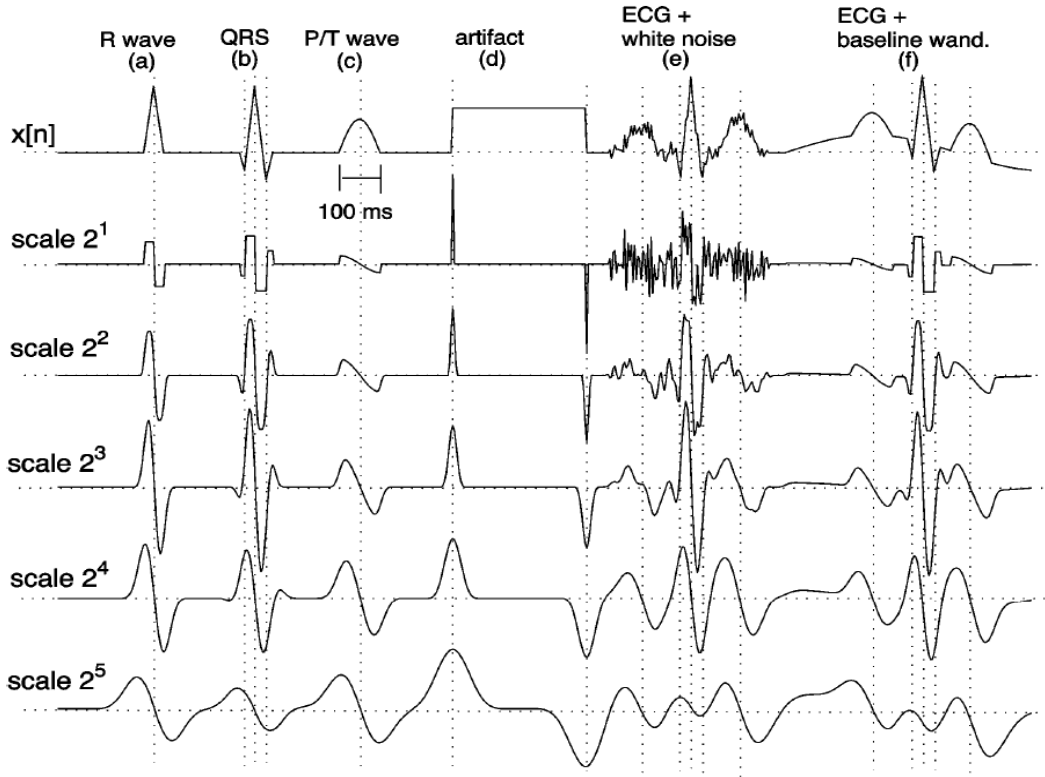


Figure 4.5 SWT at the first five scales of ECG-like simulated waves. Image adapted from [68]

4.3 Extraction Of Zero-Crossings, Peaks, And Valleys

From the spectrum of ECG signal waves with the EMG noise introduced in [2] (see Figure 3.5) and frequency responses of Spline wavelet decomposition filters introduced in [66, 67] (see Figure 4.3), it is clear that scale 2^2 of SWT contains most of the high-frequency components of QRS complexes, as well as EMG noise [65, 66, 68].

Having in mind what zero-crossings represent in SWT details (refer to section 4.2), we can say that finding zero-crossings on this scale is equivalent to finding sharp changes corresponding to waves with high frequencies in the ECG signal. However, zero crossings in wavelet details provide only the position information but do not differentiate small amplitude fluctuations from important discontinuities [65, 66, 69]. Thus, the use of local minima/maxima in the wavelet details is considered in addition to zero-crossings. This provides sufficient representation of the corresponding signal changes, originated by both the heart's electrical activity and by EMG and high-frequency contaminants.

Since the main goal is to extract the EMG noise only, multi-resolutonal analysis is used to find and exclude from zero crossings all local minima/maxima points that are most probably corresponding to QRS complexes. The residual signal is then considered as an approximate estimation of non-signal containment coefficients in the wavelet details. Essentially, some of

these points could be detected, by mistake, as QRS complex, while they are actually noises or artifacts. This however is not an obstacle when the goal is to use these points for noise level approximation and not for beats classification.

Authors in [68, 70] defined multi-resolutonal approach for QRS complex detection based on SWT and evaluated it on standard databases. They proposed amplitude thresholds (add equations) formulas for the purpose of finding pairs of maximum modules with opposite signs across the SWT scales.

These thresholds, given in (4.10), are used to find all zero-crossings, peaks and valleys which are originated by the QRS complexes amplitude changes in SWT details.

Thresholds computed for excerpts of 2^{16} samples are like so

$$\varepsilon_i = \begin{cases} RMS(W_{2^i}x[n]); i = 2, 3, \\ 0.5RMS(W_{2^i}x[n]); i = 4, \end{cases} \quad (4.10)$$

The next step is to find in scale 2^2 all zero-crossings, peaks and valleys whose absolute amplitudes exceed empirical threshold $0.5\varepsilon_2$ excluding those found in the first step as candidate of QRS complexes QRS_{cand} . Figure 4.6 illustrates the process of extraction A_{zpv} array.

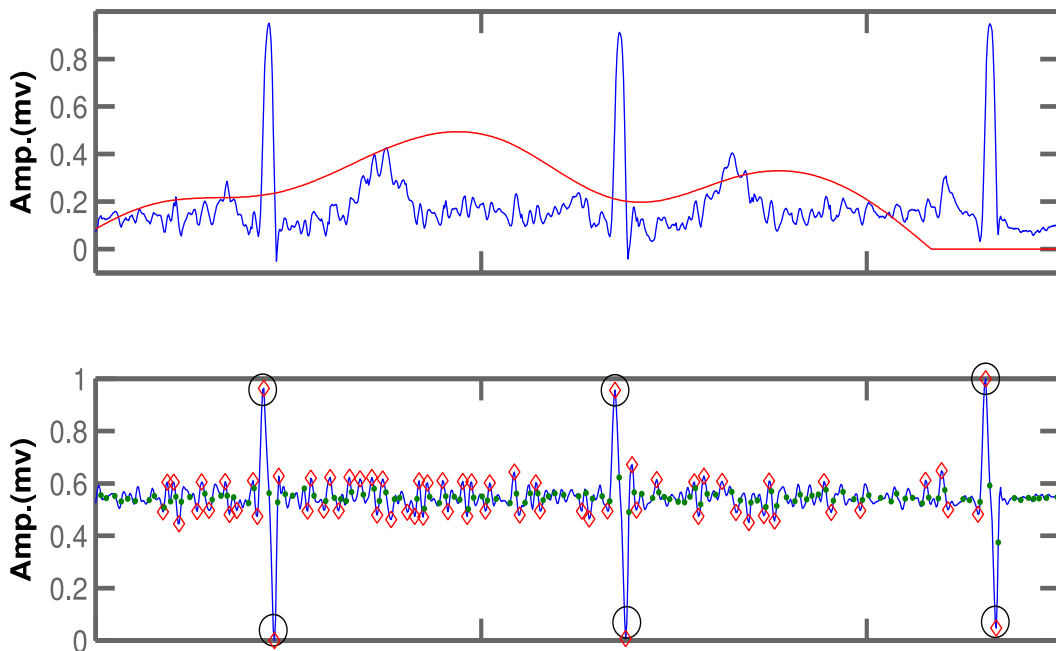


Figure 4.6 The A_{zpv} array extraction from ECG signal details. ECG signal interval from Lead 1 of MIT-BIH record 106 on the top with extracted reference signal (solid red line), and at the bottom are the details of ECG signal of scale 2^2 . Peaks and valleys are in red squares, zero-crossings are in green dots, and QRS complexes are marked as black circles.

At the end of this step, the array of zero-crossings, peaks, and valleys positions A_{zpv} is formed in the same length of the ECG signal. The array's elements are set as in (4.11).

$$A_{zpv}[n] = \begin{cases} 1 & ; W_2(x[n]) \text{ is peak or valley} \\ 0.5 & ; W_2(x[n]) \text{ is zero crossing} \\ 0 & ; n \in QRS_{cand} \\ 0 & ; \text{elsewhere} \end{cases} \quad (4.11)$$

This array is supposed to have all signal sharp changes in the second scale. This is suitable to build noise approximation taking into consideration that QRS complexes components are excluded from it.

4.4 Smoothing

In order to get a smoothed representative noise approximation from the extracted A_{zpv} in reasonable time resolution, smoothing is required. Convolution with window function's impulse response $h[n]$ is used for this purpose. This could be written as

$$\Phi[n] = \sum_{m=-\infty}^{+\infty} A_{zpv}[n] \cdot h[n-m]. \quad (4.12)$$

The extracted signal using (4.12) is called the smoothed reference signal, where its amplitude represents the rate of considered zero crossings, peaks, and valleys in wavelet details at scale 2^n .

The choice of impulse response $h[n]$ and its length N determines the representative nature of the extracted reference signal, since it affects its frequency band. Different window functions could be used, including rectangular, Hamming, and Gaussian. All of them provided desired smoothing that enables the noise presence approximation over time. However, the Gaussian windows is adopted in this paper and used for further analysis and thresholds computation.

The window length N is a more decisive parameter than the window type. If N is too large, the signal will change very slowly and thus the time resolution will not adequately reflect the changing properties of signal quality. Because the ultimate goal is to approximate the EMG noise between QRS complexes, a suitable choice of N could be

$$N = F_s \times RR, \quad (4.13)$$

where F_s is the sampling frequency used and RR is the normal resting RR interval value in seconds of the patient group. This value depends on the patients' age category and their heart

muscle special condition (infants, adults, and athletes, patients with heart blocks). This information is well known by the specialist. For example, an adult with no professional sport activities with average weight could have normal resting RR interval about 850 (ms) or equivalently 70 BPM. Moreover, this value can be estimated as the average heart rate computed after QRS candidate's detection.

Bandwidth of the smoothed reference signal is restricted to the bandwidth of the filter used (Gaussian window). Thus, it is possible to downsample this signal or to compress it without losing any amount in information.

Although downsampling could help in saving and sending the reference signal, it is important to have a reference signal of the same length as the signal it is extracted from when it is used. This is essential for the time-invariant analysis and processing of non-stationary ECG signal. Finally, it is important to highlight that smoothing of the signal is not restricted to the usage of window functions. Low pass filtering, either FIR or IIR, could be used also. There is an advantage in using Gaussian window function. The smoothed signal will always be positive which is guaranteed by the convolution with Gaussian function.

4.5 Smoothed Reference Signal Normalization

A reasonable generalization which could be concluded from the smoothed reference signal is that if its amplitude is high the noise level in the signal is high and vice versa. Actually, this is true because the clean ECG signal should have a limited number of slope changes outside the QRS complex, which is excluded from the calculation of reference signal. However, the previous statement is imprecise unless we define what is high and what is low.

In order to separate clean intervals from noise intervals and define the noise strength in noisy ones, two thresholds are defined for the smoothed reference signal. The first threshold σ_1 corresponds to an ECG signal interval with tolerable amount of EMG noise, while the σ_2 corresponds to a noisy ECG with an excessive amount of noise that makes the interval useless for analyses.

Scaling the signal between two thresholds allows us to focus on the EMG noise that really affects the clinical acceptability of the signal. So, an ECG signal interval associated with a reference signal amplitude lower than σ_1 is considered a clean signal with a tolerable amount of noise. On the other hand, signal intervals associated with the reference signal amplitude higher than σ_2 will be considered very noisy intervals.

To find these thresholds, a statistical study is conducted on the extracted smoothed reference signal from ECG signals with both normal and abnormal activity. The tested signals are from MIT-BIH database [58] along with signals recorded using commercialized ECG arrhythmia simulator (Tech Patient Cardio from HE instruments) [71] with a controlled amount of muscle noise. Both normal and abnormal rhythms are considered in this study. Table 4.1 shows the considered MIT-BIH records and the arrhythmias present in each of them. Sampling frequency of 250 Hz was used for all tested signals; therefore, the signals are downsampled from MIT-BIH database from 360 to 250 Hz. Gaussian window with length computed as in (4.13) is used for the reference signal smoothing. All rhythms episodes have the same length, and the total length of the considered arrhythmias is 7853 seconds. Heart rate range of the considered rhythms is 71-190 BPM.

Table 4. 1 Signals used for histograms generation

Rhythms	Heart Rate	Signals used
Atrial Fibrillation	105-160	201,202,217,219,222
Sinus Rhythm	70-90	103,117,119
Supraventricular Tachycardia	110-170	209,220,234
Ventricular Tachycardia	110-130	204,206,209,201,223
Accelerated Idioventricular rhythms	100-110	124
Ventricular Flutter	130-190	207, synthesized signals
Bigmeny, trigemny	70-130	106,119
Atrial Flutter	100-150	222, synthesized signals
Sinus Arrhythmia	70-90	113,115, synthesized signals
Accelerated Junctional rhythm	100-130	124, synthesized signals

Arrhythmias with high heart muscle activity such as atrial flutter, atrial fibrillation, supraventricular and ventricular tachycardia, and ventricular flutter are considered (see Table 4.1). The corresponding waves, caused by heart electrical activity in these arrhythmias, show fast changes with irregular morphology (see Figure 4.7). Taking such arrhythmias into consideration is important for avoiding misclassification between them and noise intervals, because of the high ratio of amplitude changes in the ECG signal waves in these arrhythmias. Hence, using the arrhythmias annotation and signal quality changes of MIT-BIH records, good quality intervals are isolated for both fast and normal heart rate in order to study their reference signal amplitude.

Figure 4.7 presents ECG intervals for arrhythmias with high heart rate or fast cardiac muscle electrical activity included in the statistical study. The histogram of all samples from all ECG intervals included vs. smoothed reference signal values extracted from the ECG records in Tab4.1 is shown in Figure 4.8 (a).

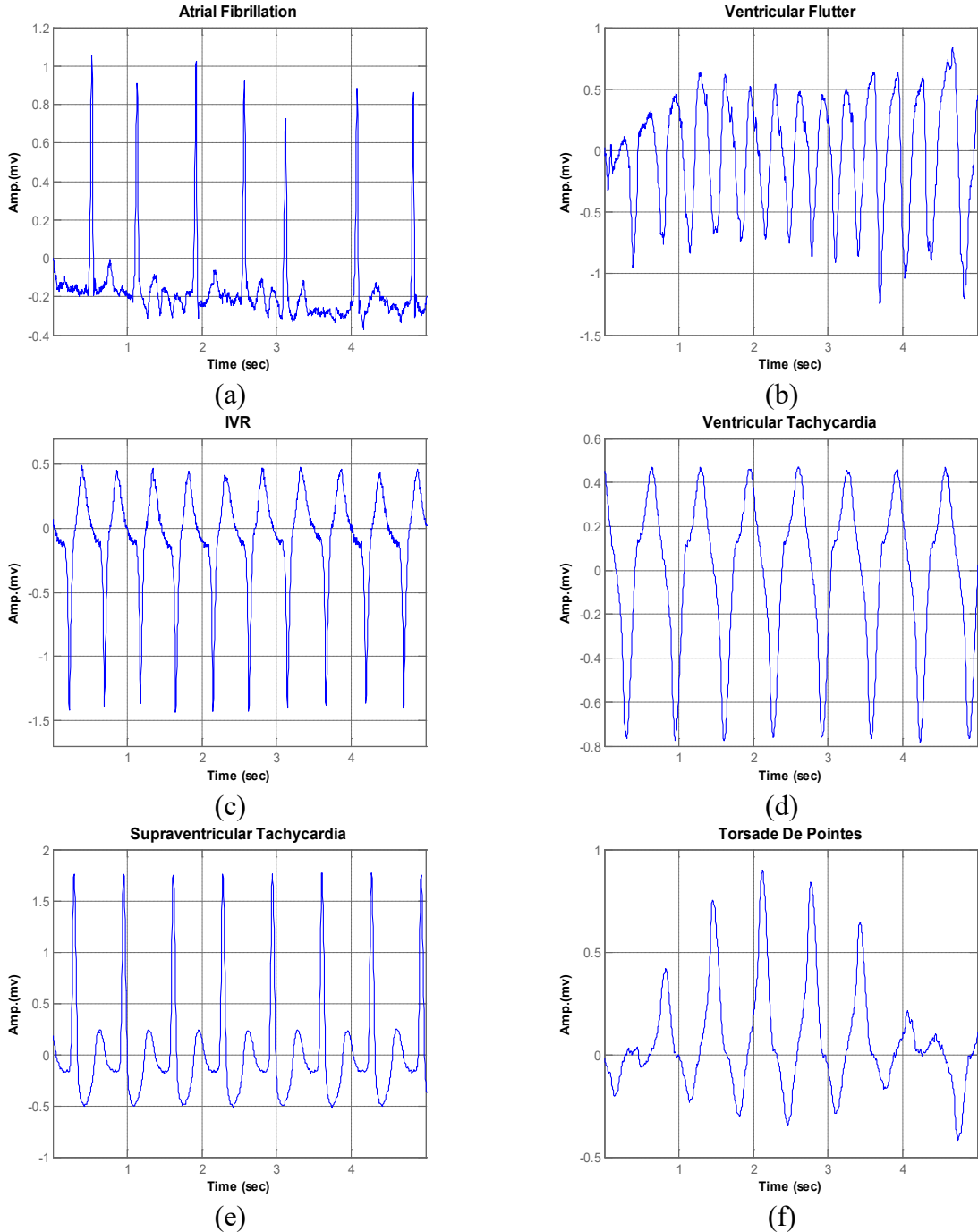


Figure 4.7 several intervals from the MIT-BIH database for arrhythmia that show fast heart rate and irregular waves morphology. (a) is for atrial fibrillation, (b) is for ventricular flutter, (c) is for idioventricular rhythm, (d) is for ventricular tachycardia, (e) is for supraventricular tachycardia, and (f) is for Torsade De Pointes.

As it could be seen from Figure 4.8 (a), the histogram fits normal distribution, and the smoothed reference signal is dispersed around the most frequent value which is lower than

0.1. To note, that higher values for the smoothed reference signal are more frequent in intervals of atrial fibrillation and ventricular flutter. This is expected considering the high ratio of amplitude changes caused by both atrial and ventricular activity of these arrhythmias. The so-called three-sigma rule is used. The value of σ_1 is defined as the average value plus three standard deviations. Applying this rule expresses that “nearly all” values, 99.7% of all possible values, lie within three standard deviations of the mean [75]. This confidence level is considered satisfactory. This value is computed and is equal to 0.13. Therefore, smoothed reference signal values smaller than this value σ_1 are considered as a clean ECG signal.

Afterwards, σ_2 is found as the smoothed reference signal value that corresponds to an unacceptable noise amount, or, equivalently, to very poor quality ECG segments. For this purpose, we added controlled amount pink, white, and brown noises as well as a real EMG noise from an MA record from the Physionet website [72]. Noise is added to whole intervals by a method described in details in section 5. Signal to noise ratio SNR ranges between -25 to +25.

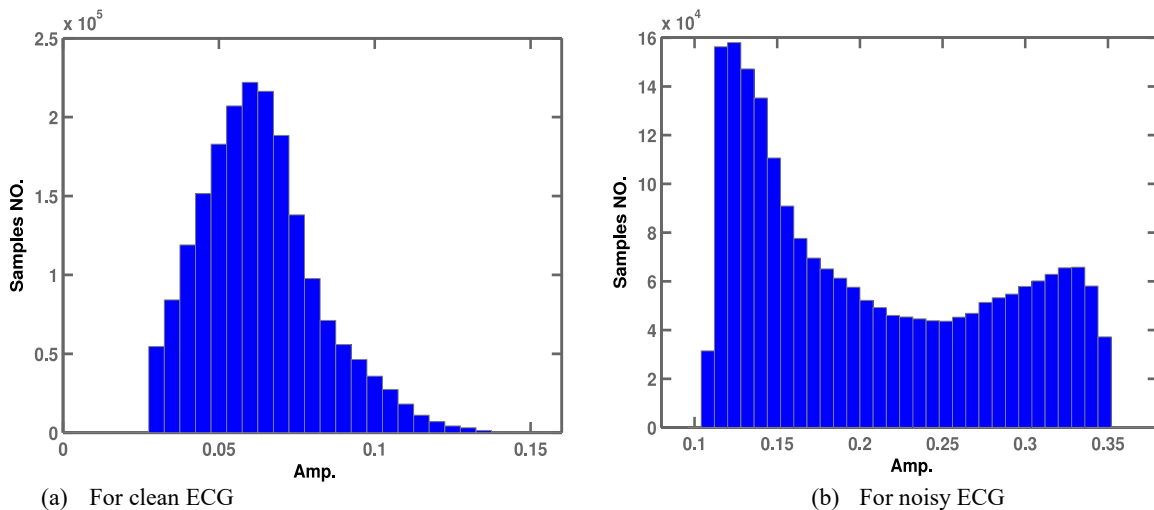


Figure 4.8 Histogram of samples number vs. smoothed reference signal values.

A histogram of smoothed reference values, corrupted by noise, was extracted from signals listed in Table 4.1 and shown in Figure 4.8 (b). The histogram of noisy signals contains different intervals that could be used for delineation or analysis, in spite of noise presence. It also includes intervals where noise is dominant, so these intervals could not be considered as acceptable signals for the ECG analysis. Therefore, two experts went through the signals and annotated the signals as “accepted” for analysis in spite of noise, or “unusable” where ECG signal's waves were overshadowed by noise. To note, unacceptable intervals or very noisy intervals were those with reference signal value larger than 0.28. These intervals were useless for any kind of analysis, and the corresponding delineation results were erroneous with

positive predictive value less than 70%. Minor changes to the σ_2 value will change the dynamic range of reference signal and the sensitivity to EMG noise level increases or decreases correspondingly.

Using the previously determined thresholds, the reference signal is normalized. This can be written as

$$\psi[n] = \begin{cases} \sigma_1; & \psi[n] < \sigma_1 \\ \sigma_2; & \psi[n] > \sigma_2 \end{cases} \quad (4.13)$$

$$\gamma[n] = \frac{\psi[n]}{\sigma_2 - \sigma_1} \quad (4.14)$$

Henceforth, the resulting normalized reference signal from (4.13) and (4.14) is referred to as the reference signal only and the amplitude values of reference signal are from (0-1).

4.6 Discussion And Results

4.6.1 Evaluation ECG Database

For the evaluation and comparison purposes, ECG signals from MIT-BIH database available on Physionet are used. This database is available publicly at Physionet and associated with both signal quality and beats annotations.

First channels of MIT-BIH records 103, 106, 117, 118, and 119 were used, because of the high signal to noise ratio in these records, according to the signal quality annotation. Therefore, these signals were considered as clean signals and used to evaluate the proposed approach and to compare it with other methods introduced in the literature. These signals were downsampled from 360 Hz to 250 Hz. Total length of signals used in the evaluation and comparison process is 10 hours. Rhythms included in these signals are sinus rhythm, ventricular and supraventricular tachycardias, ventricular Bigmeny and Trigmeny, atrial fibrillation, and heart blocks.

4.6.2 Noise Generation and Addition

In order to evaluate the performance of the presented algorithm, both real EMG noises as well as artificial colored noises are tested. The adopted colored noises are used in the literature to mimic noise in the ECG signals [3, 78].

The real EMG noise record is generated using the noise stress test database (NST), available on Physionet site, [58, 72] as standard tool to evaluate the ECG analysis algorithms. The noise record (MA) from this database was used to add real EMG noise to the tested signals. Because of the recording way, using electrodes placed on limbs in positions where the

subject's ECG signals were not visible, the (MA) noise record provides us with non-stationary real mimic of EMG noise [72]. This database is available with sampling frequency of 360 Hz, so, a downsampling is done to 250 Hz. Afterwards, baseline drift is filtered using a low pass FIR filter with cut-off frequency of 0.1 Hz to ensure that the baseline drift will not affect the evaluation of EMG noise.

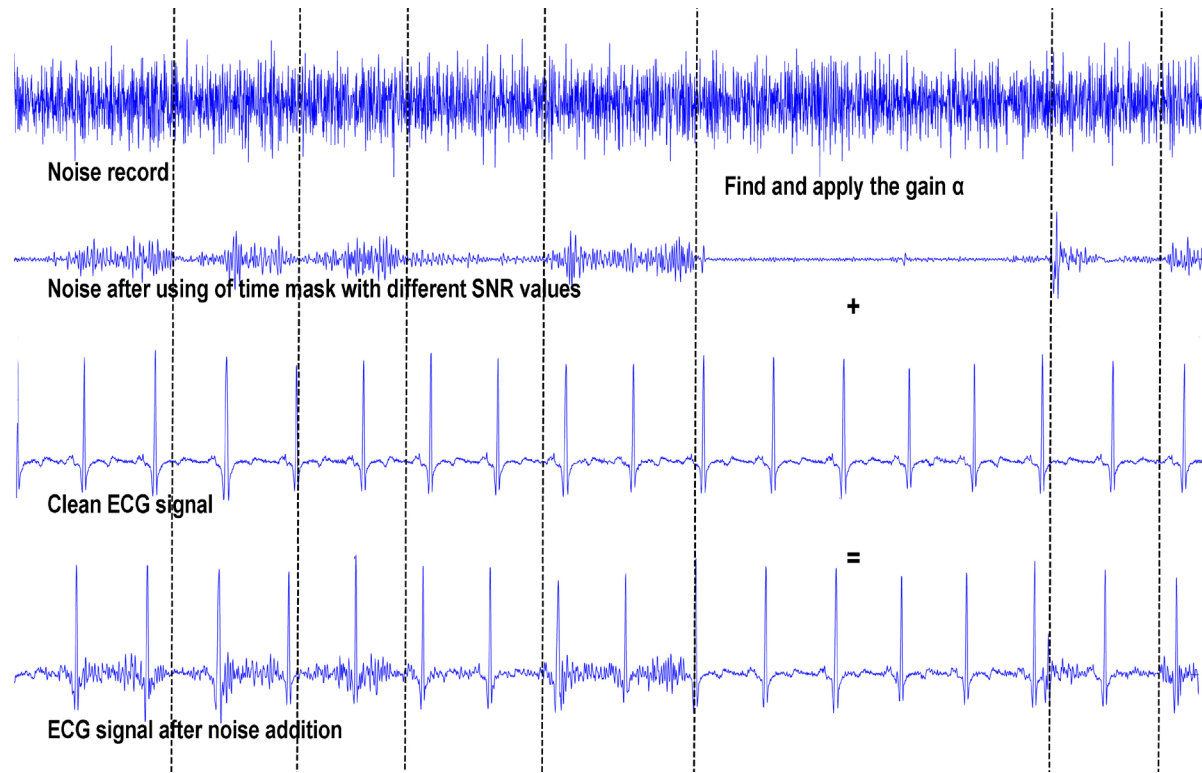


Figure 4.9The process of noise addition to the ECG evaluation signals.

On the other hand, the artificial noise records were generated at sampling frequency of 250 Hz with three noise colors. Noise color is defined by the slope of the noise spectral density function. Artificial noises are generated at sampling frequency of 250 Hz, and each noise record is generated using a different spectral density slope β . White noise is generated using ($\beta = 0$), pink noise or flicker noise using ($\beta = 1$), and the random walk noise or brown noise using ($\beta = 2$).

In order to evaluate the correlation between the measured reference signal and the SNR of the ECG signal after noise addition, and to mimic the noise non-stationarity present in the ECG signals, the noise is added using a mask of alternating intervals noise-clean-noise-clean, with alternating SNR values from -10 db to 10 db until the end of the tested ECG signal. Hence, the noise amount from the generated noise records (real EMG or MA, white, pink, and brown), that had been added to the ECG signals, is determined using the following equation,

$$\text{SNR} = 10 \log\left(\frac{S}{N * \alpha^2}\right), \quad (4.15)$$

where SNR is the desired signal to noise ratio in decibels, S is the signal power between each two successive QRS complexes, N is the noise power in the corresponding interval from noise record, and, finally α is the gain that should be applied on the noise record before being added to the ECG signal in order to reach the desired SNR value. This approach of noise addition to the ECG signal is introduced in details in [72]. Figure 4.9 illustrates the process of noise addition to the evaluation ECG signals.

4.6.3 Evaluation Results

Graphical results of the proposed method are shown in Figure 4.10 whereby signals in this figure are noisy signals from the origin, so it is unknown what the original signal looks like. Figure 4.11 and Figure 4.15 show ECG signals and a reference signal extracted as noise level approximation. Noise was added to the ECG signal as mentioned in the previous section.

The presented results are not restricted to the normal sinus rhythm. Different kinds of abnormal ECG rhythms are presented. The reference signal gives relative approximation of the EMG noise level present in the ECG signal over time. Reference signal amplitude drops at the QRS complex points and rises outside the points according to the noise amount, which is not the case when QRS complex are not detected and excluded.

Beside the graphical results, the ability of the reference signal to approximate EMG noise presence and level in the ECG signal was investigated. For this purpose, the correlation coefficient between the SNR of the ECG signal with added noise, and reference signal computed after QRS exclusion was calculated. Afterwards, SNR values, as well as smoothed reference signal average value computed from each alternating interval, were used to compute the correlation coefficient.

Correlation coefficients found for different types of noises are listed in Table 4.2 for the first and second lead of MIT-BIH signals 103,117,118. Results presented in Table 4.2 show that the reference signal is strongly correlated with the SNR of the added noise with average correlation of 0.823 ± 0.11 . The negative values are present because the reference signal approximates the noise presence and ratio to signal, while SNR is the signal to noise ratio.

Low correlation coefficients are caused by the normalization process, since EMG noise in ECG signal, with low reference signal values below σ_1 , was considered as tolerable noise as

it doesn't affect the analysis. Therefore, the average correlation coefficient of smoothed reference signal before normalization is much higher, with an average of 0.91 ± 0.05 .

Other methods described in the literature to estimate signal quality were used and tested. The correlation coefficient between the obtained signal quality and the SNR value of the ECG signal after noise addition is calculated. The best method was the averaged beats-based method which gave correlation coefficients average of 0.91 ± 0.09 while the KLT-based method gave 0.88 ± 0.08 , where bad correlation coefficients were caused by beats that are morphologically different from the average beat estimated in these methods.

Table 4.2 Correlation coefficient of reference signal with estimated SNR

	103		117		118	
	Lead1	Lead2	Lead1	Lead2	Lead1	Lead2
MA	-0.8585	-0.7303	-0.8079	-0.8455	-0.733	-0.6062
PINK	-0.9005	-0.8933	-0.9048	-0.9217	-0.8187	-0.7643
White	-0.9027	-0.874	-0.9213	-0.9443	-0.7632	-0.7736
Brown	-0.7289	-0.9283	-0.8919	-0.9242	-0.7892	-0.4987

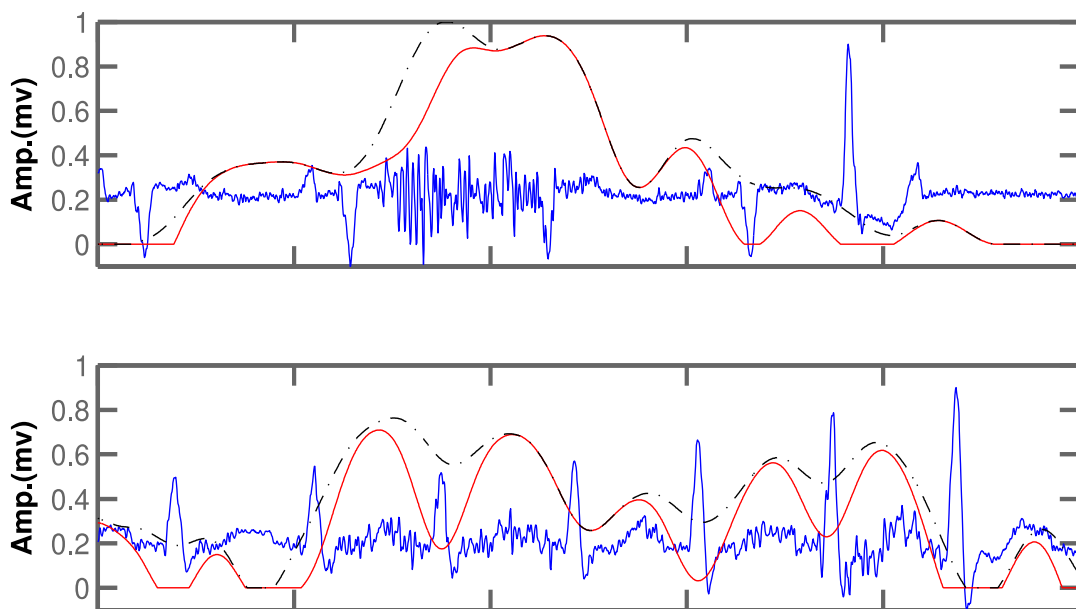


Figure 4. 10 Signals with original noise. In the top is 108 record while in the bottom is 109 record. Reference signal with (red line) and without (dashed-dotted black line) QRS exclusion. ECG signals here are noisy from the origin.

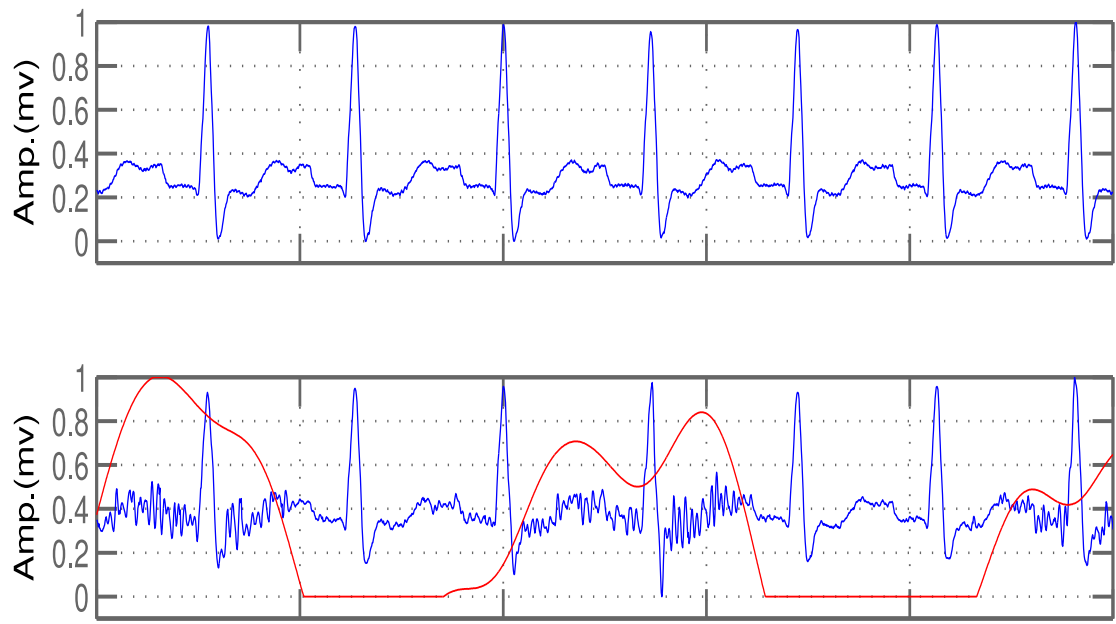


Figure 4. 11 Heart block rhythms MIT-BIH record (109), Reference signal with (red line) and without (dashed-dotted black line) QRS exclusion. Clean ECG signal from MIT-BIH record (Top), and the same signal after noise addition (bottom).

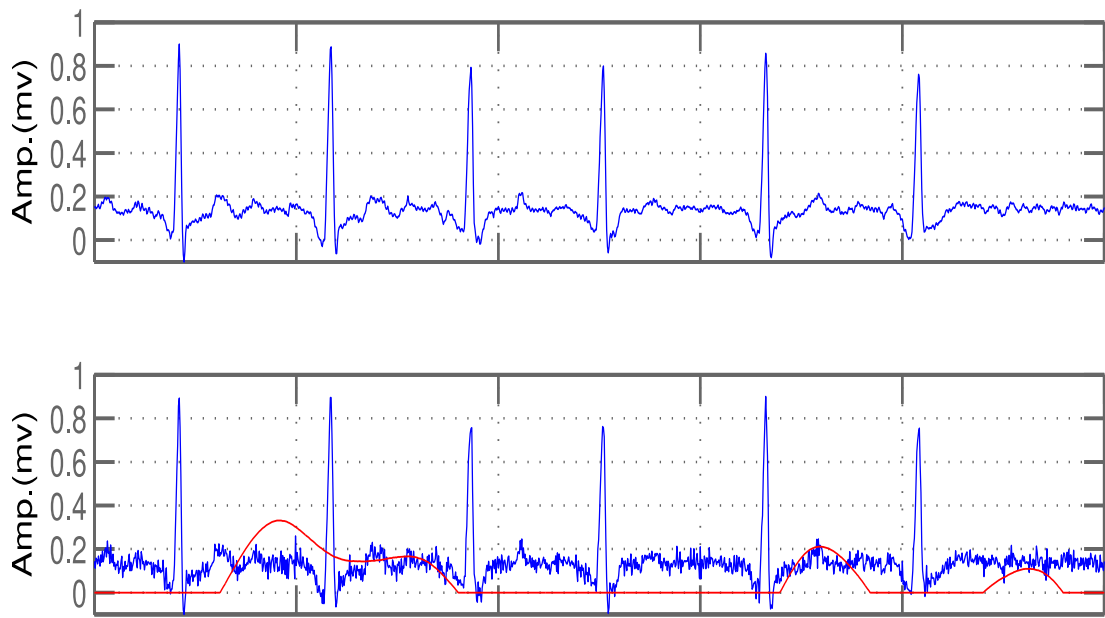


Figure 4. 12 Atrial Fibrillation MIT-BIH record (201) , Reference signal with (red line) and without (dashed-dotted black line) QRS exclusion. Clean ECG signal from MIT-BIH record (Top), and the same signal after noise addition (bottom).

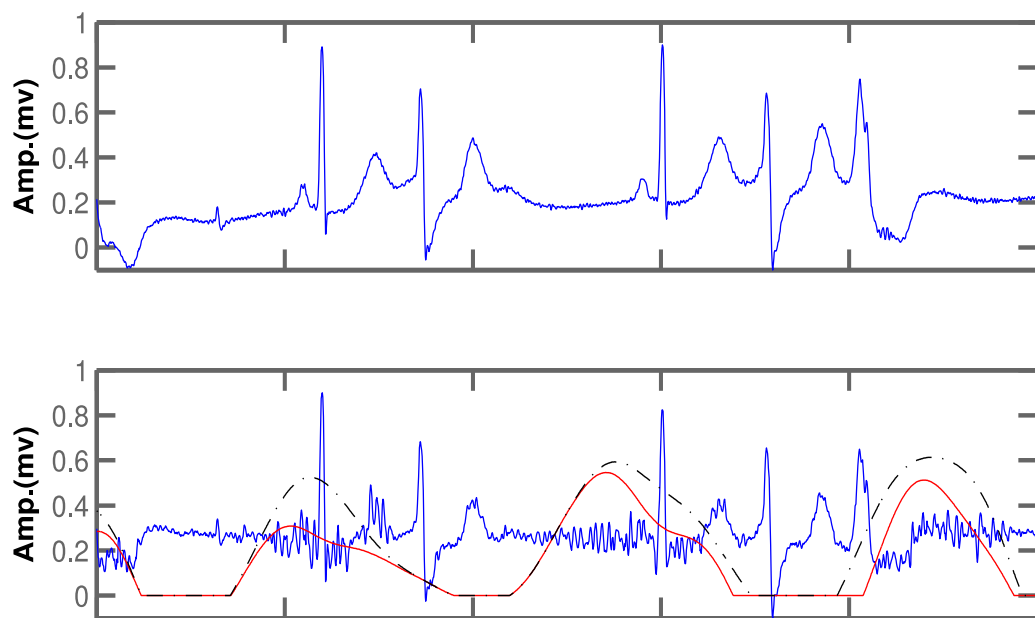


Figure 4. 13 Ventricular beats (106) record, Reference signal with (red line) and without (dashed-dotted black line) QRS exclusion. Clean ECG signal from MIT-BIH record (Top), and the same signal after noise addition (bottom).

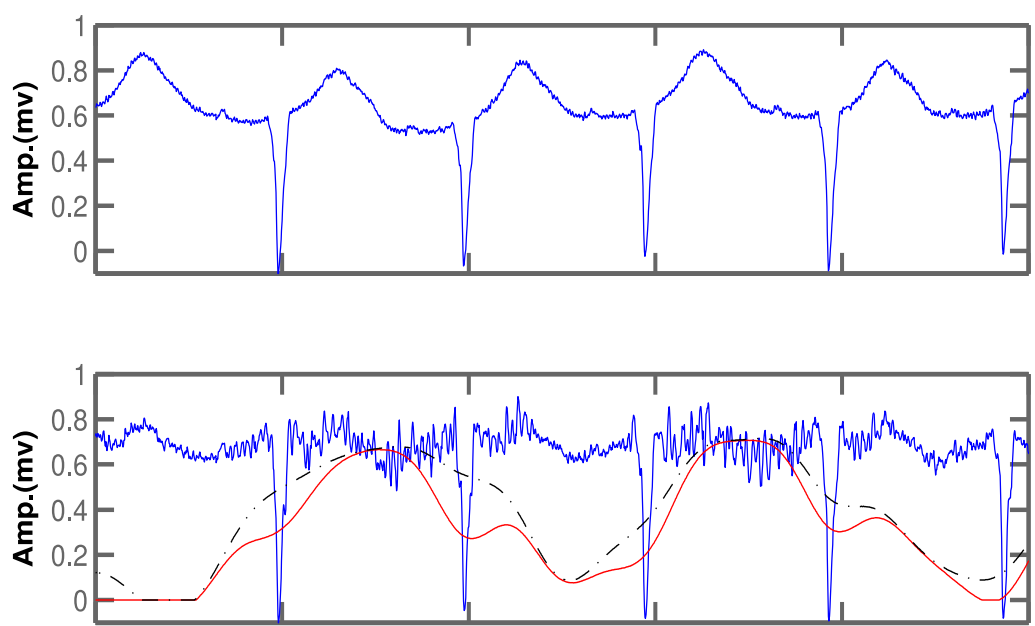


Figure 4. 14 Idio Ventricular (207) record, Reference signal with (red line) and without (dashed-dotted black line) QRS exclusion. Clean ECG signal from MIT-BIH record (Top), and the same signal after noise addition (bottom).

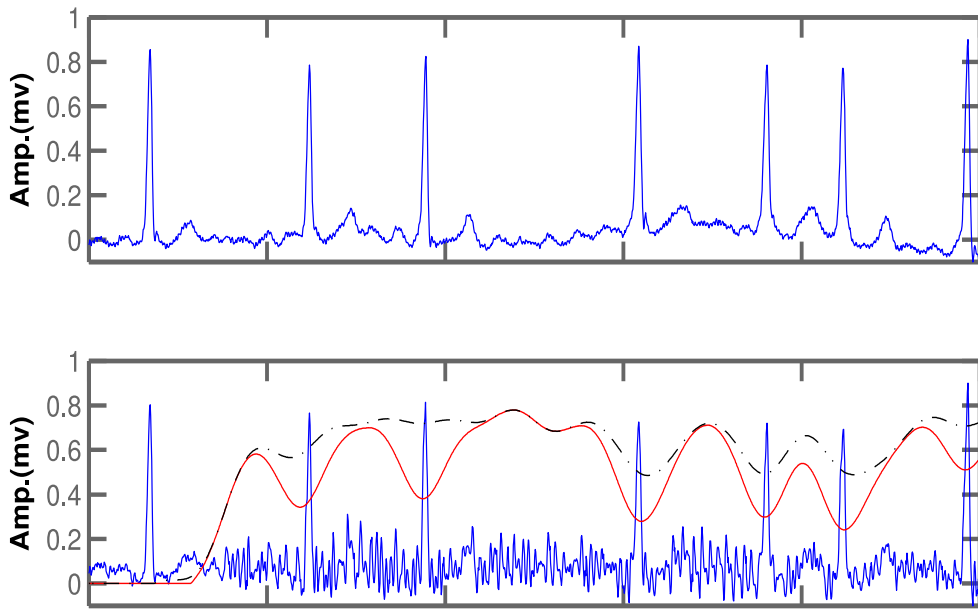


Figure 4.15 Atrial Fibrillation (201) record, Reference signal with (red line) and without (dashed-dotted black line) QRS exclusion. Clean ECG signal from MIT-BIH record (Top), and the same signal after noise addition (bottom).

EMG noise has a negative impact on the performance of QRS complexes' delineation algorithms. The delineation algorithms' positive predictive value, PPV, is the most affected value by the presence of an EMG noise, because, a delineator falsely detects EMG noise spikes as QRS complexes. Positive predictive value PPV is given as

$$PPV = \frac{TP}{TP + FN}, \quad (4.16)$$

where TP stands for the number of beats correctly detected and FN stands for the number of false positive misdetections.

The correlation coefficient of the positive predictive value with the reference signal measured on ECG intervals with different SNR values is calculated and presented. QRS single-lead delineator presented in [68] was used to detect QRS complexes from the tested ECG signals after EMG noise addition to them as described above. The positive predictive value was found after comparing QRS detection results with expert annotations available on Physionet site. The correlation coefficient of PPV with reference signal average amplitude measured upon these ECG intervals is then calculated.

The extracted reference signal gave a correlation coefficient of 0.95 ± 0.04 . Correlation coefficients between PPV and other quality estimators mentioned in the introduction were

calculated and presented in [63]. They range from 0.51 ± 0.20 for the KLT method to 0.97 ± 0.00 for the Kurtosis based method.

4.7 Reference Signal Sensitivity And Dynamic Range

Sensitivity of the extracted noise estimator depends on the thresholds σ_1 and σ_2 . In order to increase the sensitivity of the proposed method the σ_2 threshold should be decreased. This results in more noisy intervals. In other words, the dynamic range of reference signal is controllable using thresholds σ_1 and σ_2 . The thresholds, proposed in this paper, give reliable results regardless of rhythms of considered ECG signal. However, manual setting of algorithm sensitivity could be added by adding another optional parameter which controls the reference signal amplitude and subsequent usage.

4.8 Reference Signal Implementation

Running time of the proposed approach is measured after single thread implementation in C programming language. Tests were conducted on PC machine with Intel Core i3-3210 processor 3.2 GHz and memory of 8 GB on ECG signal excerpts of 5 min length. The average running time for wavelet transform along with reference signal extraction is 0.024 sec.

4.9 Applications

The proposed noise approximation method can have different applications in the ECG signal processing and analysis pipeline. In this thesis, four usages forms, which were tested and implemented, are presented.

4.9.1 Guided Leads Selection

First application is to find the best channels to be used for leads delineation combination. This could be done by studying the amount of noise on each channel over time and selecting leads according to reference signal value. For example, Lead I and Lead II could be used until the quality of Lead II drops down (reference signal amplitude values rises), and then Lead III could be used instead of Lead II, and so on. Another approach, to use the reference signal in the delineation combination, is to delineate all leads and then combine the leads' delineation results. This could be done by preferring cleaner interval delineation results when there is a mismatch in the delineation of several leads.

4.9.2 Dominant Beat Finding.

Another application of the proposed reference signal is to find the precise dominant beat from the ECG signal. This could be done by averaging only beats with reference signal amplitude below some threshold, 0.5 for example.

4.9.3 Classification And Clustering Confidence

Reference signal amplitude value indicates the noise presence ratio in the time resolution of average RR intervals. Hence, it can be used to define the certainty or the validity of the delineation, classification, and clustering algorithms applied to the signal. Usually, these algorithms are misleading when noise is present. For instance, when using classification algorithm based on template matching or distance measuring between the beats, noise causes the distance to be much larger than it should be. Consequently, the false positives are produced and the total accuracy of the analysis algorithms is negatively impacted.

4.9.4 Noisy Intervals Isolation

The reference signal could be used to make a decision about an interval's quality, and, afterwards, isolate intervals of EMG noises where noise is present. For this purpose, the usage of Rabiner's and Sambur's method is proposed to determine endpoints of isolated utterances. Therefore, EMG noise intervals' endpoints could be determined using the reference signal in the same manner sounded intervals endpoints are detected using the short time energy signal of speech signals [74]. However, using the proposed reference signal would only help to estimate signal quality vs. EMG noise. Noise in the ECG signal is more complicated and not limited to EMG noise. Other noise sources are motion artifacts and baseline noises [3]. Thus, for complete analysis that includes other noise types, other features should be extracted using other methods. A combination of features that represent different noise types could be incorporated into a special machine learning algorithm, in order to get more general classification of noisy intervals over time.

A reference signal extracted after considering QRS complexes would be more convenient for the above-mentioned applications. This is because the resulted reference signal is smoother and without amplitude variations during the QRS complexes (see Figure 5.3 in the next chapter).

4.9.5 Adaptive Noise Reduction

The usage of this signal is not restricted to quality estimation. The proposed noise approximation method provides smoothed reference signal that is suitable to be used as

guiding signal to adaptive noise reduction framework, such as adaptive filtering, filters banks, or adaptive wavelet denoising. This application is discussed in detail in the next chapter.

4.10 Conclusion

The knowledge of the statistical properties of the ECG signal, such as possible morphologies and rates, helps to find empirical thresholds. Such thresholds could be used as global thresholds in the normalization of the reference signal to increase its robustness and reliability to give more accurate results regardless of input signal rhythm.

The method, proposed in this paper, was implemented, tested, and used on real ECG signals in different parts of the ECG signal analysis pipeline. Four application of the extracted signal are proposed to be implemented in different ways. Future research is planned to develop a filtering method guided by the reference signal and to develop a machine-learning based method for customized thresholds detection according to the record properties.

Chapter 5

5. Adaptive Noise Reduction

As mentioned in the previous chapter, the usage of noise level approximation, represented by the reference signal, is not restricted to quality estimation. The proposed noise approximation method provides a smoothed reference signal that is suitable to be used as a guiding signal to an adaptive noise reduction framework such as adaptive filtering, filter banks, or adaptive wavelet denoising.

Considering arrhythmias, when the algorithm is designed, increases its reliability to give good results regardless of the input signal rhythm, which is the main reason why physicians prefer to disable all ECG signal filtering methods before interpretation. Additionally, the exclusion of zero-crossing points, peaks, and valleys, which are candidates to be a part of QRS complexes, will be translated into a reference signal that reflects the noise in the S-Q interval between each consecutive two beats. This, in turn, reduces the QRS complexes' attenuation and minimizes the distortion of any filtering method guided by the reference signal proposed in this paper. This is important because these complexes are associated with higher frequencies than other segments or waves in the ECG signal.

In this chapter, two approaches to use the noise level approximation are suggested. The first method is to develop a bank of low pass filter. The adaptive noise reduction is achieved by selecting the appropriate filter with respect to the guiding signal aiming to obtain the best trade-off between the signal distortion caused by filtering and the signal readability. This method was implemented and validated. On the other hand, a method based on wavelet wiener filtering is suggested in details without validation and implementation.

Before going into details of the proposed noise reduction methods, a brief review of some adaptive noise reduction methods is introduced. Unlike noise estimation in the ECG signal

issue, there are a plenty of reviews already published regarding the noise reduction from the ECG signal. Therefore, only the review of the most important method is included in this chapter because these methods are adopted for comparison purposes when the adaptive noise reduction method is evaluated.

For the evaluation purposes both real EMG and artificial noises are used. The tested ECG signals are from the MIT-BIH Arrhythmia Database Directory, while both real and artificial records of EMG noise are added and used in the evaluation process. Firstly, comparison with state of the art methods is conducted to verify the performance of the proposed approach in terms of noise cancellation while preserving the QRS complex waves. Additionally, the signal to noise ratio improvement, after the adaptive noise reduction, is computed and presented for the proposed method. Finally, the impact of the adaptive noise reduction method on QRS complexes detection was studied. The tested signals are delineated using a state of the art method and the QRS detection improvement for different SNR is presented.

5.1 Related work

Several methods for ECG noise reduction are presented in the literature. Linear methods for EMG noise cancellation assume stationarity in the dynamics and coloration of the noise, which is not a valid assumption in the case of real ECG signals. The classical finite impulse filtering is one of the most used methods because of its implementation simplicity. However, these methods lack the adaptation to different noise levels which makes them unsuitable for filtering the high levels of non-stationary EMG noise as they cause distortion of intervals of low noise level.

The use of discrete time wavelet transform (WT) for filtering the non-stationary ECG signals can increase effectiveness of suppression of wide-band EMG noise in comparison with linear filtering. Wavelet-based methods for EMG filtering from the ECG signals are introduced widely in the literature with different parameters and mother wavelets combinations [80, 81]. This is essentially because of the non-stationary and multi-resolutinal nature of the ECG signals, which make wavelet transform suitable as it allows a time-scale analysis. In these methods, the signal is decomposed into a set of components, where each component should represent a specific time-scale component of the original signal. The highest frequency bands (lowest time-scale components) contain EMG noise and some additive components of QRS complexes, the lower bands (higher time-scale components) contain more components of QRS complexes.

Afterwards, adjustment of the wavelet coefficients for the so called shrinkage of noise components is done in the in the wavelet domain. The coefficients thresholding is controlled by an estimation of noise-free signal or noise variance. Different parameters should be set when using the wavelet transform. Several methodologies are proposed for the automatic tuning of these parameters. The choice of the level of decomposition, the strategy of wavelet transforms coefficient thresholding/ shrinkage, and the mother wavelets used for the decomposition and reconstruction filters impact significantly on the performance of wavelet-based algorithms. Some wavelet-based methods depend to some degree on the localization of the ECG components [82].

An important feature of WT-based filtering is that it keeps additive components of QRS complexes even in the highest bands of decomposition. This property is used when the enhanced adaptive wiener wavelet filtering method is presented later in this chapter.

Other methods, such as singular value decomposition (SVD), are used for signal quality estimation and filtering [83, 84]. This method was discussed in details in chapter 3 of this thesis (refer to section 3.4.4). These methods rely largely on the detection and alignment of QRS complexes, which, in turn, are not reliable in case of noisy signals. Additionally, this method becomes unsuitable in case of arrhythemic beats presence in the signal because such beats have different morphology and could not be aligned with other normal beats to estimate the dominant QRS complex.

In addition to SVD based decomposition, other methods that rely on the averaging of successive QRS complexes are introduced. The moving average is reported to have achieved good results [36]. This method is discussed in chapter 4 of this dissertation. It relies on the periodicity of the ECG signal. The assumption behind signal averaging is that the noise at different sample times is uncorrelated, but that the signals at these times are highly correlated. Therefore, using signal averaging in time, it is possible to find the stationary portion of the signal. However, ECG signals are not periodic; therefore, it is important to solve this issue before applying averaging. Otherwise, this will have a negative impact on the final results. Stretching and shrinking operations are the bases for the conversion of quasi-periodic signals into periodic signals. The proposed algorithm exploits this feature in filtering signals with a minimum amount of distortion. After filtering the ECG signal, the residue is found by subtracting the signal average from the original input. Afterwards, the residue is filtered through a low-pass filter, and finally the filtered residue (FR) is added back to the signal average to reconstruct the output. Similar to the SVD based method, timing information is needed for the alignment of the beats. This is problematic when noise is present in the signal.

Kalman filter (KF) is also used and proposed for the purpose of ECG signal filtering [85, 86]. Similar to the SVD-based filtering, KF-based methods rely on the accuracy of the beats delineator used and their results differ largely for different rhythms.

Other methods such as adaptive filtering [87] were proposed early to filter ECG signals or even to help finding arrhythmias. However, most of these methods rely on the reference signal presented to them in order to change filters' coefficients so that the error between the filtered observations and the reference signals is minimized. This dependence makes this approach unsuitable as such reference signal is hard to find accurately. A noise level approximation or estimation is possible, though.

The classic wiener filters were also proposed for filtering of the ECG signals [88]. However, this method relies on the noise-free model presented to it, and so their performance varies depending on it [59]. Additionally, the non-stationary nature of ECG signals has a great impact on the performance of this method [82, 3] as it works in the frequency domain. This will be discussed in details later in this chapter.

In this dissertation, two approaches are presented for adaptive noise reduction approach. The main goal behind the proposed methods is to maximally preserve the useful ECG components in the clean intervals and to get the best trade-off between distortion of ECG signal waves caused by filtering and quality enhancement achieved by filtering.

5.2 Noise Level Approximation As A Guiding Signal For Filters Bank

In order to illustrate the proposed approach, a flow diagram is presented in Figure 5.1. The proposed method consists of two main parts: EMG noise extraction and adaptive reduction. The noise level approximation approach presented in [89] and discussed in chapter 4 was used in the noise level approximation block.

As mentioned in chapter 5, the stationary Wavelet Transform (SWT) is applied on the ECG signal. Using the zero-crossings, peaks, and valleys in the SWT details at scale 2^2 , a reference signal is built as translation-invariant noise level approximation. Afterwards, a multi-resolutonal analysis (MRA) at scales $2^1, 2^2, 2^3, 2^4$ was done to exclude all possible QRS complexes from the reference signal computation process. Finally, two thresholds, σ_1 and σ_2 , are used to normalize the resulting smooth signal. These thresholds were found after analyzing several recordings with different cardiac activities.

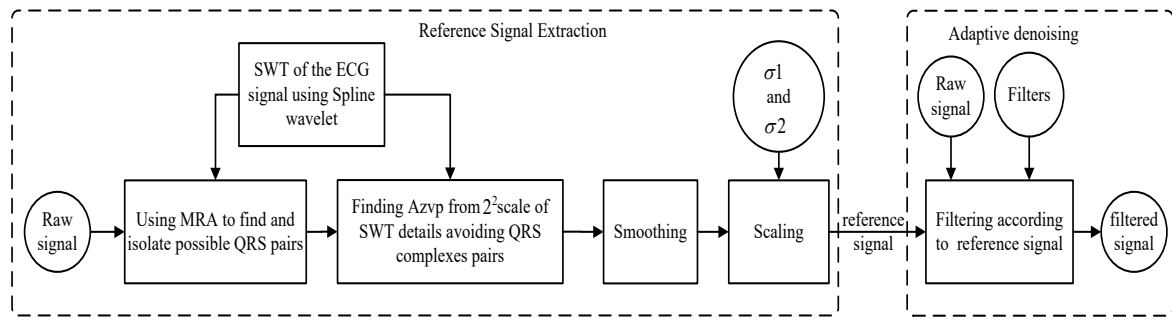


Figure 5. 1 Flow diagram for the reference signal extraction and adaptive denoising.

Scaling the signal between these thresholds allows us to focus on the EMG noise that really affects the clinical acceptability of the signal. The ECG signal interval associated with reference signal amplitude lower than σ_1 is considered as a clean signal and will not be filtered in later steps. On the other hand, signal intervals associated with reference signal amplitude higher than σ_2 will be filtered using maximal filtering strength.

Therefore, the extracted reference signal amplitude is used as a guide for adaptive noise reduction block, decreasing denoising strength in clean intervals and increasing it in noisy ones. This is realized by applying a filters bank to the signal, wherein filters are selected depending on the value of the reference signal amplitude.

5.3 Adaptive noise reduction

Filtering of ECG signals to the bandwidth of 1-30 Hz produces stable ECG with EMG noise attenuated. However, in most cases, the signal filtered in this way is not suitable for later diagnosis, because such filtering attenuates the important high-frequency components and reduces the clinical acceptability [76, 32, 77].

The proposed noise reduction method was intended to maximize the signal readability in noisy intervals and to minimize signal distortions caused by clean intervals filtering. This enhances the whole signal fidelity. Signal fidelity, after processing, measures how close the result of digital processing represents the "true" input signal [32].

For this purpose, a filters bank of 10 low pass FIR filters is used. The selection of the appropriate filters depends on the value of the reference signal at that point. The noise is removed while characteristics of the original signal are retained as much as possible at each interval. The reference signal, extracted as a noise level approximation, is quantized into 10 levels and each level is associated with one filter according to the filter strength and to the reference signal value. For instance, the ECG samples with reference signal values between 0.7-0.8 will be filtered using 7th filter in the filter bank.

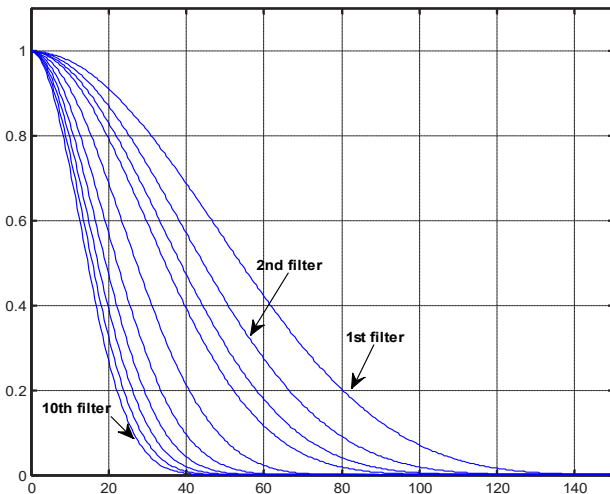


Figure 5.2 Equivalent frequency responses of filters at degree 1,...,10 for 250-Hz frequency sampling.

The filters' frequency responses (see Figure 5.2) are set to get the best trade-off between signal quality and the distortion of ECG signal caused by low pass filtering such as the attenuation of high-frequency components such as Q, R, and S waves and the widening of QRS complexes.

Filters' design and their characteristics are not the main topic in this paper, and it is important to mention that filtering with respect to the reference signal is not restricted to FIR filters.

Filters are applied only when the reference signal has the corresponding value for their activation. This could produce some glitches in the transient intervals. Smoothness of the reference signal ensures that neighboring filters are selected when the reference signal's level changes, which helps to reduce the amount of abrupt transitions and glitches in the transient intervals in the filtered ECG signal. However, this is not sufficient; special attention was given when implementing this method to compensate the delay introduced by FIR filters and to apply mean averaging within 5 samples in the transition intervals.

Exclusion of possible QRS complexes from the computation, when the reference signal is built, will be translated into a guiding signal that reflects the noise in the S-Q intervals between each consecutive two beats. Therefore, normalized reference will drop during the QRS complex. This reduces the QRS complexes attenuation and minimizes the distortion of filtering, which is important because these complexes are associated with higher frequencies than other segments or waves in the ECG signal. Figure 5.3 explains this, where filtering was done using the reference guiding signal extracted with and without the exclusion of QRS complexes.

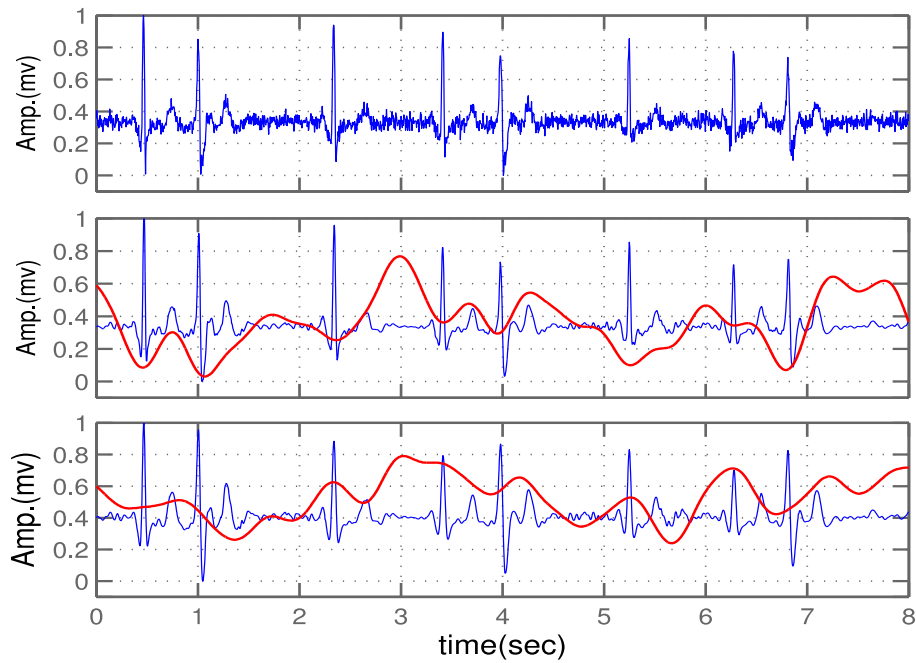


Figure 5.3 Reference signal with and without QRS exclusion.(up) Noisy ECG signal from MIT-BIH record 106, (middle) filtered signal in solid blue and reference signal extracted with exclusion of QRS components in solid red, (bottom) filtered signal in continuous blue and reference signal extracted without exclusion of QRS components in solid red.

The reference signal normalization using thresholds extracted after statistical study conducted on different heart rates and rhythms increase the reliability of its usage as the guiding signal in the filtering algorithm. Fast and abrupt changes due to arrhythmia's intervals will not be reflected in the amplitude of reference signals and, so, the proposed filtering approach will avoid these intervals.

Smoothness of reference signal ensures that neighboring filters are selected when the reference signal level change. This is important to avoid any possible glitches or abrupt transitions on transient intervals in the filtered ECG signal.

5.4 Discussion And Results

5.4.1 Noise Generation And Tested Signals

Noise generation procedure and the validation dataset used are discussed in Chapter 4. Refer to sections 4.6.1, and section 4.6.2 and to Figure 4.9.

5.4.2 Benchmark Methods And Validation

Three criterions are used to evaluate the results of the presented algorithm in this paper. Moreover, the results of the proposed adaptive noise reduction approach were compared to well-known ECG filtering methods.

For insight into how good the proposed noise reduction model is, the presented method was compared to wavelet based (WD), conventional finite impulse filtering (FIR), and Singular Value Decomposition (SVD) based filtering methods. To do this, the methods were implemented on the used evaluation data set.

The first benchmark method implemented is wavelet denoising method. The implementation of wavelet denoising was set to work with Stein's unbiased Risk Estimate (SURE) shrinkage rule, single level rescaling, soft thresholding strategy, coiflet3 mother wavelet, and, finally, 6 levels of decomposition were used. The used parameters combination gives superior results for ECG denoising [82]. The second adopted method for comparison is the well-known finite impulse filtering based on band pass filter in the recommended range of 0.4-40 Hz. The MATLAB implementation of this filter was used from the open source toolbox for ECG processing [78]. The third adopted method used the singular value decomposition (SVD) approach [82, 84]. This method performs a truncated SVD on the matrix of beats with N components. As this method relies on peaks detection, its result depends largely on the accuracy of beat's delineator. Additionally, it is sensitive to the small changes of signal morphology or noise power [82].

Graphical benchmarking results of WD, FIR, and SVD as well as the presented approach's results, with and without candidate QRS exclusion, are presented in Figure 5.2. The input ECG excerpt was selected from MIT-BIH database after the addition of real EMG noise from the MA record [72]. As it could be seen, the results of the proposed method are superior in terms of minimizing QRS complex distortion in the clean or relatively clean intervals. Additionally, a trade-off is achieved in the noisy intervals between signal quality and signal readability.

More graphical results of the proposed adaptive denoising method are shown in Figure 5.3 and Figure 5.8. The presented results are not restricted to normal sinus rhythm. Yet, different kinds of abnormal ECG rhythms are presented. Noise was added to the first four figures as mentioned in the previous section, while signals in the last two figures at the bottom were noisy signal from origin.

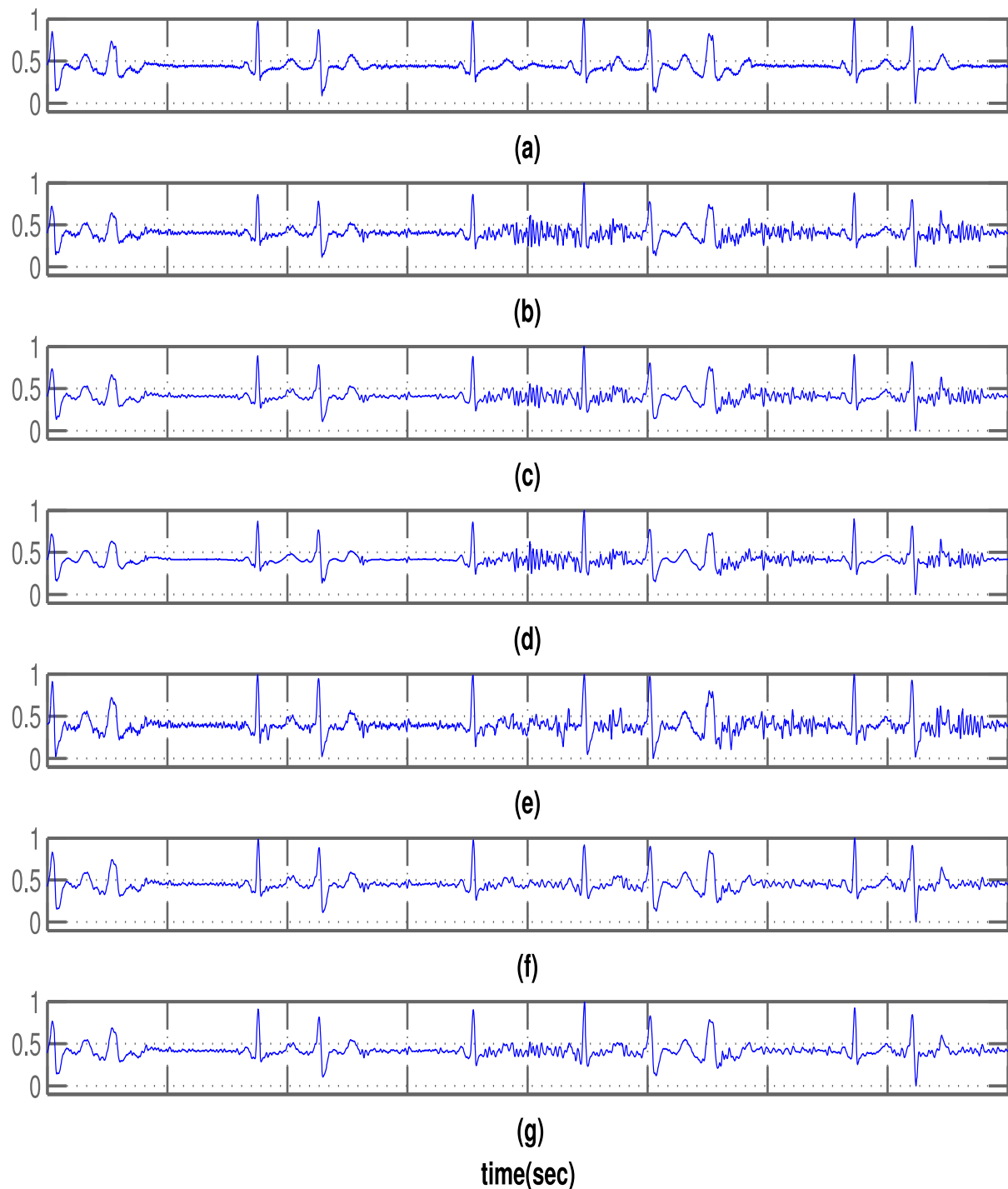


Figure 5.2 Comparison with other methods results.(a) original signal 106 record from MIT-BIH data base, (b) signal after real EMG noise addition with $\text{SNR} = 5$, (c) filtered signal with BPF,(d) filtered signal with WD, (e) filtered signal with SVD, (f) the results without the exclusion of QRS candidates, (g) the results with the exclusion of QRS candidates.

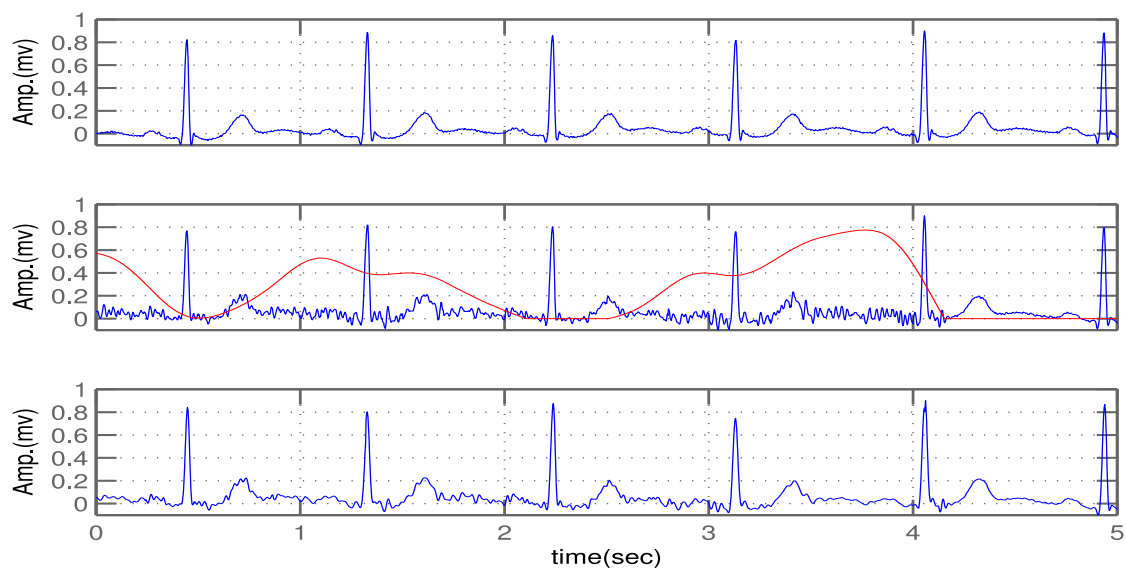


Figure 5. 3 Normal sinus rhythm MIT-BIH record(103). Adaptive denoising results. Clean ECG signal is at top of figures (a,b,c, and d), signal after noise addition is in the middle in solid blue line, while the extracted reference signal (red), and filtered signal are at the bottom.

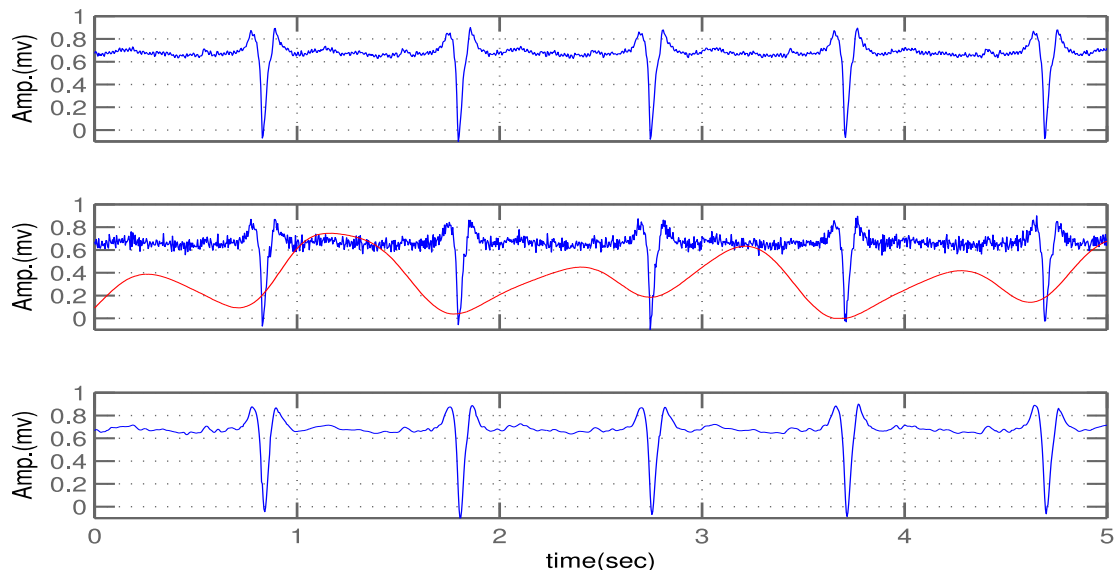


Figure 5. 4 Idio Ventricular Rhythm MIT-BIH record(207) Adaptive denoising results. Clean ECG signal is at top of figures (a,b,c, and d), signal after noise addition is in the middle in solid blue line, while the extracted reference signal (red), and filtered signal are at the bottom.

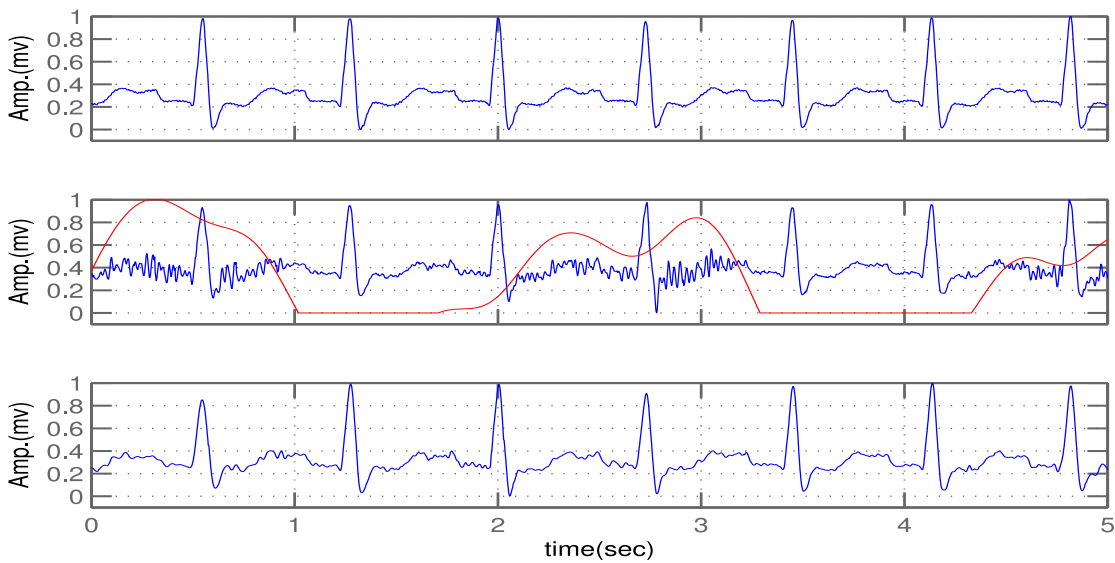


Figure 5. 5 Heart block rhythms MIT-BIH record(109) Adaptive denoising results. Clean ECG signal is at top of figures (a,b,c, and d), signal after noise addition is in the middle in solid blue line, while the extracted reference signal (red), and filtered signal are at the bottom.

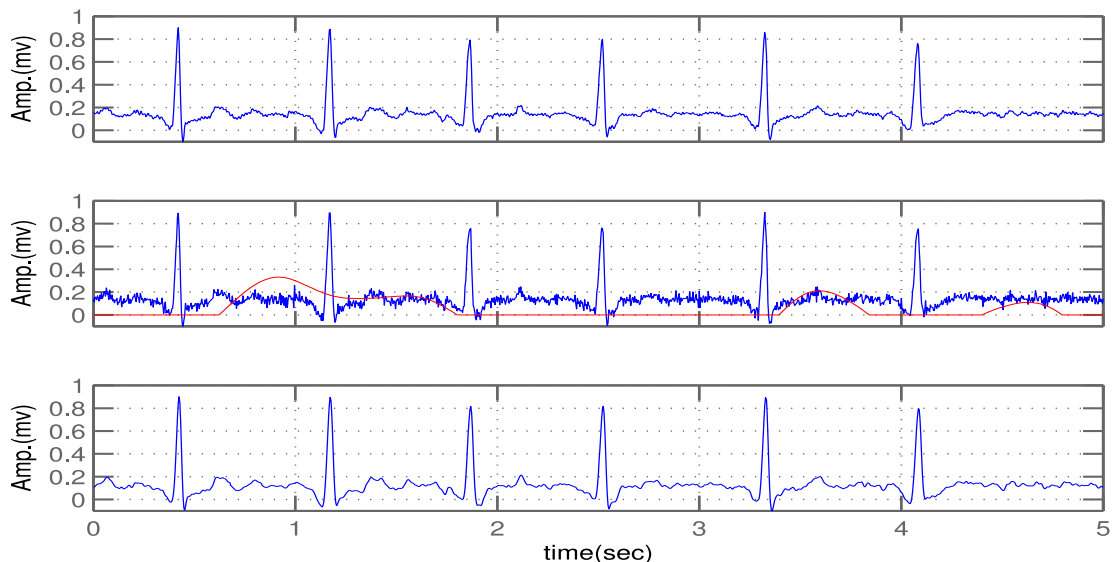


Figure 5. 6 Atrial Fibrillation MIT-BIH record(201) Adaptive denoising results. Clean ECG signal is at top of figures (a,b,c, and d), signal after noise addition is in the middle in solid blue line, while the extracted reference signal (red), and filtered signal are at the bottom.

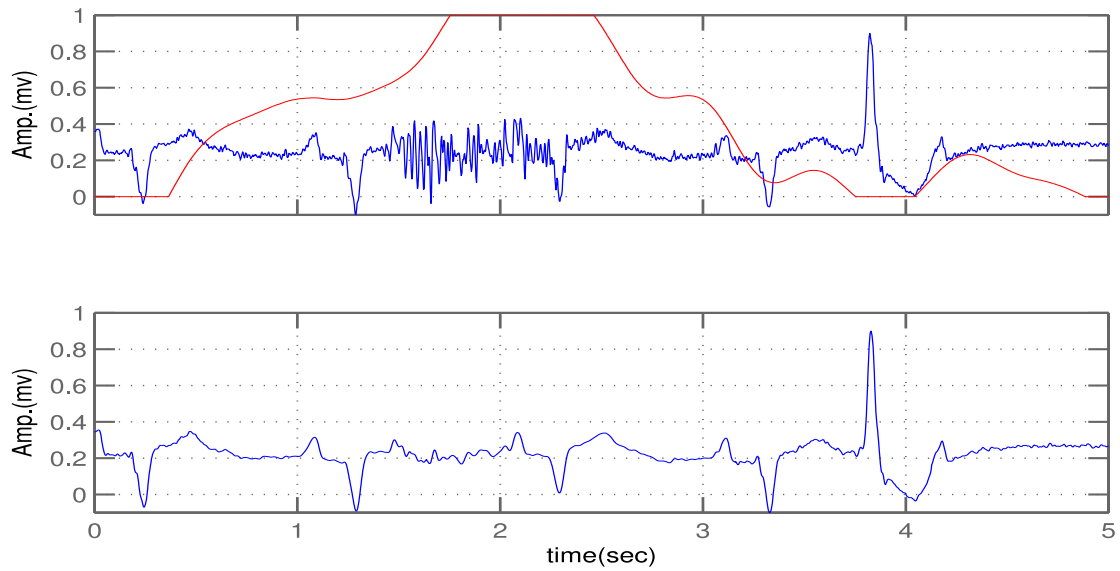


Figure 5.7 Adaptive denoising results. Filtering results of different ECG rhythms from MIT-BIH records. Noisy ECG signal from origin is at the top of figures in solid blue line, while extracted reference signal (red), and filtered signal are shown at the bottom.

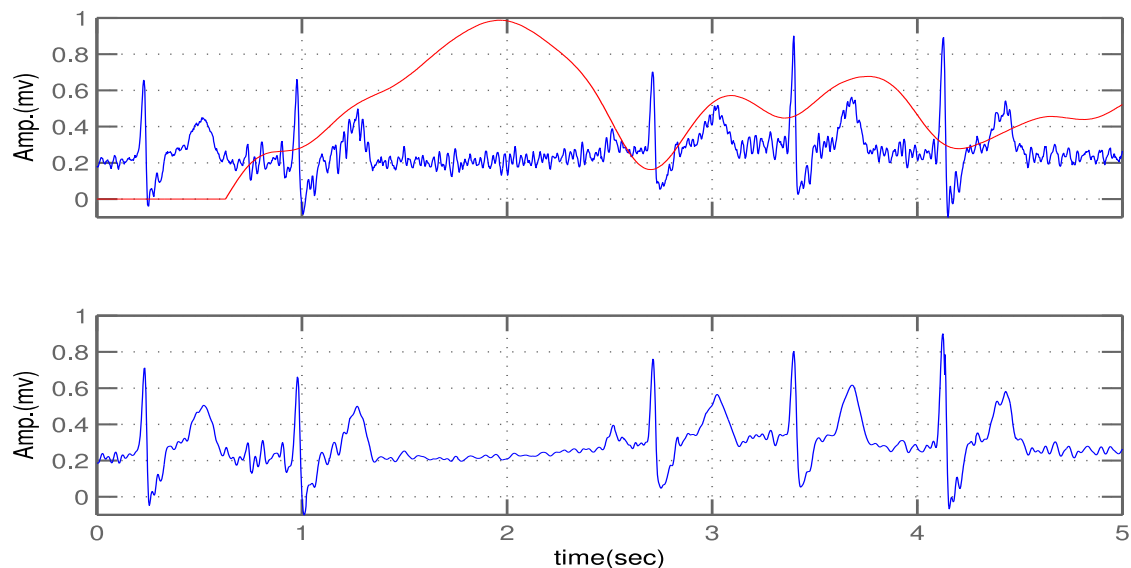


Figure 5.8 Adaptive denoising results. Filtering results of different ECG rhythms from MIT-BIH records. Noisy ECG signal from origin is at the top of figures in solid blue line, while extracted reference signal (red), and filtered signal are shown at the bottom.

In the next evaluation procedure, the fidelity of filtering method is examined. Using the proposed noise reduction method, the difference between the filtered noisy signal and the clean original signal (output-input “true”) is computed. The difference is considered as noise that is not filtered. It was used to compute the SNR value after noise reduction method is applied. SNR improvement is then computed as the difference between the input signal to added noise ratio and the output signal to remaining noise ratio. The relation of the input SNR with SNR improvement is illustrated in Figure 5.9 for first channel of MIT-BIH records 103, 117, 119.

Evidently, the presented adaptive noise reduction method enhances the positive predictivity of beats detection algorithm without affecting its sensitivity. The importance of the adaptive approach arises in the case of signals with high ratio of premature ventricular contractions (PVC) such as the MIT-BIH record 106 because QRS complexes in clean or relatively noisy intervals are not over-smoothed. This is because over-smoothing (aggressive filtering) of PVC beats misleads the delineation algorithm so to detect them as a T wave.

Beside noise attenuation and the readability enhancement, the proposed algorithm remarkably enhances the QRS delineation results in noisy signals filtered using the guided filter bank. Thus, the impact of the proposed method on ECG delineation was studies. For this purpose, a Single-Lead beats detector algorithm proposed in [68] is used to delineate both noisy signals using the time mask before and after filtering. Sensitivity and positive predictivity are computed for both signals. Table 5.1 shows the impact of adaptive denoising on delineation of first channel of MIT-BIH records 103, 106, 117, 118, and 123 for muscle noise from MA record.

Running time of the proposed approach is measured after single thread implementation in C programming language. Tests were conducted on PC machine with Intel Core i3-3210 processor 3.2 GHz and memory of 8 GB on ECG signal excerpts of 5 min length. The running time of the adaptive noise reduction is 0.008, while the reported average time of the reference signal extraction is 0.024 sec. Hence, the average total time for the entire algorithm is 0.032 for ECG signal of 5 min length and sampled with 250 Hz.

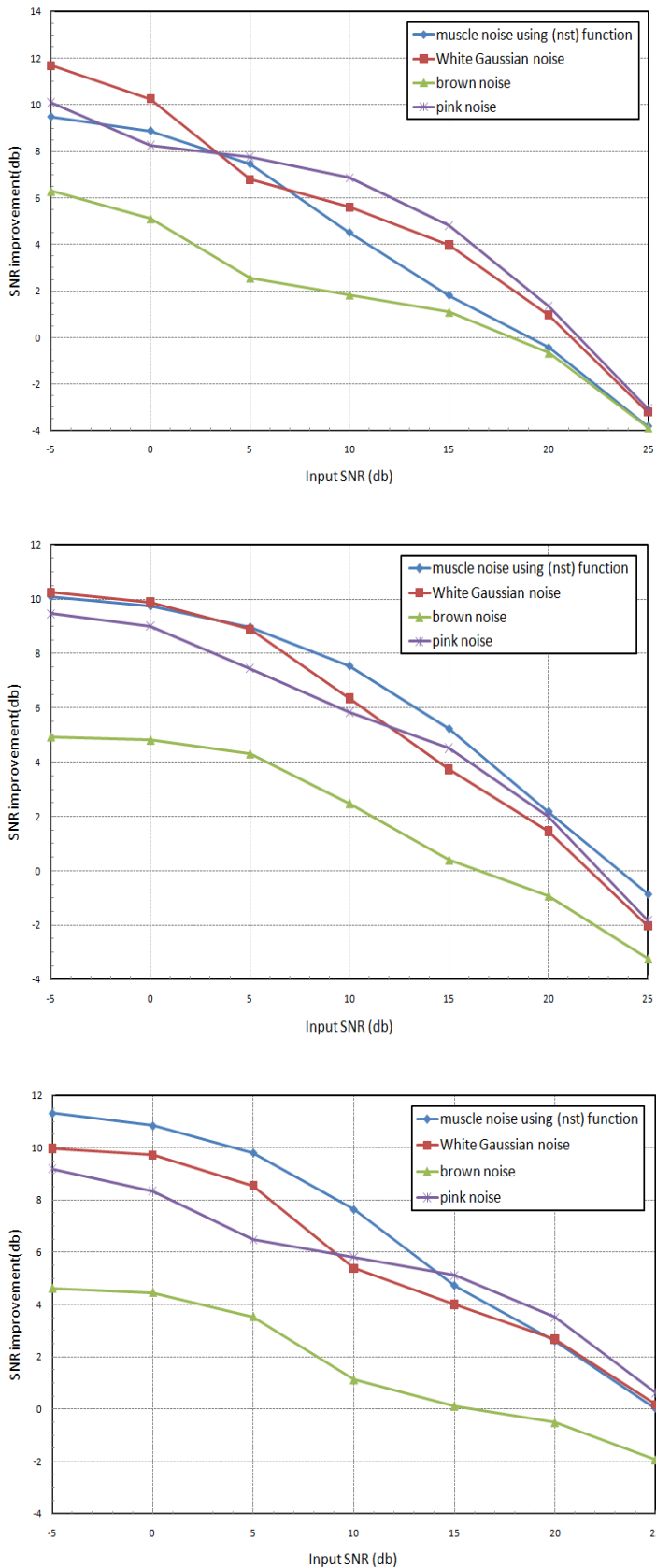


Figure 5. 9 SNR improvement after adaptive denoising of Lead I of MIT-BIH records (from top to bottom 103,117,119) computed for four types of noises.

Table 5.1 Single lead delineation results with and without the usage of adaptive denoising.

		103		106		117		118		123	
		PP[%]	SEN[%]								
SNR=-5	Raw signal	98.110	99.808	93.496	94.466	78.846	96.408	85.831	92.436	98.053	99.802
	Denoised	99.521	99.904	98.363	97.974	90.000	99.935	96.203	99.164	99.539	99.934
	improvement	1.411	0.096	4.867	3.508	11.154	3.527	10.372	6.728	1.486	0.132
SNR=0	Raw signal	99.952	99.952	99.241	96.937	92.757	99.543	97.776	98.593	99.934	99.934
	Denoised	100.000	99.904	99.899	98.172	98.710	99.935	99.649	99.912	99.868	99.934
	improvement	0.048	-0.048	0.658	1.235	5.953	0.392	1.873	1.319	-0.066	0.000
SNR=5	Raw signal	100.000	99.952	99.899	97.431	98.519	99.935	99.868	99.912	100.000	99.934
	Denoised	100.000	99.952	100.000	98.221	100.000	99.935	100.000	99.956	100.000	99.934
	improvement	0.000	0.000	0.101	0.791	1.481	0.000	0.132	0.044	0.000	0.000
SNR=10	Raw signal	100.000	99.952	99.949	97.678	99.739	99.869	99.956	99.956	100.000	99.934
	Denoised	100.000	99.952	100.000	98.221	100.000	99.935	100.000	99.956	100.000	99.934
	improvement	0.000	0.000	0.051	0.543	0.261	0.065	0.044	0.000	0.000	0.000
SNR=15	Raw signal	100.000	99.952	99.949	97.628	99.804	99.869	100.000	99.956	100.000	99.934
	Denoised	100.000	99.952	100.000	97.875	100.000	99.935	100.000	99.956	100.000	99.934
	improvement	0.000	0.000	0.051	0.247	0.196	0.065	0.000	0.000	0.000	0.000
SNR=20	Raw signal	100.000	99.952	99.949	97.727	99.804	99.869	100.000	99.956	100.000	99.934
	Denoised	100.000	99.952	100.000	97.777	100.000	99.935	100.000	99.956	100.000	99.934
	improvement	0.000	0.000	0.051	0.049	0.196	0.065	0.000	0.000	0.000	0.000
SNR=25	Raw signal	100.000	99.952	99.949	97.628	99.804	99.869	100.000	99.956	100.000	99.934
	Denoised	100.000	99.952	100.000	97.826	100.000	99.935	100.000	99.956	100.000	99.934
	improvement	0.000	0.000	0.051	0.198	0.196	0.065	0.000	0.000	0.000	0.000

Running time of the proposed approach is measured after single thread implementation in C programming language. Tests were conducted on a PC machine with Intel Core i3-3210 processor 3.2 GHz and memory of 8 GB on ECG signal excerpts of 5 min length. The running time of the adaptive noise reduction is 0.008, while the reported average time of the reference signal extraction is 0.024 sec. Hence, the average total time for the whole algorithm is 0.032 for ECG signal of 5 min length and sampled with 250 Hz.

5.5 Noise Level Approximation as a Guiding Signal For Wiener Filter

The non-causal frequency-domain Wiener filtering is one of the best models used when there is prior statistical knowledge about signal and noise dynamics. It is used to statistically estimate the unknown clear signal based on the real observations, which are, in this case, a noise-corrupted signal. A related signal should be provided as an input to this method and filtering is supposed to use it to produce the estimate as an output. In the case of noise corrupted signal, noise model or signal model should be provided and the filtering will

use them to ideally estimate the output. Hence, the Wiener filter is based on a statistical approach that is based on the statistical models of signals and noise. It assumes that both the signal and the noise are statistical (not deterministic) Signals (see Figure 5.10). For the application of filtering additive noise, the optimal (non-causal) Wiener filter is given like so

$$H(f) = \frac{S_y(f)}{S_y(f) + S_d(f)}, \quad (5.1)$$

where $S_y(f)$ is the power spectrum of the desired clear signal y , and $S_d(f)$ is the power spectrum of the noise d which we want to eliminate.

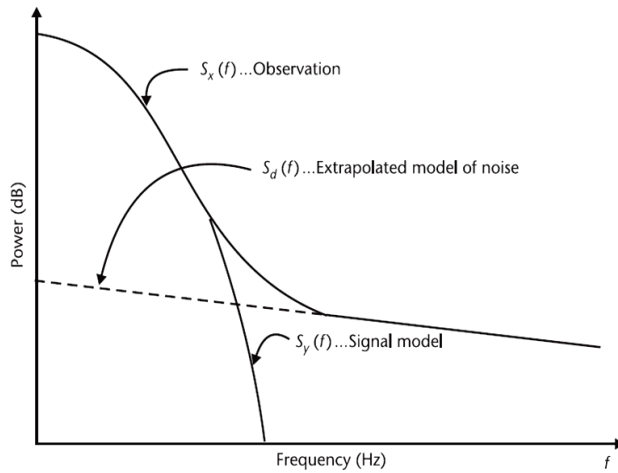


Figure 5. 10 A log representation of the power spectral components of a signal for Wiener filter.
Image adapted from [3].

Unfortunately, in the case of non-stationary ECG signals this is a tricky issue due to the unpredictable dynamics of both signals and noise as discussed in the previous chapters.

Furthermore, Wiener filtering, when applied in the frequency domain, relies on the fact that signal is stationary, since the signal is filtered in the frequency domain over the entire segment of the ECG. This also reduces its applicability on ECG signals.

Efforts are done, in the literature, to reformulate this method and to adapt it to be used for the ECG signals [3]. One of these methods is the wavelet wiener filtering. This method is a wiener-filtering model that utilizes wavelet filtering to estimate the noise free coefficients needed to calculate the correction factor of the wiener filter. The wiener filter is then applied on the wavelet coefficients of the wavelet-filtered signal and then the output coefficients are found as an output. The principles of this method were firstly proposed in [90] and a similar approach was introduced later in [91] using the DWT.

In [92], the usage of SWT instead of DWT was proposed; however, the WT was used to estimate the noise-free signal in a time-variant manner using decimation. In [93], both the

estimation and the filtering were conducted using the time-invariant SWT version of wavelet transform. This is also adapted in the method proposed in this section.

The Wiener filter requires an estimate of a noise-free signal, which is necessary to calculate the correction factor for the adjustment of transform coefficients. The classic usage of wiener wavelet filtering is shown in Figure 5.11.

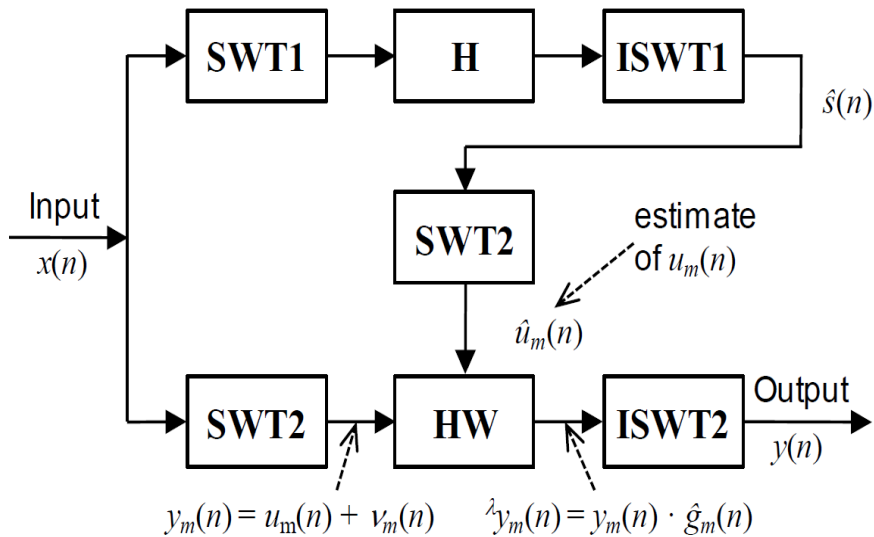


Figure 5.11 The block diagram of the Wavelet Wiener Filtering approach. The upper path is used to estimate the noise-free signal and the lower for wiener filtering using the noise-free estimation. Image adapted from [94]

So, the SWT is applied on the signal SWT1 in the upper path, then a filtering or shrinkage of SWT coefficients is done and the reverse ISWT1 is employed to reconstruct a noise free signal. This noise free signal is then used to find the noise free stationary wavelet coefficients used as an input to the wiener filter. The wiener filter, in this workflow, is supposed to filter the stationary wavelet coefficients of observation based on the noise-free estimation of these coefficients, provided from the upper path.

The upper path includes a classic wavelet filtering method where coefficients are adjusted using thresholding based on the noise variance estimation. Thresholds are defined for each level as in

$$\lambda_m = TM \cdot \sigma_{vm}, \quad (5.2)$$

where TM is an empirical threshold, and σ_{vm} is the standard deviation of the noise in the

m^{th} time-scale component. In order to obtain an adaptive threshold according to the noise level in the signal, the authors in [95, 96, 97, 98] propose an equation to compute the threshold like so

$$\sigma_{vm} = \frac{\text{median}(|y_m|)}{0.6745} \quad (5.3)$$

Using this equation, the standard deviation is calculated using a sliding window in time-dependent manner. In [94] authors propose a method to define, dynamically, the length of this window.

On the other hand, wiener filter will work in the time-scale domain of SWT and its correction factor is computed as in (5.4).

$$\hat{g}_m(n) = \frac{\hat{u}_m^2(n)}{\hat{u}_m^2(n) + \sigma_{vm}^2(n)}, \quad (5.4)$$

where $\hat{u}_m^2(n)$ is the squared wavelet coefficients obtained from the estimated noise-free SWT coefficients. This factor is then applied on the coefficients of the input signal to obtain the output signal as in

$$\lambda_{y_m}(n) = y_m(n) \cdot \hat{g}_m(n) \quad (5.5)$$

Finally the filtered coefficients are inversed back to obtain the filtered ECG output.

Authors in [94], propose a method to add more adaptivity to this method. They propose the usage of dyadic SWT in the Wiener filter and also in the estimation of a noise-free signal. The goal of that method is to find the most appropriate filter banks and also try to recommend other parameters of the Wiener filter; depth of decomposition of the input signal, size of the threshold, and the thresholding method used for estimating a noise-free signal. Selection of the appropriate parameter values was conducted with a view to maximize the average resulting signal-to-noise ratio (SNR) for all the signals tested. In order to achieve this goal, they added a new block to estimate the noise level or signal-to-noise ratio over time.

Inspired by the above mentioned method, a new approach is proposed to enhance the performance of adaptive wiener wavelet filtering. Instead of applying prior segmentation of the ECG signal in order to calculate the SNR changing value over time, the noise level approximation signal provides a better normalized smooth estimation of this value. Therefore, the reference signal could be used to enhance the performance of wavelet coefficients filtering by applying different thresholding parameters, depending on the

estimated noise over time, in a similar manner to the previously filters bank method. Therefore, the noise free estimation of the wavelet coefficients could be enhanced by applying thresholding and wavelets parameters that change smoothly over time depending on the approximated noise level. Moreover, the approximated noise level that takes arrhythmia into consideration will be more accurate in finding the noise free coefficients needed for the wiener correction factor. The block diagram of the proposed algorithm is given in Figure 5.12.

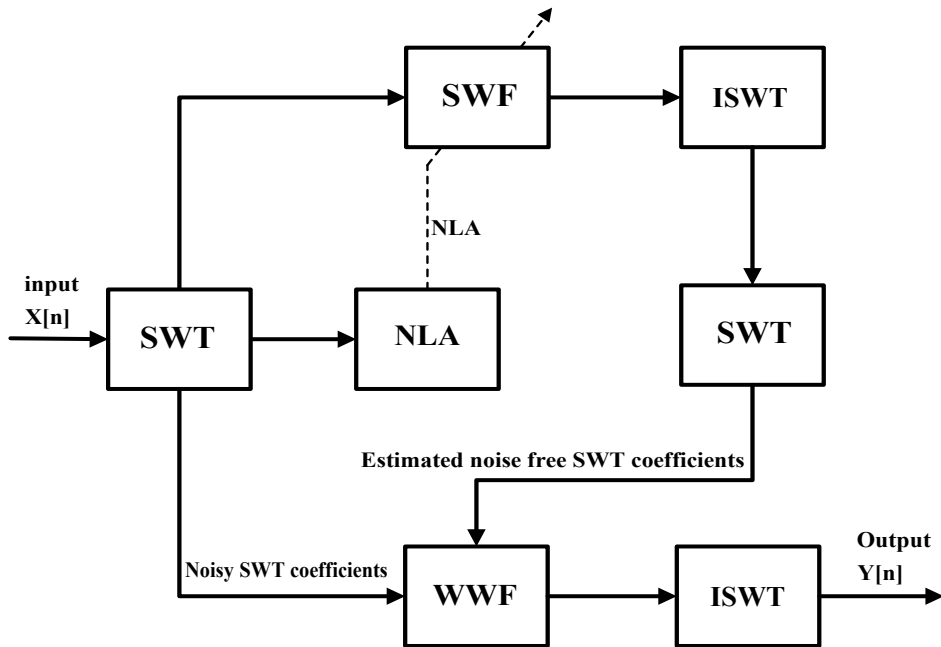


Figure 5. 12 The block diagram of the proposed Adaptive Wavelet filtering using the extracted noise level approximation (NLA) which is used to adapt the filtering of wavelet coefficients to get adaptively filtered noise free estimation. The estimated noise free coefficients are then used to compute the filtering factor of Wiener filter (WWF).

5.6 Conclusion

The proposed noise approximation method provides a smoothed reference signal that is suitable to be used as a guiding signal for an adaptive noise reduction framework. The main contribution of proposed methodologies is maintaining signal characteristics in intervals where noise reduction is not crucial for automatic analysis, while reducing the noise level adaptively in noisy intervals where noise could have a negative impact on analysis results. The guiding reference signal used takes the arrhythmia presence into consideration which increases the reliability of its application in this approach.

Chapter 6

6. Algorithms integration in a multi-purpose ECG telemetry system

The main theme of this thesis is a part of the development efforts of an ECG telemetry system. This provided a platform to evaluate and integrate all algorithms on real world data. In this chapter, the design, implementation, and validation are introduced for the multi-purpose telemetry system, where the foregoing methods are implemented and used. The proposed device is intended for recording, transmission, and interpretation of ECG signals in different recording modes. The system consists of an ECG device, a cloud-based analysis pipeline, and accompanying mobile applications for physicians and patients.

The proposed ECG device's mechanical design allows laypersons to easily record post-event short-term ECG signals, using dry electrodes without any preparation. Moreover, patients can use the device to record long-term signals in loop and holter modes, using wet electrodes. In order to overcome the problem of signal quality fluctuation due to using different electrodes types and different placements on subject's chest, customized ECG signal processing and interpretation pipeline is presented for each working mode.

Additionally, the evaluation of the novel short-term recorder design is presented. Recording of an ECG signal was performed for 391 patients using a standard 12-leads golden standard ECG and the proposed patient-activated short-term post-event recorder. In the validation phase, a sample of validation signals followed a peer review process, wherein two experts annotated the signals in terms of signal acceptability for diagnosis. It has been found that 96% of signals allow detecting arrhythmia and other signal's abnormal changes. Also, the correlation coefficient between the 12-leads golden standard ECG recorder and leads recorded using the proposed device is presented. Finally, the automatic QRS delineation

results, of both short-term post-event signals and 12-leads golden standard ECG signals, are compared and presented.

The proposed multi-purpose ECG device allows physicians to choose the working mode of the same device according to the patient status. The proposed device was designed to allow patients to manage the technical requirements of both working modes. Post-event short-term ECG recording using the proposed design provides physicians with reliable three ECG channels with direct symptom-rhythm correlation.

6.1 Background

Over the last few years, many new ECG measuring applications emerged, taking advantage of widespread use of smart phones. Patients with cardiac issues, as well as healthy people, can now record ECG signals and send them to physicians or health centers using modern communications technology, thereby enabling ECG recording regardless of place and time. Different designs of ECG devices were proposed to operate in the telemedicine system in order to make the procedure of signal recording easy and smooth for users [99, 26, 27, 100, 101].

Personal ECG devices can be divided into holter devices, and event recorders as discussed in Chapter 2. Refer to Section 2.5.4, section 2.5.5, Figure 2.11, Figure 2.12, and Fig1.3 for more details.

The main limitation of Holter monitoring is the detection of intermittent arrhythmias, because symptoms happen infrequently. Additionally, there is no real-time analysis of the recoded signals. In these cases, an event monitor could be used [22, 23, 24, 25]. The second type of ECG monitoring applications is the event monitoring. Event recording devices can be divided into loop and post-event recorders. In loop recording approach, electrodes are in long-term continuous contact with patient's skin and the event signal storing and processing is triggered by patients or by an embedded algorithm [102, 103].

Different devices emerged to make the loop ECG event recoding easier and wireless [26, 27, 100] using wearable fashion such as belts and T-shirts. However, the quality of the recorded signals is still the major impediment facing the efforts to replace signals recorded with standard wet adhesive electrodes which are still the favored choice for long-term recording [29]. Poor signal quality and, consequently, poor clinical acceptability are the main reason for imprecise delineation and misclassification of heart beats with artifacts. Moreover, the lack of signal quality makes the algorithm event-activated devices generate false alarms and store misleading intervals which increase the physician cost [22].

All of this was the motivation to develop a multi-purpose ECG device to be operated in a telemetry system platform. Both long-term holter and post-event short-term recording modes are enabled using a single device. The design and implementation of the proposed device and processing pipeline makes these different ECG recording modes smooth and easy to do for a layperson.

In the following sections, a brief description of the system design and architecture is introduced. The evaluation process and validation results are presented, and finally, a conclusion is drawn.

6.2 System Architecture and Design

The basic scheme of the telemedicine system in which the ECG device is supposed to work is shown in Figure 6.1. The system consists of three main components: an ECG device, an algorithms/storage server, and users' applications for signal recording, transmission, and cloud-based analyses. The basic concept is to allow patients to record and send ECG signals to the algorithms/storage center. Experts have instant access to the sent signals through mobile and web applications, where they can view all sent signals and the automatic algorithms' proposals for them.

Recorded signal is sent from the ECG device to algorithms/storage server either via Bluetooth to phone application. Signals are, then, sent to algorithm/storage server using the phone's GSM network Internet service, or directly via GSM/GPRS module embedded in the device. In the previous, the embedded GSM/GPRS module communicates directly with the server using the GSM operator network. The last option is important, especially for patients who don't use smart phones, such as parts of the elderly population, and for fast instant ECG signal transmission when a smart phone is not operable.

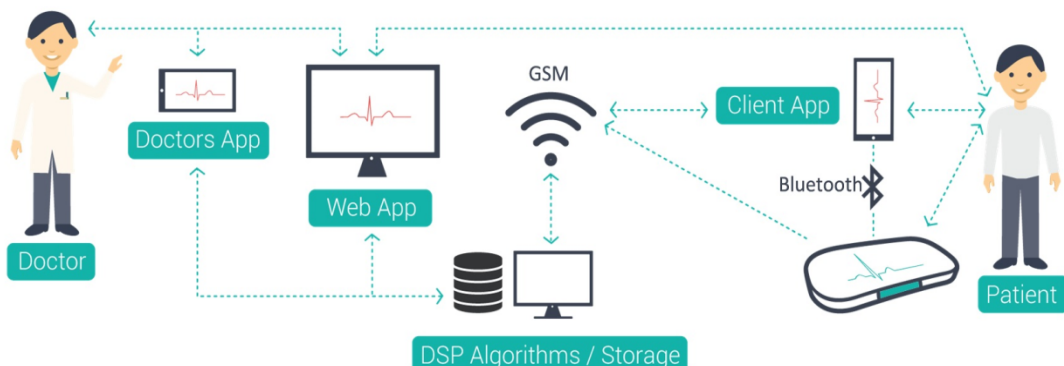


Figure 6. 1 The basic diagram of the presented platform and its principal components, where the device is wirelessly transmitting the recordings to a handheld mobile phone which transmits the signals to a cloud server. Signals could be directly transmitted to the cloud server using GSM connection

Received signals are further processed on the server and then classified into critical or urgent and uncritical signals. Urgent signals are signals sent with an urgent flag by patients or those including a rhythm that is not considered a normal rhythm by algorithms. Thus, experts receive a notification when a signal is received and an urgent notification when the signal is flagged as urgent. Processing of signals and their classification into urgent and uncritical helps to reduce the workload of physicians and reduces the cost of the whole telemedicine platform.

6.3 Mechanical Design And Working Modes

Mechanical design of the ECG device presented in this paper is shown in Figure 6.2. It mainly consists of a short-term post-event recorder body, and a long-term recorder body which is also the main ECG acquisition module. The separation of these two main parts allows the device to work in two independent modes: short-term post-event recording and long-term Event/Holter recording mode.

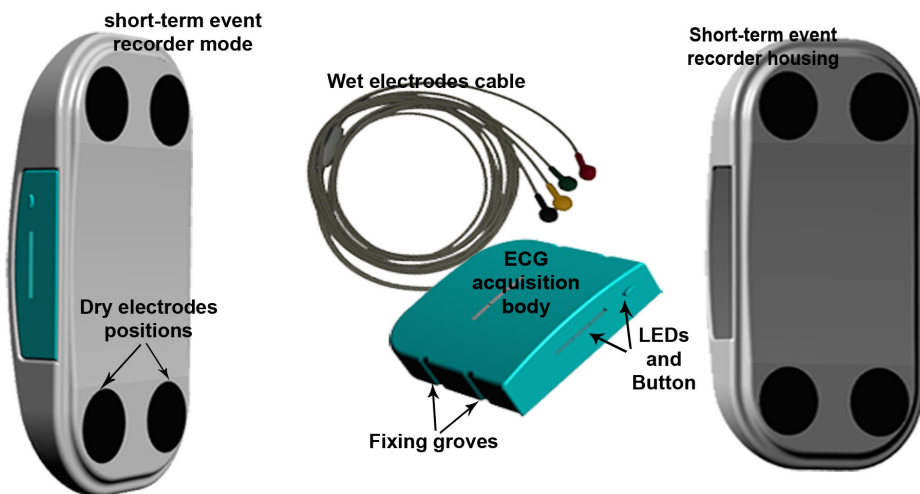


Figure 6. 2 The principal components and mechanical design of proposed ECG device, where short-term post-event recorder is enabled by inserting the ECG acquisition body in the short-term post-event recorder housing. Holter or long-term recording mode is enabled by connecting the cable of wet adhesive electrodes to the ECG acquisition body

Consequently, patients can always carry the device around in their pockets and in case of typical testing, chest pain, or other arrhythmia symptoms, they can apply the device to the chest area and start recording three ECG channels, sensed by dry electrodes, without any preparation and wires. For this reason, the event recorder housing is provided with four dry electrodes positioned in the corners of an imaginary rectangular shape whose vertices are drawn on the slightly curved housing.

The short-term post-event recorder housing has inner jumper pins that are responsible for detecting the working mode of the device. Hence, when an ECG acquisition body is inserted into the short-term post-event recorder housing, the device activates a short-term post-event recorder mode and the ECG signal recording is performed using dry electrodes. In this mode, ECG main acquisition module is locked in the event short-term housing. This is achieved by embedding several latching blocks in the short-term post-event recorder housing and, when the ECG acquisition body is inserted, they fix on several latch grooves on the side faces of acquisition body.

In order to run the device in the long-term recording mode, a user can easily extract the acquisition body using finger nails and attach the wet adhesive electrodes cable to start recording three standard ECG channels. For this reason, two slits between the ECG acquisition body and the short-term cover housing are left.

6.4 Dry And Wet Electrodes

The main problem associated with long-term ECG signal recording is signal quality vs. noise and motion artifacts. Signal quality is significantly affected by electrode-skin impedance and by electrode's stability on the subject's chest. For this reason, it is important to apply the right types of electrodes that last for a long time and are able to record a reliable ECG signal according to the selected working mode.

The stability of Ag/AgCl electrodes, along with their low electrode-skin impedance, makes them the most common and favored electrodes for ECG measurements. These electrodes are non-polarizable electrodes, so the charge can cross the electrolytic gel which is used to facilitate the electrochemical reactions and to reduce electrode-skin interface impedance. Thus, they are associated with low electrode-skin impedance, low noise and low motion artifact [29]. For these reasons, the disposable wet Ag/AgCl electrodes are used for long-term recording and electrodes' snap connectors' cable is provided with the device.

On the other hand, short term event recording requires electrodes that can last for a long time and need minimal preparation. Dry electrodes are the best choice for short-term fast event recording, mainly because they don't need any prior preparation. The materials from which the dry electrodes are made are more durable than Ag/AgCl electrodes; therefore, they do not need to be changed after recording [29, 104].

Several electrodes providers are already competing in the market to sell their technology. When the design efforts of the proposed device started, a specific type of dry electrodes had to be selected at that moment for further development. Two parameters were decisive in that

phase of development. The first parameter is signal quality, and the second one was diagnostic potential.

Signal quality was estimated using noise level approximation method proposed in this thesis. The electrocardiography signals were recorded using a prototype of the specialized analog front end for each electrode type and then the noise approximation was calculated from these recordings.

The second metric was the diagnostic potential of signals. This parameter was evaluated by expert cardiologists who investigated signal characteristics and decided on the best recordings. After this evaluation procedure, electrodes in [106] were selected.

The dry electrodes used are polarized electrodes and their skin-electrode impedance is higher in the frequency band of the ECG signal. Authors in [29, 104, 105] compared the skin-impedance of different types of electrodes made of different materials. The results of their study showed that Orbital dry electrodes give superior performance as opposed to other dry electrodes in terms of skin-electrode impedance.

Orbital electrodes have pins or spikes on their contact surface that support the strong attachment of electrodes to skin, since they penetrate the highly resistant skin stratum corneum layer. This helps to reduce the skin-electrode impedance, and stabilize the device body on the subject's chest, which positively influences the recorded ECG signal quality. Therefore, these dry electrodes [106] are used for short-term recording. In order to overcome the skin-electrode impedance difference between dry and wet electrodes, the resistance at the instrumentation amplifier input is controlled in the electrodes' analog front end. Thus, higher input impedance is used when event mode is activated to record ECG with dry electrodes. This helps to minimize the loading effect and ensures signal amplitude consistency in both modes [107].

Another important issue is the distance between electrodes and its effect on signal amplitude. The chest size has great impact on the signal recorded in the short-term event mode because the distance between the electrodes is fixed (14×7 cm) for all chest sizes. To resolve this issue, a special step, in the analysis pipeline of the signals, is added to extract reference templates and then use them in the analysis of the signals, as will be discussed in more details later in this paper.

6.5 ECG Acquisition Module

The block diagram of the ECG acquisition module is shown in Figure 6.3. All components are embedded in the ECG device except for electrodes and interconnections. The first and

most important component is the ECG signal analog front end. The on-chip device, presented in [108], was used. This chip is designed and tested following the AAMI EC11 standard to simplify the task of acquiring and ensuring the quality of the ECG signals. Wherein, it has amplifiers and analog to digital converters (ADC) able to provide up to five ECG channels in low power operation mode of 15 mW for three ECG leads. Additionally, it has an embedded right leg driver logic which was set and used for lead-off detection and noise rejection. This driver logic helps in solving the problems of broken lead occurrence, or poor electrode-skin contact and eliminating interference noise by actively canceling the interference [108]. The on-chip device was set to work at a 19-bit level in 2 KHz data rate, which is later downsampled to 250 Hz. Serial Peripheral Interface (SPI) communication is implemented to transmit data and control commands between the on-chip device and the host processor.

The ECG module also has a host processor (MCU), internal memory (eMMC) able to save patients' information, and three leads recordings up to 7 days, a lithium battery 3.7 V along with its charging facilities (battery charger chip and fuel gauge), a Bluetooth transmission module, a GSM transmission module, one button and indicating Light-emitting diodes (LEDs), a near field communication (NFC) module, and, finally, a USB I/O port for charging, testing, and wired file transmission. A universal asynchronous receiver/transmitter (UART) communication is implemented to enable the communication between the GSM and the MCU modules.

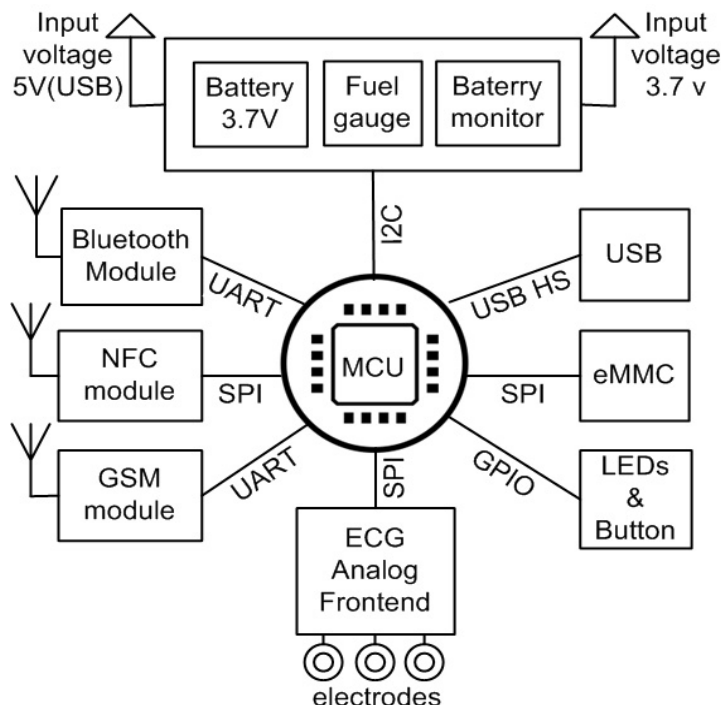


Figure 6. 3 ECG acquisition module architecture

The usage of the NFC module for telemedicine medical devices was presented in [109, 110, 111]. The near field communication module addition makes the procedure of event recording, based on mobile phones, autonomous, easy-to-use, and instant. The NFC module is embedded in the proposed device with Radio-frequency identification (RFID) tag and a field detector, and is set to work in passive mode. The automatic pairing of a smart phone and an ECG device is activated when a patient moves the back of the smart phone toward the back of an ECG recorder. Thus, when the field detector detects the mobile phone's NFC field, it activates a microcontroller by raising interrupt that starts the recording workflow. Simultaneously, the mobile phone reads the connection information from the RFID tag to launch a smart phone application and to establish a Bluetooth pairing with the ECG device.

6.6 Mobile Application

Medical data exchange between experts and patients is enabled using two smart phone applications built as a part of the telemedicine platform proposed in this paper.

The first application is the patient's, which was built to help patients record the ECG signal and exchange messages and medical information, such as symptoms, with health centers and physicians. This information will be associated with a recorded signal when it is sent to the algorithms/storage server.

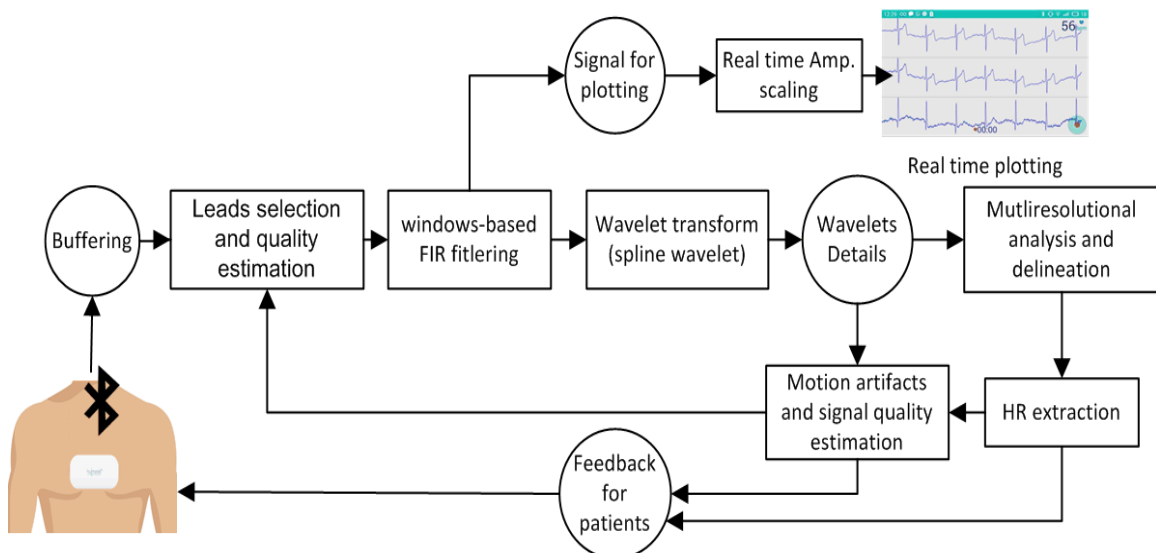


Figure 6. 4 The flowchart of ECG signal processing pipeline implemented on smart phone applications.

The second application is the expert application, which allows an expert to record and monitor ECG signals in real time, as well as to view and analyze sent recordings using algorithms running on the cloud server. Beside patient's signal viewing and analysis, experts can exchange medical advices, feedback, and messages with patients, if necessary. Additional

services were implemented to allow medical experts to exchange intervals of the ECG signal and medical knowledge or opinions with other experts who are more experienced in the field of arrhythmology.

On both applications, a library for real time event ECG signal processing and basic analysis was implemented, which allows signal plotting on mobile monitors, and provides heart rate and signal quality information as feedback to patients. The basic flowchart of the real time processing library is shown in Figure 6.4.

Hence, the received signal is buffered in a 1-s buffer, and then the signal is filtered from both baseline wandering and high frequencies noises, such as EMG noises and network interference. Filtering from high-frequency noise was done using adaptive noise reduction methodology, proposed in previous chapter.

The signal amplitude is then scaled in real time to ensure that its maximum and minimum values fit the smart phone display. A spline wavelet transform is also applied to delineate the ECG signal and, consequently, extract the heart rate. For this reason, the state of art multi-resolutional approach, presented in [68], was used. Wavelet transform details, along with the heart rate extracted in the delineation process, were used to estimate motion artifacts and EMG noise.

High frequency noise was approximated using the noise level approximation method presented in this dissertation, intervals were labeled according to the reference signal amplitude values and signal overall quality was penalized according to these amplitude values.

The difference between the original wavelet details and the aligned averaged details signal for QRS complexes is used to define signal quality at each interval in the ECG signal. This approach is presented in [36]; however, wavelet details at scale 2^2 were adapted in this method instead of the ECG signal, because most of the energy of QRS complexes lies in this scale [68, 2]. Information about estimated leads quality as well extracted heart rate are shown and updated in real time.

The mobile phone applications are native mobile applications and support both operating systems IOS and Android. Processing library is written in C language and wrapped to be used in Java for the Android application and objective C for the IOS application. Bluetooth connection was used to enable real time plotting of the received signals from the paired device. Additional pages are designed for the device, the patient, and patient parameter setting.

6.7 Algorithms and Offline Analysis

The next step, after sending signals to the algorithms/storage server, is to process the signals and provide an automatic analysis report associated with the signals. The flowchart of the automatic analysis for long-term signals, as well as for short-term signals, is shown in Figure 6.5. Both analysis workflows share the main components of pre-processing, feature extraction and delineation, and, finally, the arrhythmia detection (classification and clustering).

However, the analysis workflow of ECG signals, recorded by the proposed device, changes according to the recording mode due to different leads lengths, and different electrode positions and types. The short-term post-event signals, recorded using dry electrodes, are more difficult to be analyzed, because of the lack of dominant beat reliability caused by small beats number recorded in this mode. Additionally, the positioning of event recorder on patient's chest has a great impact on the ECG waves' morphology and polarity in the short-term post-event recording mode. This is due to different cardiac muscle positions and different axes [101].

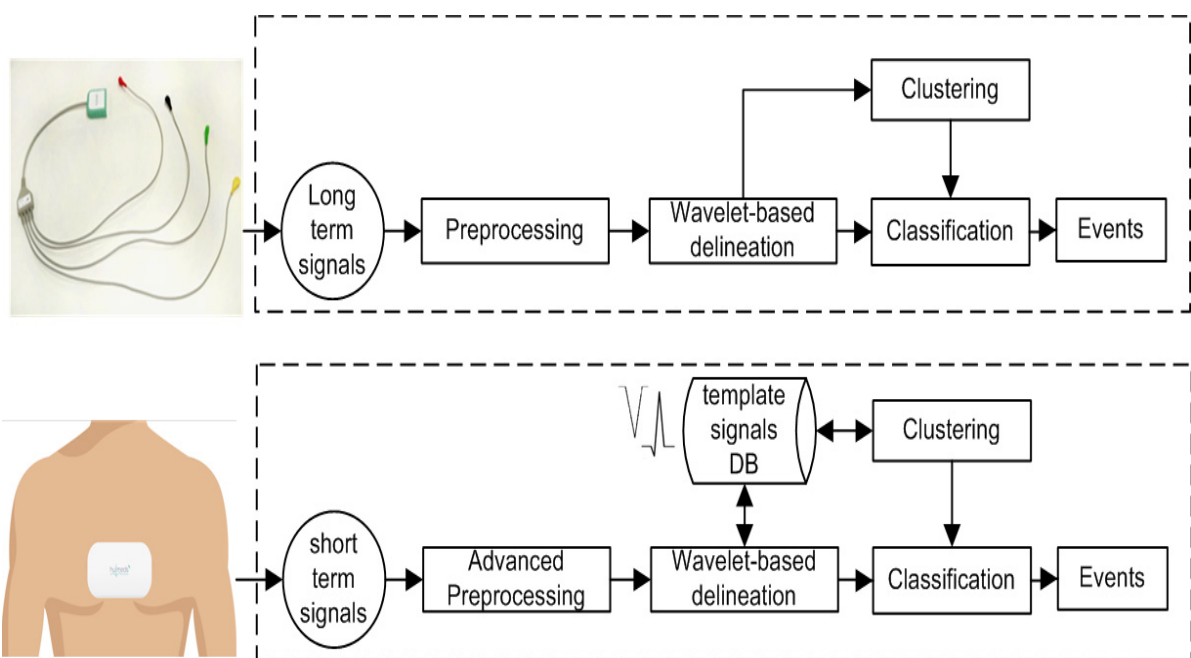


Figure 6. 5 The flowchart of ECG signals analysis for both short-term and long-term modes.

The proposed solution requires templates to be built for each patient when the patient starts using the short-term post-event recorder. The templates are built by testing relatively different positions on patient's chest the first time they use the device. The device placement that provides the best signal quality will be used and recordings from that position will become the source of normal QRS templates that are saved and used moving forward. The

tested positions are around specific position pre-defined as the standard device placement position for this device design. This is discussed in details later in evaluation section.

On the other hand, when long-term holter signals are recorded, there is no need to use any pre-defined templates in the analysis and interpretation pipeline. This is because the average beat could be dependably computed from the large number of recorded beats (central limit theory). The average beat could be used later in several steps in the analysis pipeline to estimate signal quality and to find the fluctuations of the beats' morphology.

Therefore, the first stage of both modes of the ECG signal's analysis pipeline is the pre-processing stage. Firstly, ECG signal is filtered from both baseline wandering and network interference using an FIR filter with reduced number of Taps presented in [41], while high frequency and EMG noise was filtered using FIR filtering according to the specifications and recommendations of bandwidth used in filtering [32].

Afterwards, the quality of each lead was estimated using a more sophisticated time-invariant algorithm than that used for real time processing. This algorithm is used to estimate the signal quality vs. motion artifacts and baseline artifacts and high frequency EMG noises [89]. Subsequently, the leads quality estimation is used in leads selection logic to use one, two, or all three leads for delineation, clustering, and classification stages. The right selection of leads to be used in the analysis is important since it affects ECG waves' delineation and beats classification [112, 113].

The next step is to apply spline wavelet transform to delineate ECG waves. The same algorithm used in mobile-based ECG processing was used for this purpose [68]. Then, a combination of the delineation results was done using the signal quality representation of each lead as in [114]. This approach reduces the negative impact of noisy intervals on delineation results. Additionally, the combination of single-lead delineation results increases the positive predictive values and the sensitivity values of overall QRS detections, by taking advantage of the three leads presence. Combination is achieved using several criteria. For instance, when signal quality, estimated over time for each lead, worsens for some leads, then other leads with better signal quality should be used. Another example is when a beat is detected on one lead while is absent on others. This is considered a false predictive beat.

The clustering algorithm is then built to cluster the detected beats into forms which are used in the classification stage of these beats. Wherein, each ECG beat was encoded in vector of 6 digits of KLT transform coefficients extracted as described in [56, 115], and two more digits from RR intervals as used in [115] are added. These vectors are then normalized and K-means algorithm was used to cluster the ECG beats (see Figure 6.6).

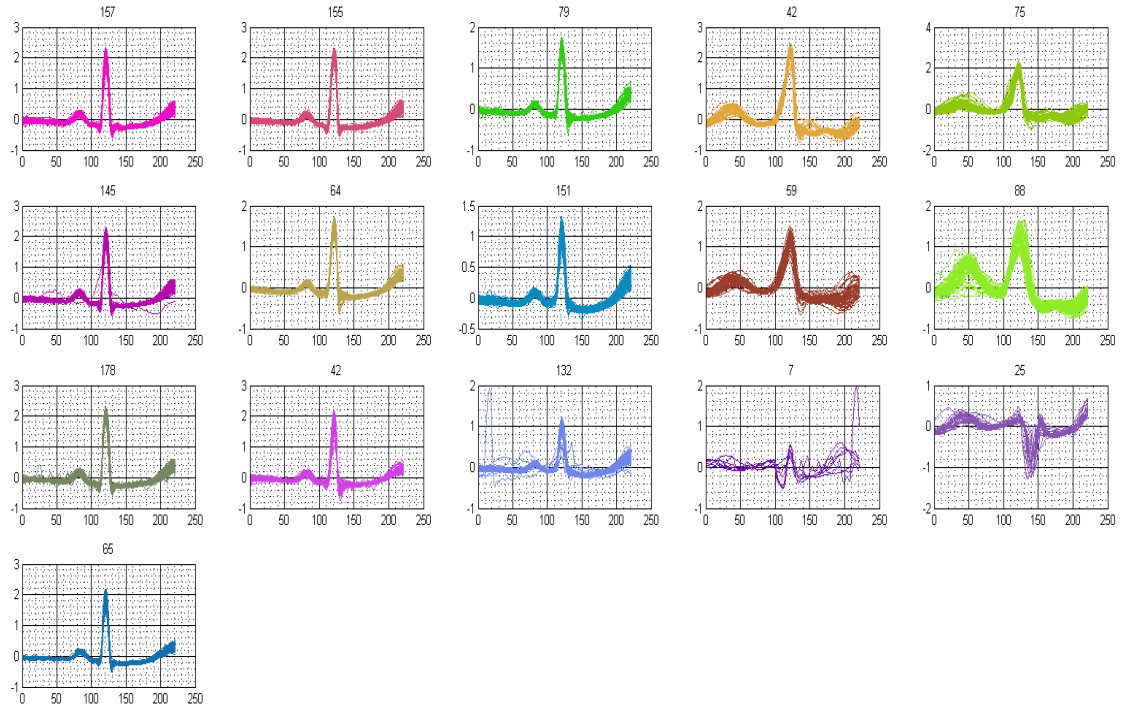


Figure 6.6 Clustering of ECG beats of first channel of MIT-BIH recording 106 using KLT coefficients vector and RR features. Noise level approximation is used in this step in the validation of clustered beats. Average cluster was calculated and beats which have Euclidean distance large larger than 2 standard deviations and whose corresponding noise level approximation value larger than 0.5 were classified as noises and isolated.

Finally, the classification algorithm, presented in [116], was used to find the class of extracted beats. For short-term signals, all beats from the cluster whose morphology is similar to the predefined normal beat morphology are associated to the normal class after considering their heart rate features. All beat annotations are mapped during the classification process into the sets N, V, S, Q (corresponding to normal, ventricular ectopic, supraventricular ectopic, unknown). Finally, a report with clusters' morphological forms, delineation statistics, along with intervals of interest is, introduced to physicians for detailed analysis.

Calibration of the patients' templates is of paramount importance. It should be taken into consideration by physicians because of the acquired template changes during the lifespan of all patients, especially the younger ones. The templates can be changed easily using the mobile phone applications by physicians or by patients themselves. Patients, who would use the device for long periods or before and after some circumstances that could change the templates morphology, must recalibrate the morphology and the analysis parameters of their personal ECG recordings.

Three groups of customizable parameters—pediatrics, adults, and special—are used as default analysis parameters. The first group; the pediatric group contains normal ECG

parameters for children aged 0–16 years divided into several age groups [117, 118]. The second group is the adult group. However, all parameters for groups can be also customized according to each patient’s case in a special group of parameters. For instance, patients with Acquired Heart Block due to surgery or medication, or with congenital Heart Block that developed after birth, should have customized analysis parameters which must be controlled by physicians, and fluctuations from those parameters should be considered as abnormal changes. Another example is in sport medicine, where athletes have special parameters that depend on their sports, special conditions, and age [119, 120]. A special set of parameters should be used to handle any special situation.

Therefore, a patient-parameters database is used. It contains used analysis parameters along with the template ECG wave for each patient. The patient-parameters database is editable and must be calibrated by physicians according to patients’ changing conditions.

All algorithms were designed firstly using MATLAB and Python Packages. They are then ported to C programming language and wrapped in python back-end so that the communication between the cloud-based web application and the wrapped algorithms is done using REST services implemented within Django REST framework.



Figure 6. 7 Screen-shot of the web analysis platform. Automatic analysis results are seen in the bottom part, while the signal is shown with colors annotating the beats classification. Physicians have an access to their patients’ recordings so they can confirm the automatic analysis results and follow their status.

6.8 Evaluation and Results

Long-term ECG signals, recorded by the proposed device, are standard holter signals recorded using wet electrodes and the long-term mode itself is not the novelty of this paper. For this reason, only validation procedures of short-term patient-activated event signals, recorded by the means of dry electrodes, are presented in this context.

To evaluate the short-term post-event recorder design introduced in this paper, a clinical study was conducted. A total population of 391 patients was tested in the evaluation process, 40 volunteers and 351 patients with non-significant cardiac issues. The average age of validation population, included in this study, was 26.90 ± 19.32 years (26.90 ± 19.32 years). The genders percentages of tested patients are 60.86% or 238 males, and 39.13% or 153 females. The adults (age > 16) percentage is 52.94% or 206 adults, while the percentage of children (age ≤ 16) is 47.05% or 184. The evaluation procedures were divided into two phases; pre-validation and validation.

The purpose of the pre-validation process was to find the best placement of short-term post-event recorder on subjects' chest. Total of 60 participants were selected in the pre-validation procedures, while the other evaluation procedures were finished with the residue validation population 331 participants.

In both procedures, the main tested body positions were supine, sitting, and standing positions. Patients recorded their ECG themselves, but all recordings were performed under the supervision of medical professionals. Measurements were done without skin preparation such as shaving or adding conductive gel on the skin surface, and signal recording was performed immediately after placing the device body on the subject's chest. The whole study was carried out following the rules of "The 1975 Declaration of Helsinki" [121]. All the evaluation procedures were approved by the Belgrade University Children's hospital ethics committee, and the participants' informed consent was given before the experiment.

6.8.1 Device Placement Versus Signal Quality

In the pre-validation phase, the goal was to find the best placement at which three most different leads are sensed. This is important for physicians because leads morphological difference reflects the heart muscle electrical activity from different angles [22, 24, 122]. For this reason, signals of 20 sec length were recorded using the proposed short-term post-event recorder with different placements on each patient's rib cage. The tested placements during the pre-validation phase are illustrated in Figure 6.7.

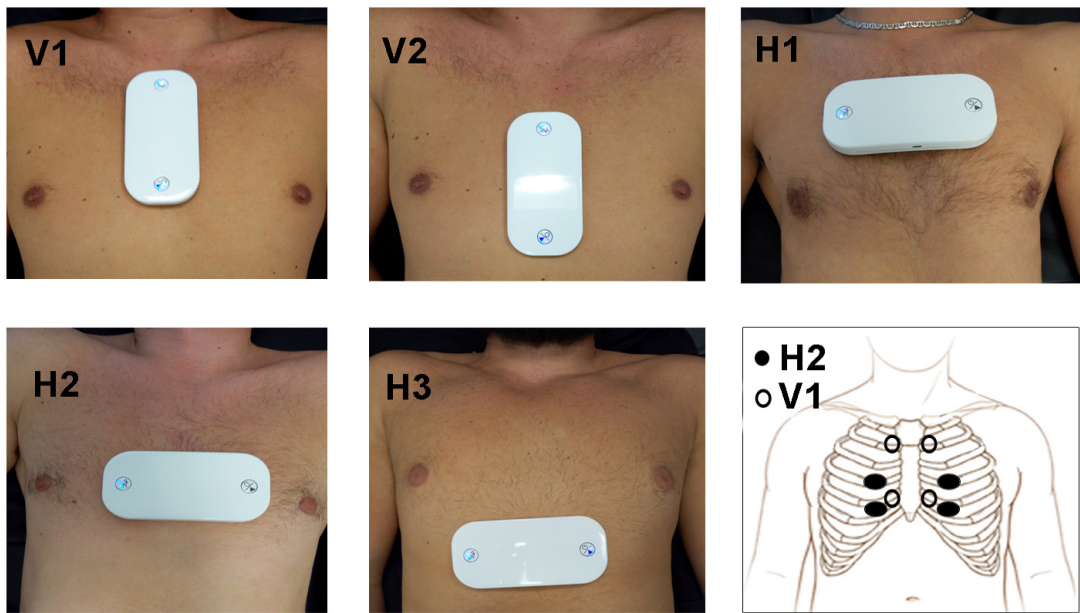


Figure 6.8 Tested device placement; two vertical (V1–V2), three horizontal (H1–H3), and finally the corresponding positions of electrodes of H2, V1 placement on human chest ribs.

Afterwards, two specialized cardiologists were asked to estimate signal quality for the analysis of the three channels recoded using dry electrodes. They went through the signals and annotated them in terms of signal quality and clinical acceptability. Signal quality refers to the presence of EMG noise, motion artifacts, and baseline wandering, while clinical acceptability refers to the presence of all PQRST waves, narrowness of QRS complex, and suitable R/T amplitude ratio. Experts were asked to give their estimate from 1 to 5, where 1 stands for unacceptable signal for analysis and 5 stands for high-quality signal, suitable for interpretation.

At the end of pre-validation process, position H2 gives the best results and was the best placement with good quality and different ECG channels morphology. This applies to a subset of the tested population which includes both adults (age > 16 years) and children (age < 16 years) with rib cage size allowing this placement. On the other hand, position V1 gives better results for children whose chest size doesn't enable recording in position H2.

The average signal quality annotated by experts of the signals at the selected positions, V1 and H1, was quantified per age group and presented in Table 6.2. Signal quality was presented with a standard error computed with a confidence interval of 95%.

Device placement illustration, according to age category is stored in the smart phone application. Instructions to help patients to find the best placement on chest, and to explain the correct usage of the proposed device, were included in the smart phone application.

6.8.2 Correlation With ECG Golden Standard Leads

In order to evaluate the quality of ECG signals recorded by the short-term post-event recorder at the selected positions, they were compared to the golden standard of 12 ECG leads. The correlation coefficient check was examined to understand the possible distortions caused by the usage of loose dry electrodes. Additionally, it was intended to find the maximum correlated lead from the golden standard 12 leads ECG to each lead from the event recorder device.

The correlation coefficient between the recorded three leads, using dry electrodes, and ECG signals recorded simultaneously using 12 leads gold standard ECG (SCHILLER CARDIOVIT CS-200 Office System) was computed.

After analyzing a sample of 100 recordings, of 20 sec length, from the validation population signals, golden standard precordial leads (V1, V2, and V3) were found as the best match with ECG leads recorded by the short-term post-event recorder, since they show high correlation with the short-term leads, recorded using dry electrodes. The computed correlation coefficients from these leads and leads recorded by the presented design are presented in Table 6.1. Thus, the leads recorded by the short-term post-event recorder are called modified V1, V2, and V3 leads. Consequently the usage of short-term leads should be equivalent to the usage of golden standard leads in terms in applicability and reliability in arrhythmias detection.

Table 6.1 The average correlation values of short-term post-event recorder Leads (L1–L3) and corresponding ECG Golden standard leads (V1–V3)

Compared leads	Correlation coefficients
V1–L1	0.888
V2–L2	0.8930
V3–L3	0.929

Figure 6.9 shows three leads of ECG signals recorded using the proposed design with dry electrodes and corresponding leads of the ECG golden standard device. The most important point to highlight and deduce from this figure is that the short-term post-event mode of the proposed device was able to record three different leads that represent the heart muscle electrical activity from different angles, exactly as the golden standard ECG recorder did. Another point that could be deduced from this figure is the equivalent signal quality regardless of different electrodes types used in each recorder.

Table 6.2 Signal quality and clinical acceptability for selected placements H1, V1

Population	Age range	Signal quality	V1	H1
Adults	17–80	4.17 ± 0.30	0	30
Children	4–16	4.10 ± 0.28	6	24
Both	4–80	4.13 ± 0.20	6	54

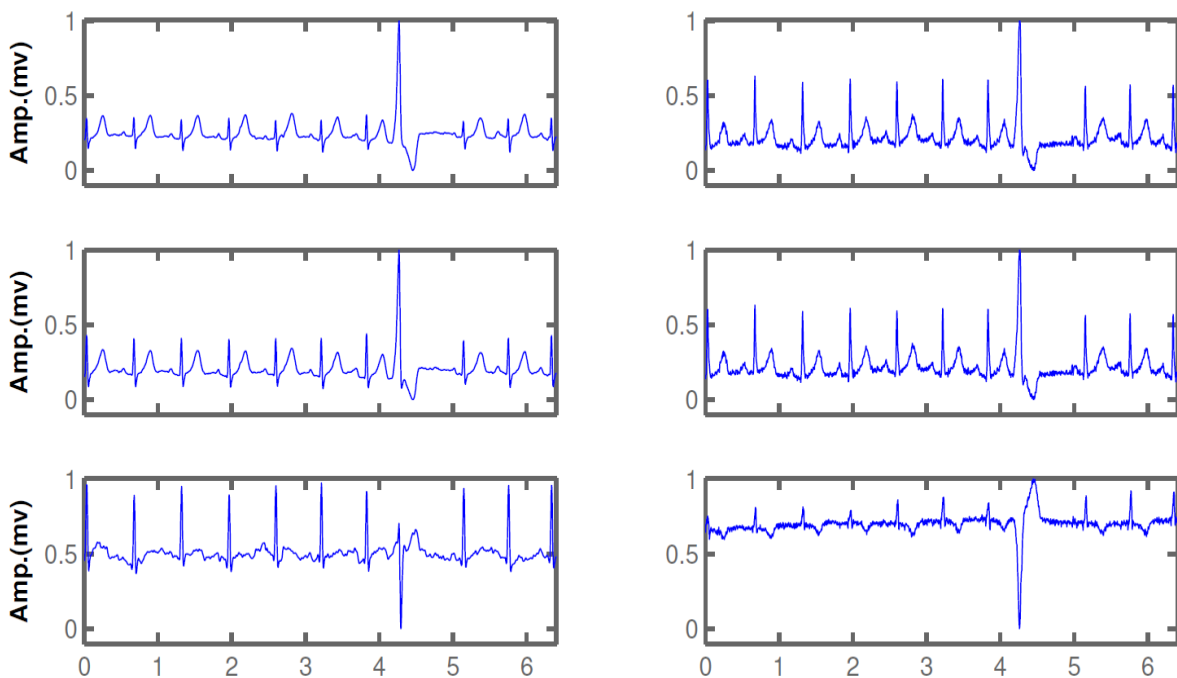


Figure 6.9 Short-term post-event signals L1–L3 (left column) versus golden standard channels V1–V3 (right column). The morphological variability could be noticed among leads recorded using short-term post-event recorder as well as golden standard leads.

6.8.3 Peer review of clinical acceptability

Quality of signal is not only restricted to the cleanliness of signal from artifacts and noises. The ability to do a detailed interpretation of ECG signals is also a paramount necessity. This includes the presence of ECG main waves (P, Q, R, S, and T), as well as suitable morphology and amplitude for them that allow experts and algorithms to measure the width and amplitude variation of ECG waves. For instance, the QRS complex should be tall and narrow (recommended amplitude >0.5 mV, but not biphasic), while T amplitude should be relatively smaller than the R wave [112, 113]. Such details have great impact on both diagnosis potential and, consequently, on automatic analysis. This is reflected in the performance of different algorithms for automatic delineation and analysis. To translate this into statistical

data, two criteria were used to evaluate the recorded signals' acceptability for interpretation; expert-based and algorithm-based.

First, a peer review process is adopted to evaluate the signal clinical acceptability. Three leads recorded by the proposed device are presented as well as the three most correlated leads recorded simultaneously from the golden standard 12 leads ECG device, to two experts. This was conducted without providing them with information about signals' origin for a sample of total 100 recordings. Experts were asked to annotate each set as valid or not valid for detailed analysis. For this reason, doctors went through the two sets A and B for each of three leads and gave their opinion as A, B, AB, none.

Results of this survey are presented in Table 6.3. Presented results show that the short-term post-event ECG signals, recorded using dry electrodes, have comparable diagnosis potential to the ECG 12 leads golden standard and could be used in arrhythmia detection.

Afterwards, the hypothesis that the validity ratio of signals, recorded with short-term mode of the proposed device Pe , is equivalent to the validity ratio of signals recorded using the golden standard ECG recorder Pg , is tested. With a confidence interval of 95%, the standard error of the tested hypothesis was 0.829 and P value is 0.796. Thus, the null hypothesis was accepted which means that both ratios are equivalent, and that short term signals could be used in similar way to the golden standard signals in heart rate variability analysis.

It was found during this validation phase that in case of consistent pressure aimed to force the electrode against the subject's skin, the signal quality of recorded leads, in terms of EMG noise and motion artifacts, was corresponding to standard ECG leads annotated by experts as the best match with the recorded short-term leads. Nonetheless, corresponding standard ECG leads signal quality in terms of baseline wandering was better than the short-term leads, recorded by the proposed device. Finally, 99% of tested patients succeeded in accomplishing a transmission test after following the instructions stored in the mobile phone application.

Table 6.3 Results of peer review of event and best match leads from golden standard ECG

Recording device	Clinical acceptability	
	Valid	Invalid
Short-term recorder	96	4
Golden standard ECG	98	2
Both devices	95	1

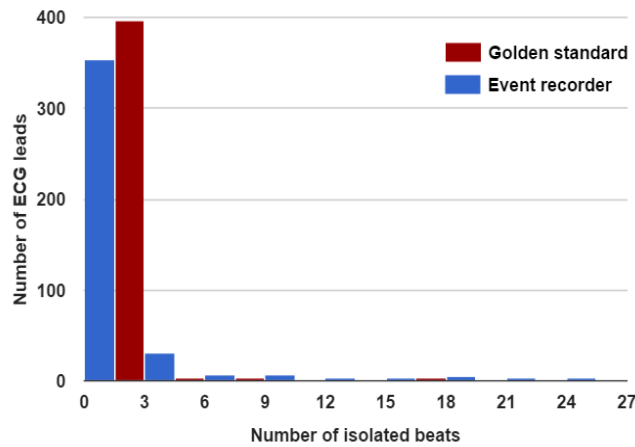


Figure 6. 10 Histogram of isolated beats or detected on each lead that are not detected on all leads.

6.8.4 Accuracy Evaluation For Heart Rate Detection

In order to examine the quality of recorded ECG signals in terms of fidelity in recording suitable ECG waves, the performance of the automatic delineator was evaluated. Both short-term post-event recorder leads, and the corresponding best-matched three leads from the golden standard 12 leads ECG, were tested. A sample of 100 recordings was used in this phase. Each recording contained 6 leads, three leads of each device. Recordings were done simultaneously using both devices and each was of 20 sec length.

Two expert annotators delineated the QRS complex independently, and their delineation was considered as the golden standard delineation for comparison. Afterwards, the delineation algorithm presented in [68] was used to detect QRS complexes automatically. Sensitivity and positive predictive value for QRS complex detection, after comparison to expert manual annotations, were computed and presented in Table 6.4.

Signals recorded using dry electrodes obtained a positive predictive value of 99.07% ,when a combination of single lead delineation results is used as it is mentioned in the algorithms section, compared to 99.34% from the corresponding leads from the golden standard ECG. These results show that automatic delineation algorithms' performance is equivalent for short-term post-event recorder signals as well as for ECG golden standard recorder. Consequently, the QRS complexes could be dependably detected and used for heart rate variability analysis, including Atrial Fibrillation detection, in the ECG signals, recorded using short-term post-event recorder.

Table 6.4 QRS complex delineation results on both short term event leads and best matched three standard ECG leads event

Leads	Event recorder				Golden standard			
	L1	L2	L3	L1-L3	V1	V2	V3	V1-V3
PPV.%	93.18	96.56	95.27	99.07	98.04	99.14	97.22	99.34
Sens.%	97.55	99.61	98.76	99.23	99.13	99.87	99.83	99.87

6.8.5 Noise Influence On Heart Rate Accuracy

To check the signal quality in terms of clinical acceptability for heart rate analysis, the percentage of detected beats on each lead, which were also detected on all leads, was calculated.

This metric was used and presented in [123, 124]. It indicates the clinical quality of ECG channels in terms of resistance to noises and motion artifacts by measuring the performance of automatic QRS delineation on all leads. Since beats detection in high-quality signals is more accurate on all leads, there are less isolated beats that are detected erroneously by algorithms on each lead separately. The aforementioned state of the art delineator was used to detect QRS waves in 400 leads of post-event short-term recorder and in the corresponding leads from the 12 leads golden standard ECG recorder.

Results are shown in Figure 6.10 and they indicate a very good performance for the automatic delineator with short-term leads, as with the corresponding golden standard ECG leads. This is an indication of equivalent signals quality and applicability for heart rate detection and subsequent arrhythmias analysis.

In order to translate the presented results from Figure 6.9 into statistical measures, the mean difference of the paired ECG delineation results (isolated beats number) is calculated and evaluated. The tested hypothesis is that the difference of isolated beats numbers of delineated leads, recorded simultaneously using the short-term mode of the proposed device and the golden standard ECG recorder, is greater than zero. With a confidence interval of 95%, the standard error of the tested hypothesis was 4.52 and P value was 0.99. So, the null hypothesis was rejected and the alternative was accepted. This means that isolated beats number ratios are equivalent.

6.8.6 Comparison With The Available Commercial Solutions

Features of the proposed device were compared with similar available commercial solutions. Table 6.5 explains the features differences of the proposed device compared to some known solutions.

Table 6.5 Features comparison with similar available commercial solutions

Name	Unit description	Channels number	Applications	Electrodes types	Recording place	Transmission methods
Alivecor system and ECG check	Smartphone protective case	Single channel	Short-term post-event tests	Dry	Fingers	FM
EPI mini	Independent unit	Single channel	Short-term post-event tests	Dry	Fingers	Bluetooth
eMotion ECG	Continuous wearing, cable set, wearable belt or fastfix	Single or three channels	Real time monitoring, holter monitoring	Wet adhesive	Chest	Bluetooth
NUVANT mobile	Continuous wearing and measuring	Single channel	Real time and holter monitoring	Wet adhesive	Chest	Bluetooth
Ambulatory ECG	Independent unit	Single channel	Post event monitoring, patient activated	Dry	Chest	Bluetooth
Omron	Independent unit	Single channel	Post event short-term monitoring, patient activated	Dry	Chest	Bluetooth
Body guardian verit	Independent unit	Three channels	Long-term and Holter monitoring	Wet adhesive	Chest	Bluetooth and cable
IEM beam	Independent unit	Three channels	Short-term loop/event recorder, record up to 3 min	Wet adhesive and dry electrodes	Chest	Bluetooth
Proposed design	Independent unit provided with NFC module for fast activation	Three channels	Long-term event and holter monitoring, post event monitoring short-term monitoring	Wet adhesive and dry electrodes	Chest	Bluetooth, GSM and cable

The most important advantage of the proposed design, compared to some of those commercial solutions, is the reliability of recorded ECG leads for deep analysis. This is achieved by using the appropriate electrodes number and types (dry and wet) with hardware customized for each of those types. Single lead devices could not be considered confident for deep ECG signal analysis [125]. On the other hand, the usage of wearable fashion to record ECG signals is still subject of debate since signals recorded using this approach suffer from motion artifacts and noises that reduce the clinical acceptability of such signals [126].

Therefore, reliable long-term recording, as well as fast reliable short-term recording, could be achieved using both dry electrodes and wet adhesive electrodes. To increase the reliability and acceptability of recorded signals analysis a customized algorithmic approach is proposed to deal with signals depending on the used electrodes, and on the patients special ECG templates in the short-term mode.

The usage of an NFC module reduces the time needed to start short-term post-event recording, which is very important for short-term post-event recording.

Finally, the hardware costs of a single device, operating as proposed herein, are significantly lower than costs of two devices, each operating in separate recording mode (short-term post-event and long-term holter).

6.9 Conclusions

The simple design and the usage of dry electrodes for short-term post-event recording and wet adhesive for holter long-term mode, allows laypersons to record reliable signals according to physician's recommendations in two working modes.

The reliability of three post-event short-term ECG leads with direct symptom-rhythm correlation is the major advantage of the short-term post-event mode. This is achieved by providing solutions to the drawbacks of already available devices while focusing on maintaining the recorded signals' reliability.

The algorithm pipeline presented is an example how noise level approximation can be utilized in several phases in the analysis pipeline for different purposes. Noise level approximation is used in the delineation, signal quality enhancements, leads selection, signal quality assessment, clustering, and classification.

Finally, the evaluation of the proposed novel design of an event recorder with dry electrodes showed that ECG signals of 96% of participants, who finished the recording and transmission, have the diagnosis potential to be used in arrhythmia detection for different age groups.

Chapter 7

7. Conclusions and Perspectives

High frequency noise is addressed in this thesis. Noise level approximation was introduced and utilized in different phases in the ECG signal analysis pipeline. The proposed method takes noise non-stationarity into consideration by introducing a short-time smoothed approximation instead of global estimation or interval based noise estimation.

In order to achieve a better isolation of the noise component from the signal component in the observed noisy ECG recordings, the stationary wavelet transform is utilized. Zero-crossings and peaks and valleys in the wavelet details were detected and were used to build the noise level approximation signal or what was called the reference signal.

The usage of time-scale stationary wavelet coefficients, as well as reference signal smoothing over time, allow the extracted signal to follow the changing dynamics of the ECG signal. This is reflected in the approximation signal amplitude. On the other hand, the knowledge of statistical characteristics of the ECG signal in terms of possible morphologies and frequencies is utilized to add global knowledge to the extracted signal. This could be considered as a semi-supervised approach to enhance the reference signal accuracy to approximate noise regardless of the included rhythm.

Smoothness of the extracted signal makes it suitable for applications such as noisy intervals detection and isolation, lead adaptive selection for delineation algorithm, and, most importantly, for adaptive noise reduction from the ECG signal. Thus, the usage of this methodology is investigated by implementing a method based on filters bank for adaptive noise reduction in the ECG signal. Results were evaluated using both real EMG and simulated noises added to the ECG signal with several arrhythmias.

The main advantage of the usage of short-time noise level approximation for adaptive noise reduction is the maintaining the ECG signal unfiltered in intervals where noise reduction is

not crucial for automatic analysis, while reducing the noise level adaptively in noisy intervals where noise could have a negative impact on analysis results.

In addition to filters bank method, a new strategy to adaptively filtering the ECG signal was proposed using the wavelet Wiener filtering. Noise level approximation in this methodology plays a crucial role to estimate the noise-free signal wavelet coefficients, which are then delivered to the Wiener Filter along with noisy wavelet coefficients. This methodology could be suitable to filter short-term signals where signal dynamics don't change a lot as in holter or long-term signals.

Finally, in the last chapter the design and implementation of the multi-purpose ECG telemedicine system that can operate in different working modes is introduced. Customized algorithms pipeline is presented and discussed in details to analyze ECG signals recorded using both dry electrodes, for short-term post-event recording, and wet adhesive for holter long-term mode.

The proposed device itself is one of the claimed contributions of this thesis. It allows laypersons to record reliable signals easily according to physician's recommendations in each of recording modes. The major advantage of using dry electrodes is to achieve correlation of symptom-rhythm which is necessary to catch in case of intermittent arrhythmia where symptoms occur infrequently.

Noise level approximation could be utilized in ECG signal processing pipeline in algorithm-triggered loop recorder. However, it needs to be associated with other algorithms that deal with other kinds of noises. For instance, the reference signal could serve as a feature along with other features representing other artifacts types to a specialized machine learning algorithm to get real-time classification of alarms raised by loop recorder algorithms. This is crucial to reduce the amount of false alarms caused by artifacts and noises. Moreover, adaptive noise reduction methodology could be used and customized to operate on fetal ECG signals. The dynamic properties of fetal signals are rather known which could be utilized to achieve better separation of this signal from noises it is usually associated with. Finally, deep learning algorithms could be fed by the noise level approximation signal as well as features or even the whole signal (using suitable representation) to classify ECG beats. The usage of the reference signal in this case will make it easier to deep network to distinguish between noise/false alarms and real arrhythmias.

References

1. G.M. Friesen, T.C. Jannett , M.A. Jadallah, Yates, S.L., S.R. Quint and H.T. Nagle, “A comparison of the noise sensitivity of nine QRS detection algorithms”, *IEEE Transactions on biomedical engineering*, vol. 37, no. 1, pp.85-98, 1990.
2. N.V. Thakor, J.G. Webster and W.J. Tompkins, “Estimation of QRS complex power spectra for design of a QRS filter”, *IEEE Transactions on biomedical engineering*, vol. 11, pp.702-706, 1984.
3. G.D. Clifford, F. Azuaje and P. Mcsharry, “ECG statistics, noise, artifacts, and missing data. Advanced Methods and Tools for ECG Data Analysis”, *Artech House Inc*, Norwood, 2006.
4. I.I. Christov and I.K. Daskalov, “Filtering of electromyogram artifacts from the electrocardiogram”, *Medical engineering & physics*, vol. 21, no. 10, pp.731-736, 1999.
5. G.J. Tortora, and M.T. Nielsen, *Principles of human anatomy*, vol. 257, Wiley, 1999.
6. <http://anatomybody101.org/muscular-system-cardiac-anatomy/>
7. <http://www.texasheart.org/HIC/Anatomy/anatomy2.cfm>
8. J.T. Koivumäki, T. Korhonen and P. Tavi. “Impact of sarcoplasmic reticulum calcium release on calcium dynamics and action potential morphology in human atrial myocytes: a computational study”, *PLoS computational biology*, vol. 7, no. 1, p.e1001067, 2011.
9. <http://www.newhealthadvisor.com/blood-flow-through-the-heart.html>
10. A.M. Katz, “Physiology of the Heart”, *Lippincott Williams & Wilkins*, 2010.
11. <https://en.wikipedia.org/wiki/File:Conductionsystemoftheheart.png>
12. <http://www.austincc.edu/apreview/PhysText/Cardiac.html>
13. <https://www.medicine.mcgill.ca/physio/vlab/cardio/setup.html>
14. Dale Dubin, “Rapid interpretation of EKG's: an interactive course”, *Cover Publishing Company*, 2000.
15. <http://www.austincc.edu/apreview/PhysText/Cardiac.html>
16. https://upload.wikimedia.org/wikipedia/commons/0/0e/EKG_leads.png
17. https://en.wikipedia.org/wiki/File:Limb_leads_of_EKG.png

18. M.D. Darrow, “Ordering and understanding the exercise stress test”, *American family physician*, vol. 59, no. 2, pp.401-410, 1999.
19. <http://www.heartrhythmspecialistsla.com/services-treadmill-stress-test-los-angeles-ca.html>
20. N.J. Holter, “New method for heart studies: continuous electrocardiography of active subjects over long periods is now practical”, *Science*, vol. 134, pp.1214–1220, 1961.
21. <http://medicalfacts.ca/index.php/services/holter-monitoring>
22. P. Zimetbaum and A. Goldman, “Ambulatory arrhythmia monitoring”, *Circulation*, vol.122, no. 16, pp.1629-1636, 2010.
23. C.C., Wu, M.H. Hsieh, C.T. Tai, C.E. Chiang, W.C. Yu, Y.K. Lin, H.M. Tsao, P.Y.A. Ding and S.A. Chen, “Utility of patient-activated cardiac event recorders in the detection of cardiac arrhythmias”, *Journal of interventional cardiac electrophysiology*, vol. 8, no. 2, pp.117-120, 2003.
24. R.A. Hegazy and W.N. Lotfy, The value of Holter monitoring in the assessment of Pediatric patients, *Indian pacing and electrophysiology journal*, vol. 7, no. 4, p.204, 2007.
25. P.P. Karpawich, D.L. Cavitt and J.S. Sugalski, Ambulatory arrhythmia screening in symptomatic children and young adults: comparative effectiveness of Holter and telephone event recordings, *Pediatric cardiology*, vol. 14, no. 3, pp.147-150, 1993.
26. K.C. Tseng, B.S. Lin, L.D. Liao, Y.T. Wang, and Y.L. Wang, Development of a wearable mobile electrocardiogram monitoring system by using novel dry foam electrodes, *IEEE systems Journal*, vol. 8, no. 3, pp.900-906, 2014.
27. R. Fensli, E. Gunnarson and T. Gundersen, “A wearable ECG-recording system for continuous arrhythmia monitoring in a wireless tele-home-care situation”, *In Computer-Based Medical Systems, Proceedings. 18th IEEE Symposium*, pp. 407-412, 2005.
28. T.T. Schlegel, Wireless Self-Acquisition of 12-Lead ECG via Android Smart Phone, 2012.
29. A. Albulbul, “Evaluating Major Electrode Types for Idle Biological Signal Measurements for Modern Medical Technology”, *Bioengineering*, vol. 3, no. 3, p.20, 2016.
30. M.H.K. Park, C. de Asmundis, G.B. Chierchia, A. Sarkozy, A. Benatar and P. Brugada, “First experience of monitoring with cardiac event recorder electrocardiography Omron system in childhood population for sporadic, potentially arrhythmia-related symptoms”, *Europace*, vol.13, no. 9, pp.1335-1339, 2011.

31. G. Kaleschke,B. Hoffmann,I. Drewitz, G. Steinbeck, M. Naebauer, A. Goette, G. Breithardt, P. Kirchhof, "Prospective, multicentre validation of a simple, patient-operated electrocardiographic system for the detection of arrhythmias and electrocardiographic change", *Europace*, vol. 11, no. 1, pp. 1362–1368, 2009.
32. JJ. Bailey, A.S. Berson, A. Garson Jr, L.G. Horan, P.W. Macfarlane, D.W. Mortara and C. Zywietz, "Recommendations for standardization and specifications in automated electrocardiography: bandwidth and digital signal processing. A report for health professionals by an ad hoc writing group of the Committee on Electrocardiography and Cardiac Electrophysiology of the Council on Clinical Cardiology", *American Heart Association, Circulation*, vol. 81, no. 2, p.730, 1990.
33. M. Lagerholm, C. Peterson, G. Braccini,L. Edenbrandt and L. Sornmo, "Clustering ECG complexes using Hermite functions and self-organizing maps", *IEEE Transactions on Biomedical Engineering*, vol. 47, no. 7, pp.838-848, 2000.
34. A. Gacek and W. eds. Pedrycz, "ECG signal processing, classification and interpretation: a comprehensive framework of computational intelligence", *Springer Science & Business Media*, 2011.
35. S.A., Israel, J.M. Irvine, A. Cheng, M.D. Wiederhold and B.K. Wiederhold, "ECG to identify individuals", *Pattern recognition*, vol. 38, no. 1, pp.133-142, 2005.
36. S. Iravanian and L. Tung, "A novel algorithm for cardiac biosignal filtering based on filtered residue method", *IEEE Transactions on Biomedical Engineering*, vol. 49, no. 11, pp.1310-1317, 2002.
37. R.M. Rangayyan, *Biomedical signal analysis*, Vol. 33, *John Wiley & Sons*, 2015.
38. P. Albrecht, J.M. Arnold, N. Judell and R.J. Cohen, "Using related signals to reduce ECG noise", *Cambridge Heart, Inc.*, U.S. Patent 5,704,365, 1998.
39. M. Blanco-Velasco, B. Weng and K.E. Barner, "ECG signal denoising and baseline wander correction based on the empirical mode decomposition", *Computers in biology and medicine*, vol. 38, no. 1, pp.1-13, 2008.
40. M. Kaur, and B. Singh, Comparison of different approaches for removal of baseline wander from ECG signal, *In Proceedings of the International Conference & Workshop on Emerging Trends in Technology*, pp. 1290-1294, 2011
41. Jan A. Van Alste, and T. S. Schilder, "Removal of base-line wander and power-line interference from the ECG by an efficient FIR filter with a reduced number of taps", *IEEE transactions on biomedical engineering*, vol. 12 , pp. 1052-1060, 1985.
42. P. Konrad, "The abc of emg", *A practical introduction to kinesiological electromyography*, vol. 1, pp. 30-35, 2005.

43. R. Sameni, M.B. Shamsollahi, C. Jutten and G.D. Clifford, "A nonlinear Bayesian filtering framework for ECG denoising", *IEEE Transactions on Biomedical Engineering*, vol. 54, no. 12, pp.2172-2185, 2007.
44. G.D. Clifford and L. Tarassenko, "Quantifying errors in spectral estimates of HRV due to beat replacement and resampling", *IEEE transactions on biomedical engineering*, vol. 52, no. 4, pp.630-638, 2002.
45. J.E. Mietus, C.K. Peng, I. Henry, R.L. Goldsmith and A.L. Goldberger, "The pNNx files: re-examining a widely used heart rate variability measure", *Heart*, vol. 88, no. 4, pp.378-380, 2002.
46. S. M. Kay, "Efficient Generation of Colored Noise", *Proceedings of the IEEE*, vol. 69, pp. 480–481, Apr. 1981.
47. R. Sameni, G. D. Clifford, C. Jutten, and M. B. Shamsollahi, "Multichannel ECG and Noise Modeling: Application to Maternal and Fetal ECG Signals", *EURASIP Journal on Advances in Signal Processing*, vol. 2007, no.1, pp.94-94, 2007.
48. R.B. Govindan, K. Narayanan and M.S. Gopinathan, "On the evidence of deterministic chaos in ECG: Surrogate and predictability analysis. Chaos", *An Interdisciplinary Journal of Nonlinear Science*, Vol.8, pp.495-502, 1998.
49. F. Badilini, A.J. Moss and E.L. Titlebaum, "Cubic spline baseline estimation in ambulatory ECG recordings for the measurement of ST segment displacements", *Engineering in Medicine and Biology Society, Proceedings of the Annual International Conference of the IEEE*, vol. 13, pp. 584-585, 1991.
50. Y. Zigel, A. Cohen and A. Katz, "The weighted diagnostic distortion (WDD) measure for ECG signal compression", *IEEE Transactions on Biomedical Engineering*, vol. 47, no. 11, pp.1422-1430, 2000.
51. V. Batchvarov, K. Hnatkova and M. Malik, "Assessment of noise in digital electrocardiograms", *Pacing and clinical electrophysiology*, vol. 25, no. 4, pp.499-503, 2002.
52. S. Oh, "A new quality measure in electrocardiogram signa", *Doctoral dissertation, University of Florida*, 2004.
53. LR. Rabiner and RW. Schafer, Digital Processing of Speech Signals, *Prentice-Hall, Englewood Cliffs*, NJ, 1978.
54. M. Yokoi, Z.I. Uozumi, N. Okamoto, Y. Mizuno, T. Iwatsuka, H. Takahashi, Y. Watanabe And S. Yasui, "Clinical evaluation on 5 years' experience of automated phonocardiographic analysis", *Japanese heart journal*, vol. 18, no. 4, pp.482-490,1977.

55. R.G. Willison, "Analysis of electrical activity in healthy and dystrophic muscle in man", *Journal of neurology, neurosurgery, and psychiatry*, vol. 27, no. 5, p.386, 1964.
56. G.B. Moody, and R.G. Mark, "QRS morphology representation and noise estimation using the Karhunen-Loeve transform", *Computers in Cardiology, Proceedings. IEEE*, pp. 269-272, 1989.
57. R. G. Mark, and G. B. Moody, "ECG Arrhythmia Analysis: Design and Evaluation Strategies", Chapter 18, in I. Gath and G. F. Inbar, (eds.), *Advances in Processing and Pattern Analysis of Biological Signals*, New York: Plenum Press, pp. 251–272, 1996.
58. Ary L. Goldberger, Luis A. N. Amaral, Leon Glass, Jeffrey M. Hausdorff, Plamen Ch. Ivanov, Roger G. Mark, Joseph E. Mietus, George B. Moody, Chung-Kang, Peng, and H. Eugene Stanley, "Physiobank, physiotoolkit, and physionet components of a new research resource for complex physiologic signals", *Circulation*, vol. 101, pp. 215-220, Jun. 2000.
59. J. Allen and A. Murray, "Assessing ECG signal quality on a coronary care unit", *Physiological measurement*, vol. 17, no. 4, p.249, 1996.
60. F. Chiarugi, V. Sakkalis, D. Emmanouilidou, T. Krontiris, M. Varanini, and I. Tollis, "Adaptive threshold QRS detector with best channel selection based on a noise rating system", *Computers in Cardiology. IEEE*, pp. 157-160, 2007.
61. J. Y. Wang, "A new method for evaluating ECG signal quality for multi-lead arrhythmia analysis", *Computers in Cardiology, IEEE*, 2002.
62. P. Raphisak, S.C. Schuckers, and A. de Jongh Curry, "An algorithm for EMG noise detection in large ECG data", *Computers in Cardiology, IEEE*, pp. 369-372, 2004.
63. B. Río Aldecoa Sánchez, T. Lopetegi, and I. Romero. "Assessment of different methods to estimate electrocardiogram signal quality", *Computing in Cardiology, IEEE*, 2011.
64. L. T. DeCarlo , "On the meaning and use of kurtosis", *Psychological methods*, vol.2, no.3, p. 292, 1997.
65. S. Mallat, "Zero-crossings of a wavelet transform", *IEEE Transactions on Information theory*, vol. 37, pp. 1019-1033, Jul. 1991.
66. S. Mallat, and S. Zhong , "Characterization of signals from multiscale edges", *IEEE Transactions on pattern analysis and machine intelligence*, vol. 14, pp. 710-732, Jul. 1992.

67. M.J. Shensa, "The discrete wavelet transform: wedding the trous and Mallat algorithms", *IEEE Transactions on signal processing*, vol. 40, pp. 2464-2482, Oct. 1992.
68. JP1. Martínez, R. Almeida, S. Olmos, AP. Rocha, and P. Laguna, "A wavelet-based ECG delineator: evaluation on standard databases", *IEEE Transactions on biomedical engineering*, vol. 51, pp. 570-581, Apr. 2004.
69. S. Mallat, and W.L. Hwang, "Singularity detection and processing with wavelets", *IEEE transactions on information theory*, vol. 38, pp. 617-643, Mar. 1992.
70. C. Li, C. Zheng and C. Tai, "Detection of ECG characteristic points using wavelet transforms", *IEEE Transactions on biomedical Engineering*, vol. 42, no.1, pp. 21-28, Jan. 1995.
71. 'Specification of tech patient cardio', :<http://www.heinstruments.com/specs.htm>.
72. G.B. Moody, W. Muldrow and R.G. Mark, "A noise stress test for arrhythmia detectors", *Computers in cardiology*, vol. 11, no.3, pp. 381-384, Sep. 1984.
73. J. Allen and A. Murray, "Assessing ECG signal quality on a coronary care unit", *Physiological measurement*, vol. 17, no. 4, p.249, 1996.
74. L.R. Rabiner and M.R. Sambur, "An algorithm for determining the endpoints of isolated utterances", *Bell Labs Technical Journal*, vol. 54, no. 2, pp.297-315, 1975.
75. F. Pukelsheim, "The three sigma rule", *The American Statistician*, vol. 48, no. 2, pp.88-91, 1994.
76. P.R. Rijnbeek, J.A. Kors and M. Witsenburg, "Minimum bandwidth requirements for recording of pediatric electrocardiograms", *Circulation*, vol. 104, no. 25, pp.3087-3090, 2001.
77. P. Kligfield, L.S. Gettes, J.J. Bailey, R. Childers, B.J. Deal, E.W. Hancock, G. van Herpen, J.A. Kors, P. Macfarlane, D.M. Mirvis and O. Pahlm, "Recommendations for the Standardization and Interpretation of the Electrocardiogram", *Circulation*, vol. 115, no. 10, pp.1306-1324, 2007.
78. R. Sameni, Open source ECG toolbox (OSET), 2006.
79. D. Marr and E. Hildreth, "Theory of edge detection", *Proceedings of the Royal Society of London B: Biological Sciences*, vo. 207, no. 1167, pp.187-217, 1980.
80. P.M. Agante, and J.P. Marques de Sa, "ECG noise filtering using wavelets with soft-thresholding methods", *Computers in Cardiology*, pp. 535-538, 999.

81. S. Poornachandra, "Wavelet-based denoising using subband dependent threshold for ECG signals", *Digital signal processing*, vol.18, no.1, pp. 49-55, 2008.
82. R. Sameni, M.B. Shamsollahi, C. Jutten and G.D. Clifford, "A nonlinear Bayesian filtering framework for ECG denoising", *IEEE Transactions on Biomedical Engineering*, vol. 54, no. 12, pp.2172-2185, 2007.
83. N. Nikolaev, A. Gotchev, K. Egiazarian and Z. Nikolov, "Suppression of electromyogram interference on the electrocardiogram by transform domain denoising", *Medical and Biological Engineering and Computing*, vol. 39, no. 6, pp.649-655, 2001.
84. J.S., Paul, M.R. Reddy and V.J. Kumar, "A transform domain SVD filter for suppression of muscle noise artefacts in exercise ECG's", *IEEE Transactions on Biomedical Engineering*, vol. 47, no. 5, pp.654-663, 2000.
85. O. Sayadi and M.B. Shamsollahi, "ECG denoising and compression using a modified extended Kalman filter structure", *IEEE Transactions on Biomedical Engineering*, vol. 55, no. 9, pp.2240-2248, 2008.
86. R. Sameni, M.B. Shamsollahi, C. Jutten and M. Babaie-Zade, "Filtering noisy ECG signals using the extended Kalman filter based on a modified dynamic ECG model", *In Computers in Cardiology*, pp. 1017-1020, 2005.
87. N.V. Thakor and Y.S Zhu, "Applications of adaptive filtering to ECG analysis: noise cancellation and arrhythmia detection", *IEEE transactions on biomedical engineering*, vol. 38, no. 8, pp.785-794, 1991.
88. P. Lander and E.J. Berbari, "Time-frequency plane Wiener filtering of the high-resolution ECG: development and application", *IEEE transactions on biomedical engineering*, vol. 44, no. 4, pp.256-265, 1997.
89. M. Marouf, L. Saranovac and G. Vukomanovic, "Algorithm for EMG noise level approximation in ECG signals", *Biomedical Signal Processing and Control*, vol. 34, pp.158-165, 2017.
90. S. P. Ghael, A. M. Sayeed, and R. G. Baraniuk, "Improved Wavelet Denoising via Empirical Wiener Filtering", *Proceedings of SPIE - The International Society for Optical Engineering*, vol. 3169, pp. 389-399, Jul. 1997.
91. H. A. Kestler et al., "De-noising of high-resolution ECG signals by combining the discrete wavelet transform with the Wiener filter," *Computers in Cardiology*, vol. 25, pp. 233-236, Sep. 1998.
92. N. Nikolaev, Z. Nikolov, A. Gotchev, and K. Egiazarian, "Wavelet domain Wiener filtering for ECG denoising using improved signal estimate," *2000 IEEE*

International Conference on Acoustics, Speech, and Signal Processing - Proceedings, vol. 6, pp. 3578-3581, Jun. 2000.

93. L. Chmelka and J. Kozumplik, "Wavelet-based Wiener filter for electrocardiogram signal denoising", *Computers in Cardiology*, pp. 771-774, Sep. 2005.
94. L. Smital, M. Vitek, J. Kozumplik and I. Provaznik, "Adaptive wavelet wiener filtering of ECG signals", *IEEE transactions on biomedical engineering*, vol. 60, no. 2, pp.437-445, 2013.
95. D. L. Donoho and J. M. Johnstone, "Ideal spatial adaptation by wavelet shrinkage," *Biometrika*, vol. 81, no. 3, pp. 425-455, Sep. 1994.
96. N. Nikolaev, Z. Nikolov, A. Gotchev, and K. Egiazarian, "Wavelet domain Wiener filtering for ECG denoising using improved signal estimate", *2000 IEEE International Conference on Acoustics, Speech, and Signal Processing - Proceedings*, vol. 6, pp. 3578-3581, Jun. 2000.
97. L. N. Sharma, S. Dandapat, and A. Mahanta, "Multiscale wavelet energies and Relative Energy based Denoising of ECG signal," *2010 IEEE International Conference on Communication Control and Computing Technologies*, no. 1, pp. 491-495, Oct. 2010.
98. S. Mallat, *A Wavelet Tour of Signal Processing*. Academic Press, 2nd ed., New York, 1999
99. B.S. Lin, N.K. Chou, F.C. Chong and S.J. Chen, "RTWPMS: A real-time wireless physiological monitoring system", *IEEE Transactions on Information Technology in Biomedicine*, vol.10, no. 4, pp.647-656, 2006.
100. D. Lucani, G. Cataldo, J. Cruz, G. Villegas and S. Wong, "A portable ECG monitoring device with Bluetooth and Holter capabilities for telemedicine applications", *Engineering in Medicine and Biology Society, EMBS'06. 28th Annual International Conference of the IEEE*, pp. 5244-5247, 2006.
101. Z. Lv, F. Xia, G. Wu, L. Yao and Z. Chen, "iCare: a mobile health monitoring system for the elderly", *In Proceedings of the 2010 IEEE/ACM Int'l Conference on Green Computing and Communications & Int'l Conference on Cyber, Physical and Social Computing*, pp. 699-705, 2010.
102. P.J. Zimetbaum, K.Y. Kim, M.E. Josephson, A.L. Goldberger and D.J. Cohen, "Diagnostic yield and optimal duration of continuous-loop event monitoring for the diagnosis of palpitations: a cost-effectiveness analysis", *Annals of Internal Medicine*, vol. 128, no. 11, pp.890-895, 1998.

103. M. Linzer, E.L. Pritchett, M. Pontinen, E. McCarthy and G.W. Divine, “Incremental diagnostic yield of loop electrocardiographic recorders in unexplained syncope” *The American journal of cardiology*, vol. 66, no. 2, pp.214-219, 1990.
104. N. Meziane, J.G. Webster, M. Attari and A.J. Nimunkar, “Dry electrodes for electrocardiography”, *Physiological measurement*, vol. 34, no. 9, p.R47, 2013.
105. K. Sparks and A. Rood, “Comparison of ECG signal quality between a novel dry electrode and a standard gel electrode”, *Med. Sci. Sports Exercise*, vol. 38, no. 1, p.S5, 2006.
106. R.N. Schmidt, F.J. Lisy, G.G. Skebe and T.S. Prince, “Dry physiological recording electrode”, *Orbital Research*, U.S. Patent 6,785,569, 2004.
107. J. Yoo, L. Yan, S. Lee, H. Kim and H.J. Yoo, “A wearable ECG acquisition system with compact planar-fashionable circuit board-based shirt”, *IEEE Transactions on Information Technology in Biomedicine*, vol. 13, no.6, pp.897-902, 2009.
108. F. Abtahi, J. Snäll, B. Aslamy, S. Abtahi, F. Seoane and K. Lindecrantz, “Biosignal PI, an affordable open-source ECG and respiration measurement system”, *Sensors*, vol.15, no.1, pp.93-109, 2014.
109. J. Morak, A. Kollmann, D. Hayn, P. Kastner, G. Humer and G. Schreier, “Improving telemonitoring of heart failure patients with NFC technology”, *Proceedings of the fifth IASTED International Conference: biomedical engineering*, pp. 258-261, 2007.
110. J. Morak, H. Kumpusch, D. Hayn, M. Leitner, D. Scherr, F.M. Fruhwald and G. Schreier, “Near Field Com-munication-based telemonitoring with integrated ECG recordings”, *Applied clinical informatics*, vol. 2, no.4, pp.481-498, 2010.
111. M.F.A. Karim and R. Muhamad, “Integration of near field communication (NFC) and bluetooth technology for medical data acquisition system”, *Proceedings of the 6th WSEAS International Conference on Signal Processing, Computational Geometry & Artificial Vision*, pp. 147-152, 2006.
112. M.G. Adams-Hamoda, M.A. Caldwell, N.A. Stotts and B.J. Drew, “Factors to consider when analyzing 12-lead electrocardiograms for evidence of acute myocardial ischemia”, *American Journal of Critical Care*, vol.12, no. 1, pp.9-16, 2003.
113. P. InCenter, “Improving ecg quality: Application note”. Phillips Healthcare, pp.1-6, 2008.
114. G.B. Moody and R.G. Mark, “Development and evaluation of a 2-lead ECG analysis program”, *Computers in cardiology*, vol. 9, pp.39-44, 1982.
115. S. Olmos, M. MillAn, J. Garcia and P. Laguna, “ECG data compression with the Karhunen-Loeve transform”, *Computers in Cardiology*, pp. 253-256, 1996.

116. E. Delgado, J.L. Rodriguez, F. Jiménez, D. Cuesta and G. Castellanos, “Recognition of cardiac Arrhythmias by means of Beat Clustering on ECG-Holter Records”, *Computers in Cardiology*, pp. 161-164, 2007.
117. P.W. Macfarlane, S.C. McLaughlin, B. Devine and T.F. Yang, “Effects of age, sex, and race on ECG interval measurements”, *Journal of Electrocardiology*, vol. 27, pp.14-19, 1994.
118. D.F. Dickinson, “The normal ECG in childhood and adolescence”, *Heart*, vol. 91, no. 12, pp.1626-1630, 2005.
119. J.A. Drezner, M.J. Ackerman, J. Anderson, E. Ashley, C.A. Asplund, A.L. Baggish, M. Börjesson, B.C. Cannon, D. Corrado, J.P. DiFiori and P. Fischbach, “Electrocardiographic interpretation in athletes: the ‘Seattle criteria’”, *British journal of sports medicine*, vol. 47, no. 3, pp.122-124, 2013.
120. J.A. Ferst and B.R. Chaitman, “The electrocardiogram and the athlete”, *Sports Medicine*, vol.5, no.1, pp.390-403, 1984.
121. World Medical Association, “World Medical Association Declaration of Helsinki. Ethical principles for medical research involving human subjects”, *Bulletin of the World Health Organization*, vol. 79, no. 4, p.373., 2001.
122. E.N. Marieb and K. Hoehn,” Human anatomy & physiology”, *Pearson Education*, 2007.
123. G.D. Clifford, J. Behar, Q. Li and I. Rezek, “Signal quality indices and data fusion for determining clinical acceptability of electrocardiograms”, *Physiological measurement*, vol. 33, no. 9, p.1419, 2012.
124. Q. Li, R.G. Mark and G.D. Clifford, “Robust heart rate estimation from multiple asynchronous noisy sources using signal quality indices and a Kalman filter”, *Physiological measurement*, vol. 29, no. 1, p.15, 2007.
125. D.D. Mehta, N.T. Nazir, R.G. Trohman and A.S. Volgman, “Single-lead portable ECG devices: Perceptions and clinical accuracy compared to conventional cardiac monitoring”, *Journal of electrocardiology*, vol. 48, no. 4, pp.710-716, 2015.
126. T. Martin, E. Jovanov and D. Raskovic, “Issues in wearable computing for medical monitoring applications: a case study of a wearable ECG monitoring device”, *Wearable Computers, The Fourth International Symposium*, pp. 43-49, 2000.

Biography

Mohamed Marouf was born on July 8, 1986 in Masyaf area, Syria, where he finished elementary and high school studies. He, then, started his undergraduate studies in Electronic Engineering, Department of Computer Engineering at the Faculty of Electrical and Electronic Engineering, Aleppo University. In June, 2009, Mohamed graduated with very good qualifications, 76.6 average score.

In 2011, Mohamed got a scholarship to pursue PhD studies in Serbia. He attended the Electronics Program at the School of Electrical Engineering, University of Belgrade. His research interests include Digital Signal and Image Processing, Bioinformatics, and Machine Learning.

During his PhD studies, Mohamed worked as an R&D engineer for the HTEC group and, afterwards, for Seven Bridges Genomics. Right now, he is working as a Machine Learning scientist in Systems Biology at the Center for Molecular Neurobiology, in Hamburg, Germany.

Mohamed published several papers in international and regional conferences as well as two publications, related to this thesis, in international journals.

Author's publications

Journals

- [A1] Mohamed Marouf, Lazar Saranovac, Goran Vukomanovic, "Algorithm for EMG Noise level Approximation in ECG Signals", *Biomedical Signal processing and Control*, Vol.43, pp. 158-165, 2017, <https://doi.org/10.1186/s12938-017-0371-6>.
- [A2] Mohamed Marouf, Lazar Saranovac, Goran Vukomanovic, Miroslav Bozic "Multi-purpose ECG telemetry system", *Biomedical Engineering Online*, Vol.16, SP. 80-96, 2017, <https://doi.org/10.1016/j.bspc.2017.02.002>.

Conferences

- [B1] Mohamed Marouf, Lazar Saranovac, "Adaptive EMG noise reduction in ECG signals using noise level approximation", *Proc. SPIE 10613, 2017 International Conference on Robotics and Machine Vision*, Japan 2017; <http://dx.doi.org/10.1117/12.2299841>

- [B2] Mohamed Marouf, Jelena Popović Božović, Ivan Popović, "FPGA Implementation of Neural Network Processing Element in Ice Detector", *NEUREL 2012, 11th Symposium on Neural Network Applications in Electrical Engineering*, pp. 81 - 84, Belgrade, 2012; <https://doi.org/10.1109/NEUREL.2012.6419970>.
- [B3] Dragomir El Mezeni, Mohamed Marouf, Lazar Saranovac, “Adaptive wavelet based edge detection in noisy images”, *INFOTEH-JAHORINA Vol. 13, March 2014*, p683-688.
- [B4] Mohamed Marouf, Ivan Popović, “Ice Detector Embedded System Design”, *International Conference on Electrical, Electronic and Computing Engineering ETRAN, 2012*.

Изјава о ауторству

Име и презиме аутора Мохамед Мароуф

Број индекса 5048/2011

Изјављујем

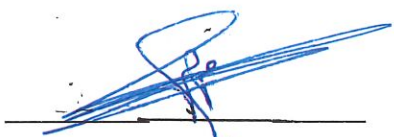
да је докторска дисертација под насловом

Апроксимација И Адаптивно Смањење Високофреквентног Шума У ЕКГ Сигналима

- резултат сопственог истраживачког рада;
- да дисертација у целини ни у деловима није била предложена за стицање друге дипломе према студијским програмима других високошколских установа;
- да су резултати коректно наведени и
- да нисам кршио/ла ауторска права и користио/ла интелектуалну својину других лица.

Потпис аутора

У Београду, 18/12/2017



Изјава о истоветности штампане и електронске верзије докторског рада

Име и презиме аутора Мохамед Мароуф
Број индекса 5048/2011
Студијски програм Електроника
Наслов рада Апроксимација И Адалтивно Смањење Високофреквентног Шума
У ЕКГ Сигналима
Ментор Др. Лазар Сарановац, Ванредни Професор

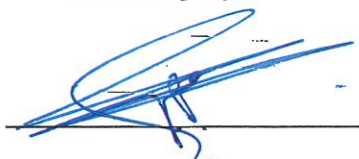
Изјављујем да је штампана верзија мого докторског рада истоветна електронској верзији коју сам предао/ла ради похађења у **Дигиталном репозиторијуму Универзитета у Београду**.

Дозвољавам да се објаве моји лични подаци везани за добијање академског назива доктора наука, као што су име и презиме, година и место рођења и датум одbrane рада.

Ови лични подаци могу се објавити на мрежним страницама дигиталне библиотеке, у електронском каталогу и у публикацијама Универзитета у Београду.

Потпис аутора

У Београду, 18/12/2017



Изјава о коришћењу

Овлашћујем Универзитетску библиотеку „Светозар Марковић“ да у Дигитални репозиторијум Универзитета у Београду унесе моју докторску дисертацију под насловом:

Апроксимација И Адаптивно Смањење Високофреквентног Шума У ЕКГ Сигналима

која је моје ауторско дело.

Дисертацију са свим прилозима предао/ла сам у електронском формату погодном за трајно архивирање.

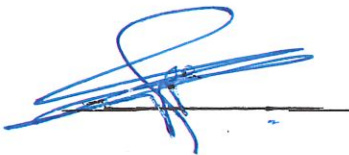
Моју докторску дисертацију похрањену у Дигиталном репозиторијуму Универзитета у Београду и доступну у отвореном приступу могу да користе сви који поштују одредбе садржане у одабраном типу лиценце Креативне заједнице (Creative Commons) за коју сам се одлучио/ла.

1. Ауторство (CC BY)
2. Ауторство – некомерцијално (CC BY-NC)
- 3 Ауторство – некомерцијално – без прерада (CC BY-NC-ND)
4. Ауторство – некомерцијално – делити под истим условима (CC BY-NC-SA)
5. Ауторство – без прерада (CC BY-ND)
6. Ауторство – делити под истим условима (CC BY-SA)

(Молимо да заокружите само једну од шест понуђених лиценци.
Кратак опис лиценци је саставни део ове изјаве).

Потпис аутора

У Београду, 18/12/2017



- 1. Ауторство.** Дозвољавате умножавање, дистрибуцију и јавно саопштавање дела, и прераде, ако се наведе име аутора на начин одређен од стране аутора или даваоца лиценце, чак и у комерцијалне сврхе. Ово је најслободнија од свих лиценци.
- 2. Ауторство – некомерцијално.** Дозвољавате умножавање, дистрибуцију и јавно саопштавање дела, и прераде, ако се наведе име аутора на начин одређен од стране аутора или даваоца лиценце. Ова лиценца не дозвољава комерцијалну употребу дела.
- 3. Ауторство – некомерцијално – без прерада.** Дозвољавате умножавање, дистрибуцију и јавно саопштавање дела, без промена, преобликовања или употребе дела у свом делу, ако се наведе име аутора на начин одређен од стране аутора или даваоца лиценце. Ова лиценца не дозвољава комерцијалну употребу дела. У односу на све остале лиценце, овом лиценцом се ограничава највећи обим права коришћења дела.
- 4. Ауторство – некомерцијално – делити под истим условима.** Дозвољавате умножавање, дистрибуцију и јавно саопштавање дела, и прераде, ако се наведе име аутора на начин одређен од стране аутора или даваоца лиценце и ако се прерада дистрибуира под истом или сличном лиценцом. Ова лиценца не дозвољава комерцијалну употребу дела и прерада.
- 5. Ауторство – без прерада.** Дозвољавате умножавање, дистрибуцију и јавно саопштавање дела, без промена, преобликовања или употребе дела у свом делу, ако се наведе име аутора на начин одређен од стране аутора или даваоца лиценце. Ова лиценца дозвољава комерцијалну употребу дела.
- 6. Ауторство – делити под истим условима.** Дозвољавате умножавање, дистрибуцију и јавно саопштавање дела, и прераде, ако се наведе име аутора на начин одређен од стране аутора или даваоца лиценце и ако се прерада дистрибуира под истом или сличном лиценцом. Ова лиценца дозвољава комерцијалну употребу дела и прерада. Слична је софтверским лиценцима, односно лиценцима отвореног кода.